MASTER'S THESIS

MSc INTEGRATED WATER RESOURCES MANAGEMENT (IWRM)

TH Köln (University of Applied Sciences)
ITT – Institute for Technology and Resources Management in the Tropics and Subtropics

Universidad Nacional de Córdoba (UNC)
Laboratorio de Hidráulica (LH) - Centro de Estudios y Tecnología del Agua (CETA)

HYDROLOGICAL MODELLING OF LA PICASA LAGOON (ARGENTINA)

Juan Sebastián Salva

September 11th, 2018

ITT
Institute for Technology and Resources Management in the Tropics and Subtropics

Technology
Arts Sciences
TH Köln

Master's Thesis

Hydrological Modelling of La Picasa Lagoon (Argentina)

Thesis to obtain the Degree of

MASTER OF SCIENCE

INTEGRATED WATER RESOURCES MANAGEMENT (IWRM)

DEGREE AWARDED BY COLOGNE UNIVERSITY OF APPLIED SCIENCES

PRESENTS:
JUAN SEBASTIÁN SALVA

SUPERVISOR OF THESIS ITT:
Prof. Dr. Jackson Roehrig

SUPERVISOR OF THESIS LH:
Prof. Dr. Andrés Rodriguez

DATE OF SUBMISSION
September 11th, 2018

Presented by

Juan Sebastián Salva Student no.: 11117464 Email: juansebastiansalva@gmail.com

Abstract

La Picasa basin, an interjurisdictional endorreic basin of 5282 km^2 located in the "Central Pampa" in Argentina, has suffered repeated flooding caused by an increasing water level of La Picasa lagoon, affecting livelihoods, infrastructure, transportation and agriculture. Although water infrastructure has been built to regulate water excesses, it has not been effective in reducing the flood risk.

To improve the knowledge of the hydrological system, the master's thesis aimed to develop a water balance model of La Picasa lagoon at a monthly time step between the hydrological years 2007/2008 and 2016/2017. Specifically, the objectives were to identify and quantify the most important components and processes determining its water level, area and volume and to propose hypothetical simulation scenarios based on different pumping operation schemes.

The description of the conceptual model and implementation of a sensitivity analysis allowed to identify the inflow and outflow components of the water balance and quantify their relative contributions, namely precipitation, water discharge from channels, surface runoff from surrounding sub-basins of the lagoon, evaporation and pumping. The performance tests applied to the model during the calibration and validation showed a very good performance. Additionally, two simulation scenarios were proposed, namely potential pumping and adjusted pumping, which reflected different trajectories of the water balance.

The master's thesis concluded that precipitation and evaporation were the most determinant inflow and outflow components in the water balance of La Picasa lagoon respectively. However, the flooding event in 2016/2017 was caused by a simultaneous reduction of net evaporation and an increase in water discharge, surface runoff and intermittent pumping. The simulation scenarios suggested that an optimal operation of the pumping stations could have been effective to increase the storage capacity of the lagoon. However, during longer humid periods, it might not be enough to outweigh additional inflows.

Keywords: water balance, hydrological modelling, La Picasa lagoon, flooding,

Resumen

La cuenca de la laguna La Picasa, una cuenca interjurisdiccional y endorreica de 5282 km^2 ubicada en la Pampa Central Argentina, ha sufrido recurrentes inundaciones causadas por crecientes niveles de la laguna La Picasa, afectando viviendas, infraestructura, transporte y la actividad agrícola. A pesar de que ya se han construido obras de infraestructura para regular los excesos hídricos, las mismas no han sido eficaces para reducir el riesgo de inundación.

Para mejorar el conocimiento del sistema hidrológico, el objetivo general de la tesis de maestría fue desarrollar un modelo de balance hídrico de la laguna La Picasa a paso mensual entre los años hidrológicos 2007/2008 y 2016/2017. Los objetivos específicos fueron identificar y cuantificar los componentes y procesos hidrológicos más importantes que determinan el nivel del agua, área y volumen de la laguna, y por otro lado proponer escenarios de simulación hipotéticos basados en diferentes esquemas de bombeo.

La descripción del modelo conceptual y la implementación de un análisis de sensibilidad permitieron identificar los componentes de ingreso y egreso del balance hídrico y cuantificar sus contribuciones relativas, específicamente precipitación, caudal de canales de entrada, escorrentía superficial proveniente de subcuencas aledañas a la laguna, evaporación y bombeo. Los análisis de desempeño aplicados al modelo durante la calibración y validación mostraron un muy buen ajuste. Además, dos escenarios de simulación fueron propuestos, bombeo potencial y bombeo ajustado, reflejando diferentes trayectorias del balance hídrico.

La tesis de maestría concluyó que la precipitación y evaporación representaron los componentes hidrológicos de ingreso y egreso más importantes del balance hídrico de la laguna La Picasa respectivamente. Sin embargo, las inundaciones ocurridas en 2016/2017 fueron causadas por una reducción de la evaporación neta simultáneamente con un incremento de caudal de llegada, escorrentía superficial y bombeo intermitente. Por su parte, los escenarios de simulación propuestos mostraron que una operación óptima del bombeo pudiera haber incrementado efectivamente la capacidad de regulación de los excedentes hídricos de la laguna. De todas maneras, durante largos períodos húmedos, el bombeo podría no ser suficiente para balancear los incrementos en ingresos.

Palabras clave: balance hídrico, modelación hidrológica, laguna La Picasa, inundaciones

Acknowledgements

First of all, I want to express my gratitude to my supervisor Prof. Dr. Jackson Roehrig for his professional guidance to define and structure the master's thesis and his suggestions in the analysis of preliminary results, which were key inputs in the process to achieve the objectives.

Second, my recognition to Prof. Dr. Andrés Rodríguez and members of the partner institution in Argentina 'Laboratorio de Hidráulica (LH) - Universidad Nacional de Córdoba' for giving me the opportunity to develop my master's thesis in the framework of the current activities of the institute, providing me with the required work place, infrastructure and information. Moreover, the culmination of this study would not have been possible without the assistance of Juan Carlos Bertoni, Secretary of Water Resources of Santa Fe, who provided endless help in contacting and establishing the interviews with local stakeholders and making possible the organization of the field trips to conduct the bathymetries. In this regard, a special recognition to Ing. Alfredo Raparo, who supplied key information about La Picasa basin in general, but also most of the water discharge data, pumping stations, maps, reports and photographs. In this line, an acknowledgement also to Adolfo Villanueva from the National Water Institute, who exchanged some of his preliminary results of an ongoing project about the hydrological modelling of La Picasa basin.

The possibility of achieving this stage of the master's thesis would not have been possible without the financial support from the Deutscher Akademischer Austauschdienst (DAAD) to study at the Institute for Technology and Resources Management in the Tropics and Subtropics (ITT) of the Cologne University of Applied Sciences and to conduct the field trip to Argentina.

Finally, I want to express my infinite gratitude to my family and friends who have been always an immense support, without which I could have not reached this goal in my life.

Table of Contents

List of Figures

List of Tables

List of Photographs

List of abbreviations

ADCP	Acoustic Doppler Current Profiler
ALOS	Advanced Land Observing Satellite
BCCBA	Bolsa de Cereales de Córdoba (Grain Exchange of Córdoba)
CN	Curve Number
CRL	Centro Regional Litoral (Litoral Regional Center)
CRLE	Complementary Relationship Lake Evaporation Model
DAE	Differential Algebraic Equations
DEM	Digital Elevation Model
ENSO	El Niño-Southern-Oscillation
EU	European Commission
FAO-LCCS	Food and Agriculture Organization of the United Nations-Land Cover Classification System
GLDAS	Global Land Data Assimilation System
GNSS	Global Navigation Satellite System
GPS	Global Positioning System
GRACE	Gravity Recovery and Climate Experiment
HSG	Hydrologic Soil Group
HWSD	Harmonized World Soil Database
IDW	Inverse Distance Weighted
IGN	Instituto Geográfico Nacional (National Geography Institute)
INA	Instituto Nacional del Agua (National Water Institute)
INTA	Instituto Nacional de Tecnología Agropecuaria (National Institute Of Agricultural Technology
LH-CETA	Laboratorio de Hidráulica – Centro de Estudios y Tecnología del Agua (Laboratory of Hydraulics – Center for Studies and Water Technology)
MAH	Ministerio de Asuntos Hídricos de Santa Fe (Ministry of Water Resources of Santa Fe)
MAGyA	Ministerio de Agricultura y Ganadería de Córdoba (Ministry of Agriculture and Livestock Production of Córdoba)
MODIS	Moderate Resolution Imaging Spectroradiometer
POSGAR07	Posiciones Geodésicas Argentinas 2007 (Argentinian Geodetic Positioning)
PPM	Parts per million
SCS	Soil Conservation Service
SRH	Secretaría de Recursos Hídricos de Santa Fe (Secretariat of Water Resources of Santa Fe)
SsRH	Subsecretaría de Recursos Hídricos de la Nación (Under-Secretariat of Water Resources of Argentina)
TIN	Triangulated Irregular Network Dataset
UNC	Universidad Nacional de Córdoba (National University of Córdoba)
UNISDR	United Nations International Strategy for Disaster Reduction
UNRC	Universidad Nacional de Rio Cuarto (National University of Rio Cuarto)
USDA	United States Department of Agriculture
UTM	Universal Transverse Mercator Coordinate System
WGS84	World Geodetic System 1984

1. Introduction

Although floods have been recognized as one of the most important disasters worldwide (UNISDR, 2009), there are many regions in the world that still lack a deeper understanding of the hydrological systems and the effective tools to counterbalance their negative effects (Cobby *et al*., 2009). One of these regions is the "Central Pampa" in Argentina, characterized by large flat areas, where the basins do not have clear limits due to undeveloped drainage networks (Latrubesse and Brea, 2009). In many cases, the water slowly flows through these networks creating temporal wetlands and finally occupying dells (shallow depressions), which are regularly flooded depending on the climatic conditions, forming larger lagoons or shallow lakes (Bohn *et al*., 2016; Iriondo and Drago, 2004).

A representative example of a flat plain basin in the Central Pampa is La Picasa, an interjurisdictional endorreic basin characterized by a longitudinal depression and a dell located at its easternmost sector, which functions as a sink receiving the water excesses from the basin, where the homonymous lagoon "La Picasa" is formed (Pedraza, 2000). As many other lagoons in the region, La Picasa is sensitive to climate variability, such as the typical alternation between humid and dry periods that are expressed by floods, seasonal cycles and droughts (Giordano *et al*., 2017; Bohn *et al*., 2016). In response to these variations, the lagoon undergoes a considerable areal and volume increase or decrease in short periods of time, being reflected in the alteration of its water level.

In the last two decades, the alternation between higher and lower water levels of La Picasa lagoon has caused two important flooding events. The first one occurred after intense precipitations over the basin between the hydrological years 1999/2001, when the water reached 105.3 m above sea level (Pereira *et al*., 2014; Pedraza, 2000). The second one happened between the hydrological years 2016/2017, when the water level exceeded that one of the previous flooding event, reaching 105.75 m (SsRH, 2017). As a consequence, the repeated flooding has affected productive land destined to agriculture, damaged public infrastructure, disrupted transportation and the overall socio-economic development of towns and cities nearby, increasing the degree of conflicts between the different jurisdictions involved (Rosenstein *et al*., 2009).

After the first flooding episode, a specific water infrastructure was built aiming to regulate the water excesses in the basin, thus reducing the flooding risk. It consists of a main channel that conducts the water coming from the fields through a series of regulation reservoirs, other channels connecting either the reservoirs to the lagoon as the final sink or a diversion channel that avoids the water flowing into the lagoon, and pumping stations to regulate the water level of the lagoon between 98.5 m and 102.5 m above sea level (INA, 2016; SsRH, 2015). However, the fact that a second and larger flooding event happened eighteen years after the first one clearly shows that not only changes in the hydrology of the basin might have occurred but also that the measures taken so far have not been as effective as required. Subsequently, there is a need to update the current scientific knowledge of La Picasa basin in general, and the lagoon in particular.

In this respect, hydrological models aiming to improve the planning and management of the water resources of the basin and reduce the risk of overflow of the lagoon have already been conducted (Pedraza *et al*., 2010; A. Villanueva, personal communication, April 27th, 2018). Nevertheless, they have not attempted to develop a water balance model of the lagoon and to explain its most

important hydrological components and processes. In contrast, most of them have pursued to develop distributed or semi-distributed hydrological models to gain an overall understanding of the functioning of the basin. In this regard, Viessman and Lewis (as cited by Rodríguez *et al*., 2006) has already suggested that a water balance model should be the first approach in the analysis of any basin.

Consequently, after the recent flooding event, there is a specific need to contribute to the knowledge of the hydrology of La Picasa lagoon in order to support appropriate and more effective planning and management practices by the basin committee, farmers, local and national governments to mitigate the negative effects of floods. Therefore, the master's thesis aims to develop the water balance model of La Picasa lagoon in order to understand the most important hydrological components, their relationships and current status. The master's thesis was conducted as a contribution to the Project 'Aportes para una Gestión Integrada de una Cuenca Hidrográfica Interjurisdiccional de Impacto Nacional: Cuenca Laguna La Picasa (Córdoba, Santa Fe, Buenos Aires)' in cooperation with LH-CETA, UNC, Argentina.

2. La Picasa basin

The study area of the master's thesis is La Picasa basin, an interjurisdictional endorreic basin of 5282 km^2 located in central Argentina between 33° 54' and 34° 30' South Latitude and 62° 05' and 63° 34' West Longitude (Pedraza, 2000), between the provinces of Córdoba (46.6%), Santa Fe (36.2%) and Buenos Aires (17.2%).

The basin is crossed from Southeast to Northwest by railways that were formerly used by the 'General San Martin' Railways and the National Route 7, the so-called bi-oceanic corridor between Brazil, Uruguay, Argentina and Chile, being at the same time the main access between the most important cities in the basin, such as Rufino, Laboulaye, Aarón Castellanos and Diego de Alvear (Herzer, as cited in García Montaldo, 2012). In turn, La Picasa lagoon occupies a dell located in the Southeastern sector of the basin (Figure 1).

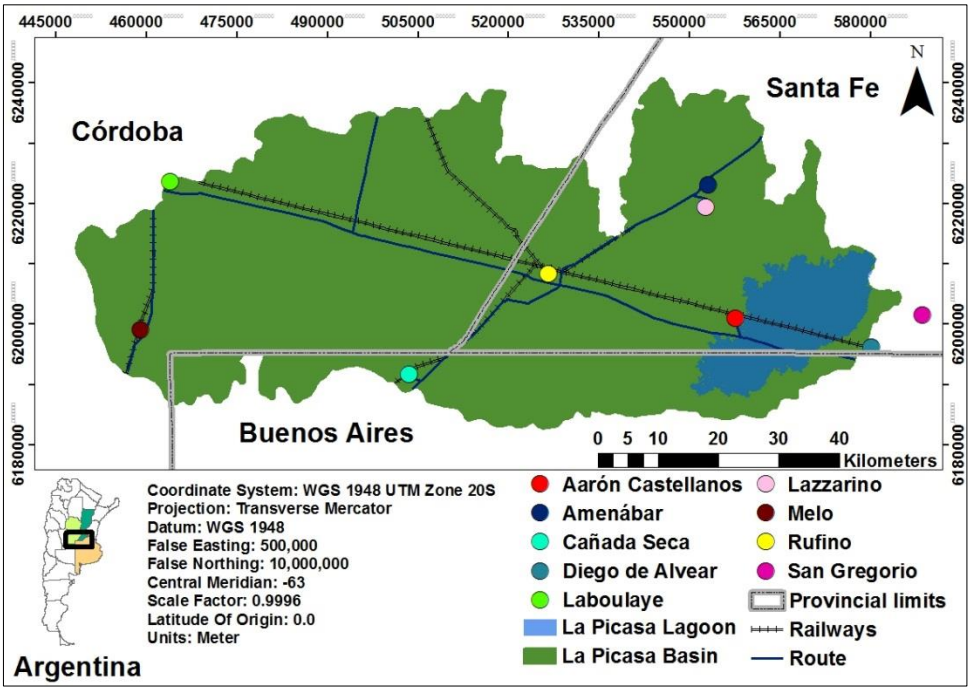

Figure 1 Location of La Picasa basin

Source: own elaboration based on SsRH (2017)

The basin is part of the ecoregion Central Pampa, specifically the so-called Pampean Sand Sea (Iriondo and Kröhling, 2007; Iriondo and Drago, 2004). The geology of the region is characterized by two quaternary aeolian formations, the Teodelina Formation, a 10 to 12 meters thick layer composed by sandy coarse silt and silty fine sand formed in the Late Pleistocene, and the San Gregorio Formation, a 7 meters thick layer made of loose, massive and very fine to fine sand formed in the Late Holocene (Iriondo and Kröhling, 2007).

Related to these geological formations, the geomorphology was described as the result of a sequence of aeolian sedimentary processes (Tripaldi and Forman, 2016), which fostered the configuration of a large flat landscape with slopes lower than 0.4% (Latrubesse and Brea, 2009; Fili *et al*., 2000). The landscape is dominated by longitudinal sand dunes in directions S-N and SSW-NNE corresponding to the San Gregorio Formation, partially covering a generally flatter area with an upper layer of loess sediments, which is the limit of the Teodelina Formation (Iriondo and Kröhling,

2007) (Figure 2). The thickness of the sand layers ranges from few meters to more than 10 meters in the 'Diego de Alvear' dune, the eastern limit of La Picasa basin (Fili *et al*., 2000). Another type of geomorphological formation is a dell, a shallow depression resulting from deflation processes, where wetlands and lagoons, such as La Picasa, are usually formed (Iriondo and Kröhling, 2007; Aradas and Thorne, 2001; Fili *et al*., 2000).

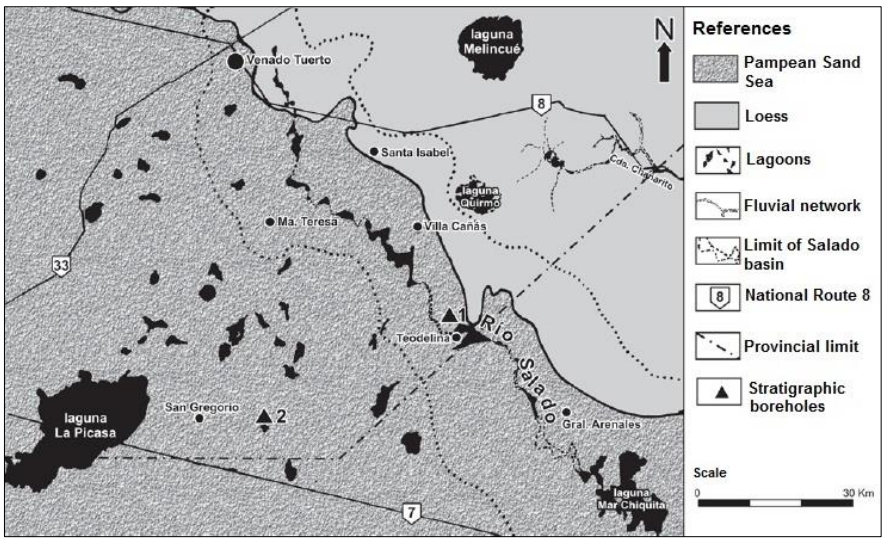

Figure 2 Pampean Sand Sea

Source: adapted from Iriondo and Kröhling (2007)

The soils of the basin are mainly represented by Mollisols, which in the higher parts of the landscape are deep, well drained, with textures ranging between sandy loam to sandy (Viglizzo and Frank, 2006). On the contrary, in the lower and depressed areas, soils are composed by finer textures varying from very fine silty sand with minor clay to fine silty sand, thus presenting a limited drainage capacity (Pedraza, 2000).

Based on Thorntwaite classification, the climate ranges from sub-humid in the eastern sector to semi-arid in the western sector, with a mean annual precipitation of 900 mm and potential evapotranspiration of 1,247 mm (Pedraza, 2000). The climate shows an intra-annual variability, with a dry season between March and September and a humid season between October to February (Iriondo *et al*., 2009). However, it is important to highlight that one of the most typical climatic characteristics of the Central Pampa is the inter-annual variability, expressed by the occurrence of alternatively humid and dry periods (Tanco and Kruse, 2001) (Figure 3).

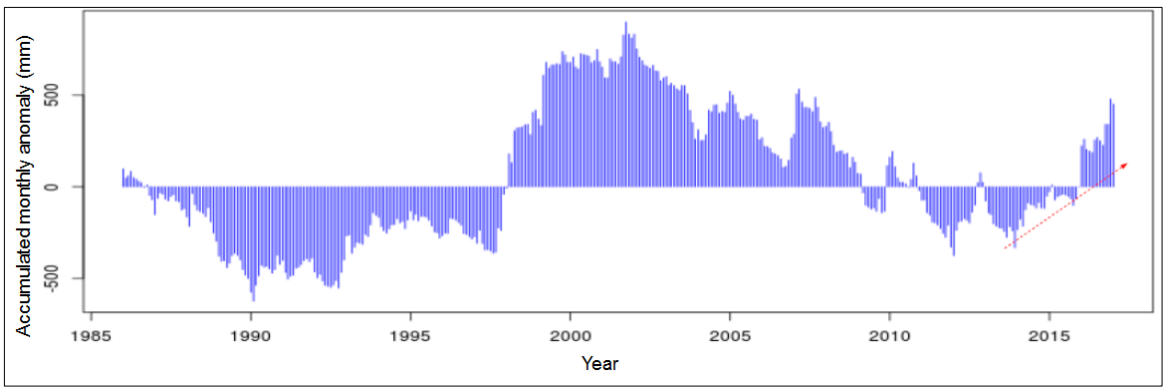

Figure 3 Accumulated monthly precipitation anomaly in Laboulaye (1986-2015)

Source: adapted from Giordano *et al*. (2017)

For instance, Figure 3 shows that between 1986 and 2015 the accumulated monthly precipitation anomaly in Laboulaye, a city located in the headwaters of the basin (see Figure 1), fluctuated following dry and humid periods that lasted for approximately 10 years. In the context of the last flooding event in the basin, it is also worthwhile mentioning that the Central Pampa is facing one of the humid periods that started in 2012 (Giordano *et al*., 2017). In this sense, it has been suggested that the inter-annual variability is mainly determined by ENSO (Guerra *et al*., 2016).

Regarding the long-term climatic variability in the region, an aspect to consider is that during the first half of the twentieth century an overall decline of precipitation has been reported, after which a shift on the trend towards more humid conditions occurred (Iriondo *et al*., 2009; Viglizzo and Frank, 2006). Especially after 1970, a positive trend in mean precipitation, shown by a westward displacement of isohyets, has been highlighted in several studies (Pereira *et al*., 2014; Brandolin *et al*., 2012; Venencio and García, 2011; Viglizzo and Frank, 2006; Aradas and Thorne, 2001). In this case, the decadal to multidecadal variability is mostly defined by atmospheric-ocean coupled oscillations over the Atlantic and Pacific Oceans (Guerra *et al*., 2016).

Originally characterized by native grasslands and later perennial pastures, the land cover of the Central Pampa has changed in the last four decades to agriculture, mainly annual monoculture production systems, such as soybean, wheat, maize, sunflower, or in rotation with annual pastures (oat, triticale, rye) or perennial pastures (alfalfa and grasses) for livestock production (Nosetto *et al*., 2015; Viglizzo and Frank, 2006). Thus, it became the core of the agricultural and farming production systems in Argentina (Labrubesse and Brea, 2009). Only a minor proportion of land remains uncultivated, such as dense grasslands and herbaceous plants in flooded areas (Figure 4).

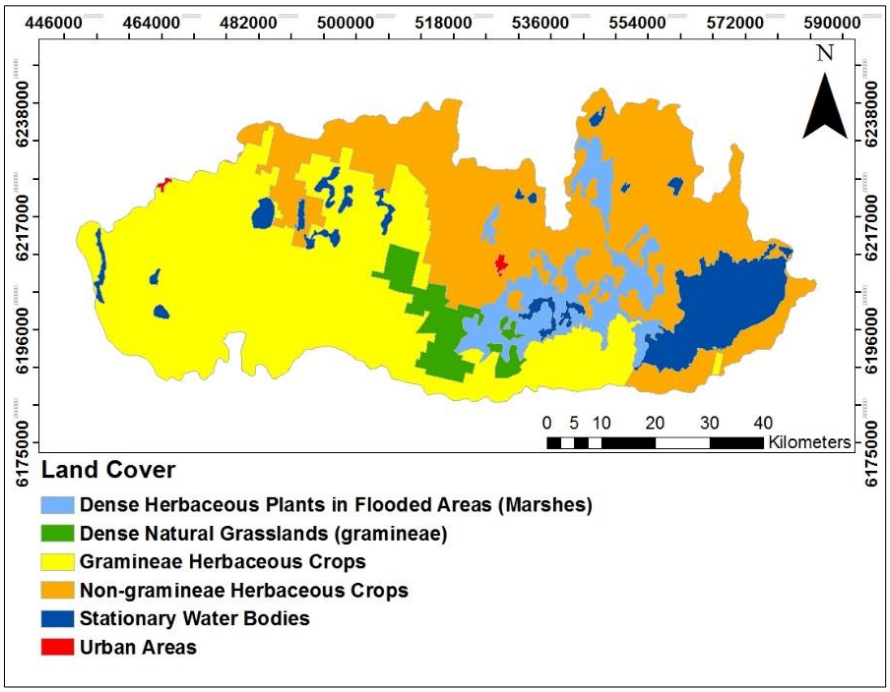

Figure 4 Land cover in La Picasa basin

Source: own elaboration based on FAO-LCCS (2007)

The geomorphological, climatic and vegetation features of La Picasa basin define its main hydrological processes. Since it is a flat basin, the water balance is generally determined by vertical components, namely precipitation, infiltration, percolation and evapotranspiration (Aradas and

Thorne, 2001). However, these processes show differences depending on the general climatic conditions, i.e. whether there is a humid or a dry period. During normal or dry periods, the hydrological dynamic is typically endorreic (Pedraza, 2000). When precipitation reaches the soils, the water is directly evaporated from bare surfaces or transpired by vegetation, while a proportion contributes to surface runoff, flowing through the undeveloped drainage network towards depressions (dells) or local lagoons (Iriondo and Kröhling, 2007; Pedraza, 2000). The remaining water is infiltrated into the soils and a proportion recharges the groundwater table due to deep percolation (Kuppel *et al*., 2015; Nosetto *et al*., 2012). On the other hand, during humid periods groundwater table rises to almost ground surface feeding local lagoons and, if their storage capacity is surpassed, they can in some cases link together to form temporary local flux networks, flowing towards water bodies, such as lagoons or lakes (Paoli, 2015; Latrubesse and Brea, 2009; Iriondo and Kröhling, 2007; Pedraza, 2000). In relation to the water flowing into these water bodies, it has been mentioned that the transportation of suspended solids is generally insignificant, yet the transportation of dissolved salts is high, especially chlorides (Iriondo and Kröhling, 2007).

In particular, two different types of water bodies can be found in the study area, namely lotic and lentic (Iriondo and Drago, 2004). The first ones are commonly represented by transient marshes (‘bañados’), which are non-permanent wetlands occupying depressions of the landscape that are regularly flooded due to extreme precipitation events (Iriondo and Drago, 2004). From the second ones, most of them are permanent endorreic lakes or lagoons that exhibit marked intra or inter-annual water level fluctuations, such as La Picasa lagoon (Iriondo and Kröhling, 2007; Iriondo and Drago, 2004).

In relation to the water resources management of La Picasa basin, since Argentina is characterized by a federal system of government and the basin is shared by three provincial states, a coordinated management is a complex task to solve. In this regard, Córdoba, Santa Fe and Buenos Aires have signed an agreement to create the Interjurisdictional Committee of La Picasa basin, whose objective is to implement a rational and coordinated water resources management and to develop projects and measures aiming to solve the problems of floods and droughts that regularly affect the basin (INA, 2016; García Montaldo, 2012).

3. Problem analysis

La Picasa basin, as many others in the Central Pampa, is facing the consequences of a changing water balance. Not only a positive trend in precipitations has been suggested in the region (Giordano *et al*., 2017), but also land use changes from grasslands and perennial pastures to annual crops have diminished the water use from vegetation, one of the most important water losses in an endorreic basin (Nosetto *et al*., 2012). At the same time, the reduction in water lost due to evapotranspiration has led to an enhanced deep drainage, which fostered the elevation of the groundwater table (Nosetto *et al*., 2015). For example, in Laboulaye the mean groundwater table depth was at 5.23 m between 1916 and 1989, while between 1980 and 1989 it was already at 2.25 m (Fili *et al*., 2000). The same happened Southeast of La Picasa basin, in the region A1 of the Río Salado basin, where it has risen 7 m since 1970 (Aradas and Thorne, 2001). In many cases, it continued to rise and reached the surface level, leading to an augmented surface runoff (Pedraza *et al*., 2010; Aradas and Thorne, 2001), resulting in an increased flooding risk (Nosetto *et al*., 2012).

These changes caused not only groundwater flooding in many areas of the basin, but also led to a first flooding episode between 1999 and 2001, when the water level of La Picasa lagoon, which receives all the water excesses from the basin, rose up to 105.3 m above sea level (Pereira *et al*., 2014). In this context, the Federal Plan for Flood Control (Plan Federal de Control de Inundaciones) was developed, aiming to diminish the frequency of flooding events, recover productive land and protect towns and infrastructure (SsRH, 2015). One of the objectives of the plan was to drain water excesses throughout the basin and regulate water fluxes coming into the lagoon to be able to keep the water level variations within a safe range between a minimum of 98.5 m and a maximum of 102.5 m above sea level (INA, 2016). In this way, it would be possible to have a sufficient water storage capacity to retain water excesses during humid periods.

This objective was supposed to be achieved through the execution of a specific regulation and water drainage infrastructure organized in three different modules (Figure 5). The Module I comprise a main channel with its associated water flux control structures and water discharge gauges connecting the reservoirs along the basin (SsRH, 2015). The Module II comprise a series of 7 retention and regulation reservoirs that were built in lowlands along the main channel with the objective to alleviate discharge peaks and control the water fluxes, with the additional benefit of water evaporation from their surface (SsRH, 2015; Pedraza *et al*., 2010). The Module III comprise diversion channels and pumping stations, namely the North Pumping Station and South Pumping Station. The first one has a capacity of 5 $m^3 s^{-1}$, connecting La Picasa lagoon to 'El Chañar' lagoon through the channel 'Alternativa Norte' (SsRH, 2015) (Photograph 1). The second one connects La Picasa lagoon with the channel 'Las Horquetas'. It is characterized by a drainage channel from La Picasa lagoon at 98.5 m above sea level to the station, which comprises 4 pumps of 1.8 $m^3 s^{-1}$ capacity each, yet one of them is left for contingency cases (SsRH, 2015) (Photograph 2).

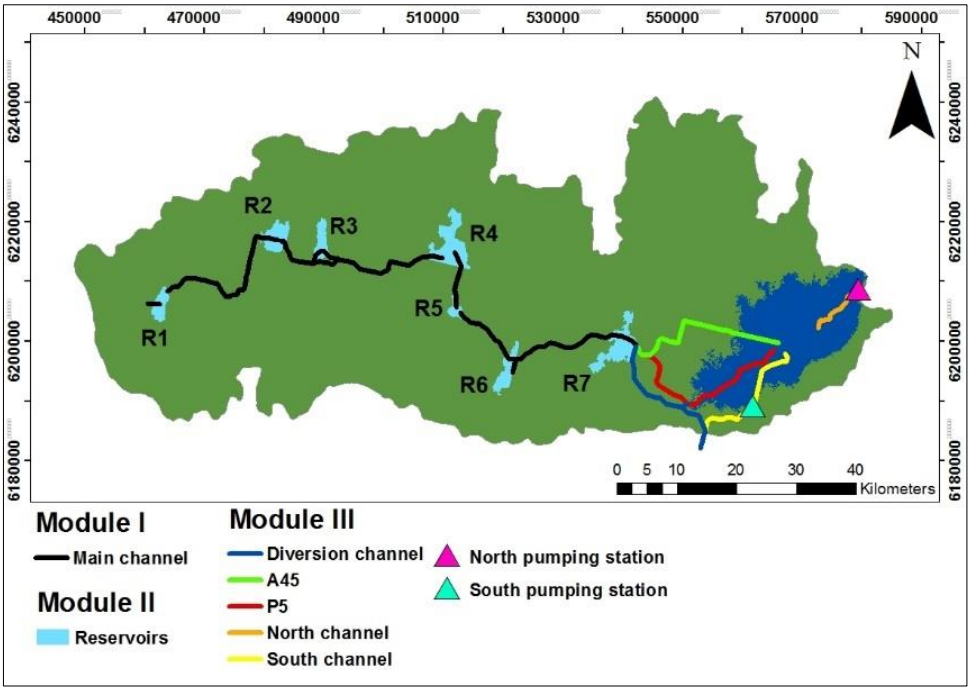

Figure 5 Water infrastructure

Source: own elaboration based on SsRH (2015)

The water infrastructure was designed in a way that during humid periods with water excesses, the water reaches the last regulation reservoir (R7) and from there it can flow either into La Picasa lagoon through two different channels (A45 and P5) or can be diverted to 'Las Horquetas' channel. At this point a specific diversion scheme was defined in order to cope with the limit imposed by Buenos Aires Province to accept a maximum water diversion of 5 $m^3 s^{-1}$ from Santa Fe Province. If the water flux reaching R7 is less than 5 $m^3 s^{-1}$, they continue to Buenos Aires through the diversion channel without entering to the lagoon and the rest of the discharge is completed with the South Pumping Station. If there is a water discharge above 5 $m^3 s^{-1}$, the exceeding discharge continues to the lagoon, either through the channel A45 or the channel P5 (INA, 2016).

Photograph 1 North Pumping Station

Source: SsRH (2015)

Besides the problems of floods, the projected infrastructure generated a conflict between Santa Fe and Buenos Aires. The reason was the construction of a channel connecting the North Pumping Station with Teodelina in Santa Fe to alleviate the emergency situation (Bertoni, 2017), after which

the water was diverted to the Río Salado basin in Buenos Aires, before having agreed on a specific alternative. As a result, Santa Fe and Buenos Aires started a long-lasting conflict, which needed the intervention of the Supreme Court of Justice to arbitrate between the provincial governments (García Montaldo, 2012).

Photograph 2 South Pumping Station

Source: SsRH (2015)

After the first flooding event and the construction of the water infrastructure, there was a period with no water fluxes in the main channel or flowing into the lagoon, especially during the years 2008, 2009, 2011 and 2013 (SsRH, 2017). After 2015, when an increase in precipitations above average in the region was registered (Giordano *et al*., 2017), extraordinary water discharges of approximately 70 $m^3 s^{-1}$ were measured flowing into the lagoon (SsRH, 2017). In relative terms, it represented 20 $m^3 s^{-1}$ more than the maximum water discharge registered in the previous flooding event (Fili *et al*., 2000). Among the reasons of the increased water discharge, it was found that the design of the water infrastructure was inadequate, i.e. the regulation function of the reservoirs was not optimal (INA, 2016). In addition, the existence of several irregular drainage channels built by farmers throughout the basin to evacuate water excesses from their properties was reported (García Montaldo, 2012).

It is also important to highlight that during this period the initial objective for which the pumping stations were built was partially achieved. This objective was expressed by Rodrigo Silvosa, Sub-secretary of Hydraulic Infrastructure of Buenos Aires, who stated that these stations were an important component as a strategy to reduce the water level of the lagoon during dry periods and increase its storage capacity (Silvosa, 2017). However, the extraordinary water excesses coming into the lagoon could not be pumped as fast as required because the pumping stations were either out of service or needed maintenance (INA, 2016; SsRH, 2015; Raparo, 2009, 2012, 2015). In fact, although the water level of the lagoon was temporary kept bellow the maximum level of the safe range, after the noticeably increase in water discharge in 2015 and 2016, the pumping capacity was finally outweighed, thus it was no longer possible to keep the water level below 102.5 m.

As a result, the combined natural and anthropogenic factors led to an extreme water level rise, reaching the historical maximum of 105.75 m in 2017 (SsRH, 2017). Hence, the region has been facing numerous negative consequences. The most important one is the higher flood risk to small towns located near the lagoon (INA, 2016). For instance, the towns that have borne the highest

direct flooding risk are Aarón Castellanos and Diego de Alvear (see Figure 1). In the first one, defenses against flooding have already been built with the help of Civil Protection and members of the Secretary of Water Resources of Santa Fe (Bertoni, 2017). Moreover, the city of Rufino, located approximately 30 km to the west of Aarón Castellanos, has been suffering indirect impacts of the increased water level of the lagoon. It was mentioned by local citizens that not only the general economy has been impacted, but there has also been a deterioration of the infrastructure and an overall social disorganization of the city and disruption of livelihoods (Rosenstein *et al.*, 2009).

The second consequence was the disruption of roads and transportation. On one hand, the most conspicuous indicator was the damage to public infrastructure, interrupting the local, national and international transportation, such as the National Route 7 and the railways (Photograph 3). Although it was already attempted to protect the National Route 7 with embankments against the effect of waves and water erosion, different degrees of deterioration were registered (INA, 2016).

Since the lagoon flooded approximately 45,000 ha of the most productive land in Argentina (Sammartino, 2017), the third consequence was the considerable impact to local farmers, who lost most of their properties and belongings, such as houses, fences, roads and agriculture fields.

Photograph 3 Disruption of infrastructure in La Picasa lagoon

Source: J. Salva (2018)

From the current situation, it is clear that La Picasa basin is another example in the Central Pampa, in which short-term solutions to reduce the flooding risk have been prioritized by the institutions involved (Collins, 2005) by building infrastructure to regulate the water excesses with a rather low effectiveness to control the water level of La Picasa lagoon. In any case, long-term solutions require to understand and integrate the underlying causes that have led to the flooding events. Therefore, to assist the Interjurisdictional Basin Committee in improving the knowledge of the hydrological system and to promote an integrated water management approach, it is critical to elaborate studies that quantify the hydrological balance not only of the basin in general, but of La Picasa lagoon in particular. It is particularly important to provide information on the main drivers that determine the temporal variations of the water level, area and volume and their relative importance in the overall water balance of the lagoon.

4. State of the art

The required knowledge of the temporal and spatial variation of the components and processes of a certain hydrological system can be pursued with the use of different types of hydrological models. In general terms, a model is a "simplified representation of a real-world system and consists of a set of simultaneous equations or a logical set of operations contained within a computer program" (Wheater, 2007). In other words, it is a mathematical representation of the dynamics of a real-world system, characterized by components that are interrelated through certain processes (Rodríguez *et al*., 2006). In this sense, there is a myriad of models with different objectives, input data, degrees of complexity and representation of reality. According to their objectives, there are models that aim to predict future system behaviors under certain conditions or to understand and describe different hydrological components and processes (Devi *et al*., 2015). As can be deduced, the best model is the one whose outcomes represent the reality as accurate as possible with the minimum requirement of input parameters and model complexity (Devi *et al*., 2015).

Based on the criteria considered, there are different classifications of hydrological models. One way of classifying them is differentiating between lumped or distributed models, based on the variation of the parameters as function of space and time (Devi *et al*., 2015). In the first case, the hydrological system (basin or lagoon) is analyzed as a single unit without considering any spatial variability, while in the second case the system is divided in discrete units and the spatial variability is considered by assigning different inputs to each unit and obtaining different outputs (Moradkhani and Sorooshian, 2009). Another classification distinguishes between deterministic models, those which do not account for random variability, meaning that for the same group of input parameters there is only one possible output, from stochastic models, those which account for random variability (Rodríguez *et al*., 2006). Finally, one important classification is the one that separates models between empirical, conceptual and physically-based models. The difference between them is that empirical models are mathematical equations that involve the use of input data based on observations without considering the characteristics of the basin (Devi *et al*., 2015). On the other hand, the second and third ones consider the hydrological processes and the features of the basin, yet the second one represents them by a series of reservoirs (lagoon) connected by a certain number of processes of inflow (i.e. precipitation) and outflow (i.e. evaporation), while the third one uses variables that are measurable and are functions of space and time (Devi *et al*., 2015).

In the Central Pampa, different models have been applied so far as a decision support tool to explain the components and processes of the hydrological systems in the frame of flooding situations. Since the region has a complex groundwater-surface water interaction, many distributed models attempted to simulate it. For instance, a distributed model MODFLOW was coupled with ISISMOD to generate flood risk maps, evaluate different drainage alternatives and predict existing flooding frequency in the Río Salado basin in Buenos Aires province (Aradas and Thorne, 2001). A second model also applied in the same basin was MIKE SHE, a distributed physically-based model suggested to account simultaneously for groundwater – surface water interaction within the same modelling framework (Badano *et al*., 2012). Similarly, the distributed physically-based model SHALL3 was applied in the Ludueña basin in Santa Fe province to represent the hydrological processes occurring in this flat area, linking the interactions between surface, vadose zone and saturated zone by means

of a vertical flow sub-model (Zimmermann and Riccardi, 2003). In turn, the AQUA model was applied to a smaller basin in the center of Buenos Aires province, using a relaxation parameter to account for flow resistance and an infiltration function to represent the downward movement of water coupled with a DEM obtained from radar interferometry to account for gradual topographic features (Dalponte *et al*., 2007). Finally, the model OCRED-2, a non-linear, continuous, distributed model based on the kinematic wave equations was applied to La Picasa basin with the use of FORTRAN programming language to simulate the overland saturation flow during the hydrological year 1999/2000 (Pedraza, 2000). Applying a rainfall-runoff method, the overland saturation flow was modelled with a variable effective area based on variations of groundwater table depth (Pedraza, 2000). This study concluded that there is not a lineal relationship in precipitation-runoff processes because of the effect of temporal variations of the groundwater table, which modify the area contributing to runoff (Pedraza, 2000). During dry periods, the area contributing to runoff is a small proportion of the basin, while during years with precipitations above average, the water excesses percolate and recharge the groundwater table, which rises accordingly. If these humid periods are maintained over time, the groundwater table might rise to the surface. Consequently, when these conditions in the basin occur, overland saturation fluxes appear. Therefore, the effect of groundwater table rises is that the area contributing to surface runoff is variable over time (Pedraza *et al*., 2010).

A second type of model applied to the flat basins of the Central Pampa are semi-distributed models, such as SWAT and HEC HMS. The first one is a continuous, processed-based model. Although water balance is the main factor explaining all the simulated processes, it has been applied for different purposes. For example, SWAT was used in the Lower Carcaraña River basin in Santa Fe province to simulate the effects of different land management practices on water, crop yields, nutrient plant uptake as well as runoff and deep percolation processes under different soil types and land management conditions (Romagnoli *et al*., 2017). Furthermore, the same model was employed to simulate a long-term time series of soil water content in data scarce areas to simulate drought episodes (Havrylenko, 2016). The other semi-distributed model HEC HMS was applied to assess the interferences of the projected channel between the North Pumping Station and the Pavón creek to the adjacent sub-basins between La Picasa and Los Patos lagoon and to verify the design parameters of the channel in the frame of the project to divert the water excesses of La Picasa lagoon to the Paraná river (Giacosa *et al*., 2005). In addition, a HEC HMS model is currently being developed in the frame of an ongoing project from INA aiming to represent the hydrological processes of La Picasa basin (A. Villanueva, personal communication, April 27th, 2018). In this model, La Picasa lagoon is represented as a reservoir receiving water discharges from the channels, expressed as reaches concentrating water excesses from surrounding sub-basins, and losses water from the pumping stations or evaporation.

A third type of model applied in the Central Pampa is the lumped parameter model, especially utilized to represent water balances, which means to represent the dynamic processes of the system with the use of mathematical equations that measure the balance between the storages and the transferences between them (Phillips *et al*., 1986). In particular, one of these hydrological systems can be a lake or lagoon, whose components are defined by storages, such as the water body “lagoon” itself, tributaries, effluent rivers, groundwater and atmosphere (Rodríguez *et al*., 2006). Also, the components are linked by different transferences, such as inflow due to

precipitation or tributaries or outflow due to evaporation, effluents or seepage (Rodríguez *et al*., 2006). These interactions can be represented by means of analytical solutions to DAE defined by the mass balance of water (Siniscalchi *et al*., 2018), which can be used for different purposes. For instance, they allow the acquisition of the value of an unknown parameter when all other parameters are known, or the simulation of scenarios when all parameters are known (Rodríguez *et al*., 2006). One of these models was applied in the Chasicó Lake, located in the Southwest of the Chaco-Pampean plain, with the aim to develop flood control strategies based on the determination of an optimal lake tributary diversion flowrate, which makes possible to keep the lake at a specific level (Siniscalchi *et al*., 2018). To achieve this objective, a simulation of scenarios was conducted based on climate and hydraulic data together with morphometric relationships of the lake (Siniscalchi *et al*., 2018). Another lumped-parameter model was applied in La Picasa basin in 2001, specifically a hydrodynamic unidimensional model called ISIS Flow, utilized to represent the behavior of the channel 'Alternativa Norte' connecting La Picasa lagoon to Los Patos Lagoon (Collins, 2005).

In spite of their usefulness to explain the water balance of lakes, the lumped-parameter model has not been applied so far as a decision support tool to define flood control strategies to the case of La Picasa lagoon. Nevertheless, after a thorough antecedent analysis, it has been found that INA-CRL (2007) had already developed a morphometric water level-area-volume relationship of this water body based on two bathymetries, which is a necessary step for the application of a water balance model.

The bathymetries of the lagoon conducted by INA were completed in two stages. The first one in 2005, following transects in direction East-West with 500 meters distance between them (INA-CRL, 2007). In 2007, the second stage was executed aiming to replace the perimeter transects to determine the contour line 102.5 m by parallel transects to the ones conducted in 2005 but this time separated every 125 m. The objective was to densify the measurements between 98 m and 100 m above sea level, thus improving the precision of the DEM of the flooded areas of the lagoon (INA-CRL, 2007). Complementing these studies, another bathymetry was conducted by MAH in cooperation with SsRH during the years 2005, 2006 and 2007 with the objective to extend the North Channel that connects La Picasa lagoon with the North Pumping Station as part of the Federal Plan for Flood Control (SsRH, 2008). Thus, the bathymetric measurements of the northeastern area of the lagoon were densified following the same itinerary as INA-CRL (2007) (SsRH, 2008).

5. Knowledge gaps

As already mentioned, although some research institutions elaborated distributed models or are currently attempting to develop semi-distributed models in La Picasa basin, none of them has applied a water balance model of La Picasa lagoon. The outcomes of this model would be important to provide sufficient technical information to define flood control strategies. In this sense, Viessman and Lewis (as cited by Rodríguez *et al*., 2006) stated that a water balance model should be the first approach in the analysis of any basin. In line with these authors, it is crucial to first develop the conceptual model of this water body to improve the understanding of the most important inflow and outflow components and processes of the hydrological cycle that determine its water balance.

Despite the usefulness of the previously developed morphometric relationships water level-area-volume of La Picasa lagoon, there is a need to update them to include modifications to the basic bathymetric studies for two reasons. First, in order to have more precise measurements in the deepest areas of the lagoon, it is necessary to densify the bathymetric results from INA below 98 m above sea level, which were not considered in their bathymetry conducted in 2007. Second, after the lagoon reached a historical maximum water level, there is a need to include new topographic measurements encompassing altitudes above 102.5 m for the whole perimeter, integrating the shallowest areas of the lagoon.

Additionally, after eighteen years of the first hydrological modelling, La Picasa basin has undergone several changes not only in natural components of the water cycle, such as precipitation regime, but also in anthropogenic factors. Among these, the most important ones have been land use changes and the execution of the water infrastructure that regulated and modified the drainage and surface runoff. Therefore, the need to update the hydrological studies in the basin was already expressed in the frame of a public audience in the Supreme Court of Justice of Argentina (Silvosa, 2017).

In this context, one of the consequences of changing conditions in the basin is the lack of information regarding the drivers of floods, yet there is a certain consensus on highlighting the anthropogenic factor as the main one. For example, according to INA (2016) the last flooding did not occur during years with water excesses, stressing that the inflow volume from channels was considerably superior than precipitation. Furthermore, Bertoni (2017) also highlighted the anthropogenic factor as the main driver of the last flooding. However, there are not studies that quantify the relative contribution from natural or anthropogenic components to the water balance of the lagoon.

Concerning precipitation, although Pedraza (2000) calculated the mean areal precipitation not only for the sub-basins but also for reservoirs, it was conducted for one hydrological year at a daily time step during the first flooding event. However, the volume accounted as inflow into the lagoon is determined by both the amount of precipitation and its area (Troin *et al*., 2010; Rodríguez *et al*., 2006). In the subsequent years leading to the second flooding event, the proportion of the volume accounted as inflow due to precipitation remained a component of the water balance that still needed to be estimated (A. Raparo, personal communication, April 19th, 2018).

Likewise, the total volume of water accounted as outflow due to evaporation is a component of the water balance that is function of the area of the lagoon (Troin *et al*., 2010; Vallet-Coulomb *et al*., 2006; Rodríguez *et al*., 2006). Despite the drawbacks that have already been investigated in the use of evaporation pans to estimate evaporation for large water bodies (Wang *et al*., 2018; Vallet-Coulomb *et al*., 2006; Morton, 1983a), the evaporation estimations for La Picasa basin and La Picasa lagoon used in the previous models have been obtained from evaporation pans. For instance, Pedraza (2000) estimated evaporation in La Picasa basin using monthly time series from evaporation pan from INTA in Pergamino. More recently, SsRH (2017) estimated the mean daily evaporation from La Picasa lagoon for each month also by means of an evaporation pan from UNRC but located in Laboulaye (see Figure 1). Finally, the evaporation time series currently being used as input of the HEC HMS modelling are mean monthly values (A. Villanueva, personal communication, April 27th, 2018), which do not consider their intrinsic variability. Therefore, based on the analysis of the available evaporation estimates for the lagoon, there is a need for a systematic quantification of evaporation rates based on more accurate and reliably methods.

One of the water balance components that still remain unclear is the linkage between groundwater and the lagoon. As it is known in this flat region, groundwater and surface water interactions are complex (Aradas and Thorne, 2001). In this respect, there are authors that have suggested that some of the water flowing into the basin might be part of groundwater discharge areas of other basins, representing an inflow component as well (Alconada Magliano *et al*., 2011). Conversely, Fili *et al*. (2000) expressed that both groundwater inflow from aquifers (approximately 0.02 $m^3 s^{-1}$) and seepage from the bottom of the lagoon have no influence in the water balance. So far, the effects of groundwater have been only considered in La Picasa basin as increasing or reducing the amount of surface runoff according to the groundwater table depths (Pedraza *et al*., 2010; Pedraza, 2000). Nevertheless, it is not clear whether this contribution has changed in the last eighteen years and what could be its relative contribution to the dynamic water balance of the lagoon.

So far, the only alternative to mitigate the impacts of floods has relied on the use of pumping stations. Though, it is not clear whether the pumping component is capable of reducing and controlling the water level of the lagoon, since in the current situation they continued to rise. Indeed, it is not known whether the water level rose because the pumping stations worked intermittently or because their pumping capacity is not sufficient in the overall water balance of the lagoon. In this sense, Juan Carlos Bertoni expressed that this alternative represents a medium-term solution and its importance lies on its continuous contribution over time, suggesting the need to couple the pumping stations with a channel connecting La Picasa lagoon with the Paraná river as a new alternative to increase the outflows (Bertoni, 2017).

Therefore, two main knowledge gaps related to the pumping component can be identified. In first place, there are no clear definitions neither from the governmental institutions nor from local stakeholders or researchers on what is the real contribution of the pumping stations to the overall water balance of La Picasa lagoon and what is their temporal variability. Secondly, in the current scenario any other alternative suggested to cope with the flooding situation in the short term would not be based on a water balance of the lagoon, thus there is a risk to repeat a wrong design and construction of the water infrastructure that might not effectively reduce its water level and the flood risk in the region.

6. Objectives

The flooding situation in La Picasa basin has been recognized as a disaster, not only by governments but also by local citizens and stakeholders (Rosenstein *et al*., 2009). The solutions attempted so far have involved either the reduction in water inflows with diversion channels or the increase in water outflows with pumping stations. In this context, given the importance of the impact in one of the most productive land in Argentina, new solution approaches are being projected aiming to transfer the water excesses to other basins. Either way, the alternatives have not been successful in controlling the water level of the lagoon or mitigating the impacts of floods to towns, infrastructure or agriculture in the short term.

At the same time, the suggested solutions have been designed upon incomplete information about the factors determining the water balance of La Picasa lagoon, their temporal variability and relative importance. Therefore, it is considered that any future solution should be based on information about which components of the water balance play a major role.

In order to contribute with answers to the recognized knowledge gaps, the goal of the master's thesis is to develop a water balance model of La Picasa lagoon as a decision support tool to elaborate effective mitigation measures aiming to tackle the current flooding situation in the basin. Therefore, the general objective is to define and quantify the most important components determining the actual volume of the lagoon, thus the water level and its variability. To reach this objective, it is necessary to update the morphometric relationships water level-area-volume of the lagoon together with a quantification of the relative contribution and variability of inflow and outflow components to employ as inputs in the water balance model. Once all the components are known, the second objective is to propose hypothetical simulation scenarios based on different pumping operation schemes aiming to analyze the possible dynamics of the water volume of the lagoon.

7. Methodology

7.1. Conceptual model

The conceptual model describes all the components of the hydrological system that define the water balance of La Picasa lagoon. It shows the sub-systems representing the different physical elements, such as the lagoon, atmosphere and water reservoirs (rectangular prisms), interconnected by water fluxes (arrows) (Figure 6).

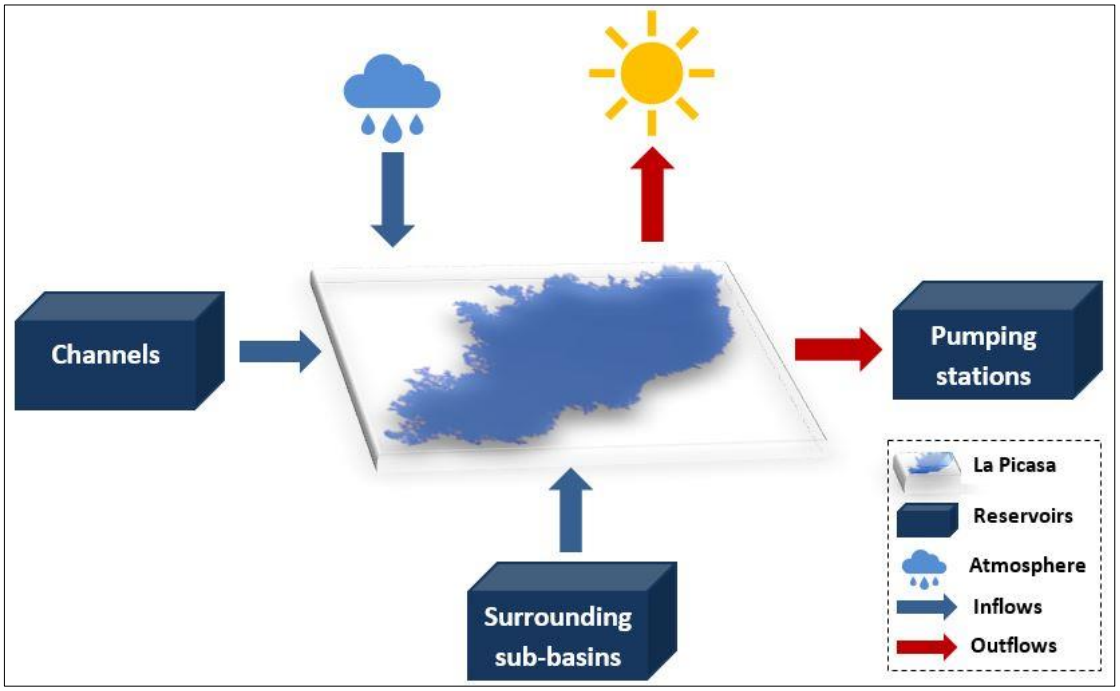

Figure 6 Conceptual model

Source: own elaboration

La Picasa lagoon, the water body under analysis, represents one of the components of the hydrological system for which a dynamic water balance model was applied to estimate the volume variations based on the inflows and outflows. These are expressed as a function of the water level, obtained from the quantitated morphometric relationships water level-area-volume.

The atmospheric component interacts with the lagoon via two vertical inflow and outflow processes, namely precipitation and evaporation. These have been suggested to be the most important hydrological processes affecting the status of the lagoon (Fili *et al*., 2000). The reason is the limited slope of the basin, which has led to extremely low groundwater and surface water hydraulic gradients, thus preventing the development of reaches and drainage networks, a typical characteristic of the basins in the Central Pampa (Badano, 2010). In other words, these basins normally show a reduced horizontal water transport, which causes that the water balance is primarily driven by precipitation and evaporation (Kuppel *et al*., 2015).

One of the water reservoirs considered in the conceptual model are the drainage channels (tributaries), specifically the Module I and Module II of the water infrastructure described in Figure 5. In spite of the low hydraulic gradients described before, it was mentioned that the water

infrastructure had an effect on the drainage, not only increasing the velocity of water transport throughout the basin (INA, 2016), but also receiving and accumulating water drainages from irregular channels (García Montaldo, 2012). The inflow represents the water flowing into the lagoon from the channels A45 and P5.

The surrounding sub-basins also represent a water reservoir in the sense that the precipitation occurring over them and being transformed into surface runoff is not considered within the Modules I and II because the sub-basins are located downstream in relation to the water infrastructure. Therefore, the surface runoff originated from them mainly flows into the lagoon from West, Southwest and Northwest. Moreover, it is also believed that water inflows from East might be considerable, especially during humid periods, but very irregular (Fili *et al*., 2000). Although surface runoff was considered as part of the inflow processes, it was mentioned that it might play a secondary role in explaining the water balance of the lagoon (Kuppel *et al*., 2015; Fili *et al*., 2000). Even less important is groundwater inflow from aquifers, which was suggested to be not considered as playing a relevant role in the water balance because it represents a negligible inflow of approximately 0.02 $m^3 s^{-1}$ (Fili *et al*., 2000).

On the other hand, since La Picasa lagoon is an endorreic water body, the outflow is mainly due to evaporation. Groundwater outflow due to seepage from the bottom of the lagoon has no influence in the water balance, thus was not considered as part of the conceptual model (Fili *et al*., 2000). In addition, the pumping stations were designed as part of the Module III of the water infrastructure in the basin to work as an artificial outlet. Therefore, they were considered as one of the water reservoirs, being interconnected to the lagoon by one of the outflow processes described as water lost from pumping.

The variation of the volume of La Picasa lagoon was calculated with a deterministic water mass balance model combining the inflow and outflow parameters together with the quantitated morphometric relationships water level-area-volume equations. The structure of the model represents the components and processes described in the conceptual model as expressed in Equation 1:

$$\frac{\Delta V(h)}{\Delta T} = A(h) * (P - EV) + QA45 + QP5 + SR - AN - AS \quad (1)$$

Source: own elaboration

Where: ΔV(h)/ΔT is the variation of the volume at a monthly time step, estimated with the morphometric relationship water level-volume; A(h) is the area of the lagoon also estimated as a function of the water level (h); P is the precipitation over the lagoon; EV is the evaporation from the open water of the lagoon; QA45 and QP5 are water discharges from the channels A45 and P5; SR represents the surface runoff from surrounding sub-basins; AN and AS represent water outflows from the North and South Pumping Stations.

The model was built based on the study of the relationships between parameters considering a period of ten hydrological years between September 2007 to August 2017 (Pedraza, 2000), taking the period between 2007 and 2016 for the calibration process and the last hydrological year for the validation process.

7.2. Bathymetry

A bathymetry was conducted together with researchers from LH-CETA, SRH and a private company in charge of the GPS in two field trips, the first one between April 17th to April 20th, 2018 and the second one between the May 8th to May 12th, 2018. It aimed to update and complete the existing bathymetric studies, densifying the measurements in the deepest area of the lagoon, that is below the altitude of 98 m above sea level (Figure 7). To achieve the objective, different itineraries were defined, either parallel lines with varying directions and width or spirals. Finally, the chosen itinerary was characterized by transects every 300 meters and a total length of 70.78 km.

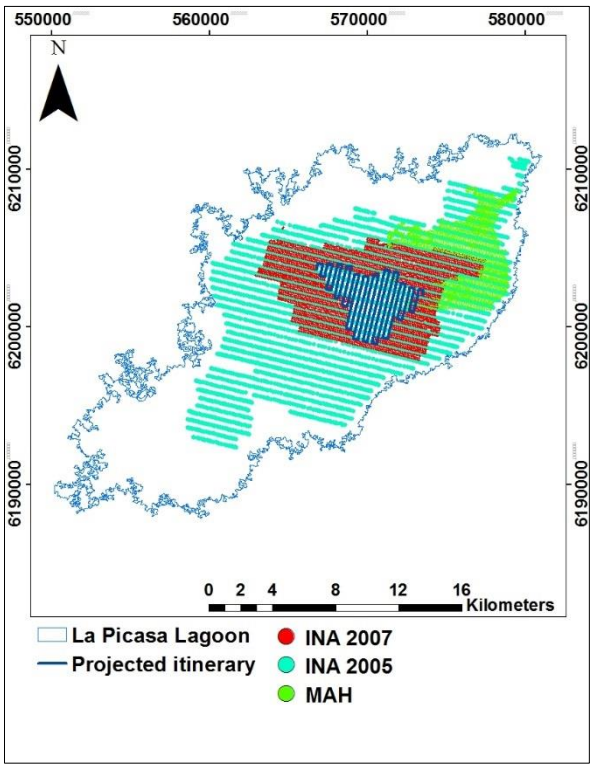

Figure 7 Previous bathymetries and projected itinerary

Source: own elaboration

Aiming to increase the redundancy of the collected data, three different equipment were used. The first one was an Echo-Sounder SDE-28S coupled to a GPS, namely a GNSS with an RTX Spectra Precision System. The precision obtained with this equipment is approximately 0.1% of the water depth (South, 2014), which considering a mean depth of La Picasa lagoon of 2 meters, represents 0.002 m. The coupling of a GPS to the Echo-Sounder was done in order to join the geographical coordinates and water depths measurements. The connectivity between the Echo-Sounder and the GPS was tested in situ and a hook between the antenna carrying the equipment and the boat was adapted so that it was rigid. The second and third equipment were two ADCP Sontek River Surveyor M9, with a precision of 0.03 m (Sontek, 2011), that were carried from the boat with ropes, as length as required to avoid interferences with the boat.

Before the measurements, a system test was performed according to the pre-measurement test suggested in the manual of the equipment (Sontek, 2011), during which cables and connections of both River Surveyor M9 were checked and different parameters were calibrated, such as battery voltage, compass, temperature sensor, among others (Photograph 4).

Photograph 4 Calibration of ADCP Sontek River Surveyor M9

Source: J. Salva (2018)

After the calibration process, the measurements were conducted with two boats, one belonging to SRH and the other one to Civil Protection from Santa Fe. The equipment was distributed in both boats, one carrying the Echo-Sounder coupled to the GPS/RTX together with one of the ADCP Sontek River Surveyor M9 and the other one carrying another ADCP Sontek River Surveyor M9. Both followed the same itinerary, with a frequency of measurements of 1 meter in each case (Photograph 5). Although the boats followed the same itinerary without interferences with the measurements and all of the equipment registered bathymetric levels, the data collected with the Echo-Sounder SDE-28S coupled to the GPS/RTX was considered for the current study because of the its higher precision.

Photograph 5 Boat with Echo-Sounder SDE-28S and ADCP Sontek River Surveyor M9

Source: J. Salva (2018)

In the first field trip, the itineraries started where the calibration process took place, this is from the western border of the lagoon located next to the National Route 7, while in the second field trip a better access was found nearby Aarón Castellanos. In both cases, the distance travelled between the starting point and the area of interest in the lagoon was not considered. As a result, the complete itinerary registered with the Echo-Sounder SDE-28S were eight transects, which after a post-processing of the data were combined into one (Figure 8).

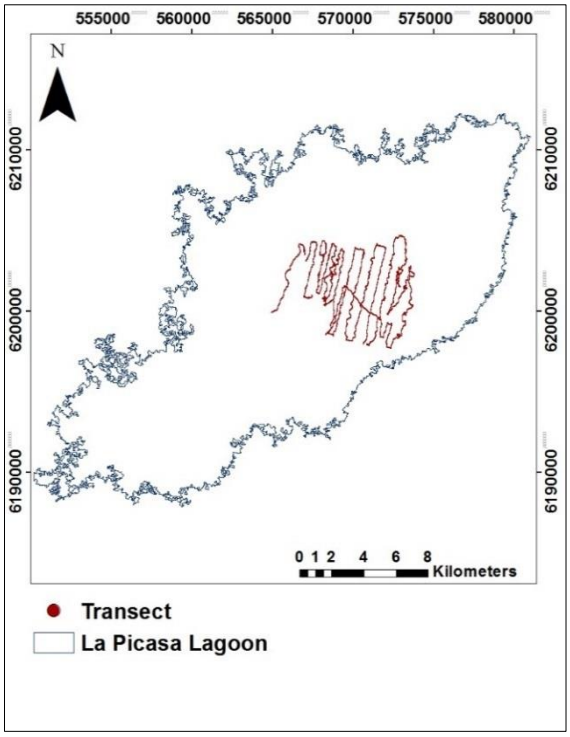

Figure 8 Bathymetric transect with the Echo-Sounder SDE-28S

Source: own elaboration

After the raw data from the Echo-Sounder was collected, a post-processing was conducted. The first step was the format transformation of the files retrieved from the equipment. Indeed, these files were acquired with a '.org' format and were subsequently transformed to '.csv' format for the eight files corresponding to the transects to make them directly readable. The data recorded of every transect were the geographical coordinates of the points from GPS/RTX, the altitude of the GPS, length of the antenna between the GPS and the Echo-Sounder and the water depth. The altitude of the Echo-Sounder was calculated as the difference between the altitude of the GPS and the length of the antenna. The geographical coordinates were projected to a coordinate system UTM 20 South with a Datum WGS84. Afterwards, all the transects were compiled into one file in order to reduce the post-processing time.

In the second step, a correction of the altitude of the Echo-Sounder was conducted by calculating the orthometric altitudes at each measured point. In general terms, altitude is a measure of the elevation of a point above a predetermined reference surface (Odumosu *et al*., 2018). In the case of GPS devices, the predetermined reference surfaces commonly used are ellipsoids, which in the present study was WGS84. In turn, the orthometric altitude was defined as the "distance of a point above a specified surface of constant potential; the distance measured along the direction of gravity between the point and the surface" (Odumosu *et al*., 2018).

In practical terms, the orthometric altitude of the Echo-Sounder was calculated as the difference between the ellipsoidal altitude and the geoid undulation (Rabah *et at*., 2017) (Figure 9). To calculate the geoid undulation at every measured point, the data was processed with the tool 'Calculadora Online Geoide-AR 16', which uses a gravimetric geoid model (Geoide-Ar 16) adjusted to POSGAR 2007 (IGN, 2016). Firstly, the data was transformed to shapefile format (.shp) and projected in POSGAR07. With the new coordinates, the correction factor accounting for the geoid undulation calculated for every measurement point resulted in 18.7443 m.

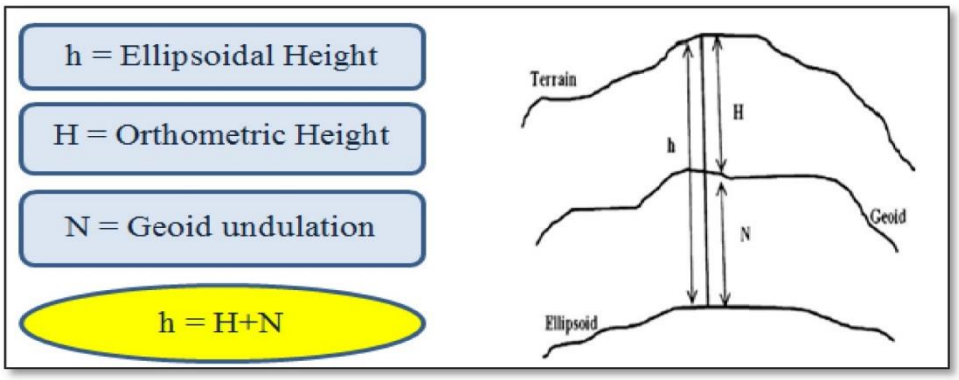

Figure 9 Relation between ellipsoid altitude, orthometric altitude and geoid undulation

Source: Rabah *et al*. (2017)

Third, atypical values were checked and removed. To that end, the altitudes were ordered from smallest to largest and those ones resulting in "zero" were removed. This might have been due to the movement of the boat because of waves, where the Echo-Sounder did not correctly register the water depths.

The resulting values could not be directly used to calculate the altitude of the bottom of the lagoon because of the effect of waves. Therefore, in the fourth step a bias correction was performed. The concept is that the altitude registered by the Echo-Sounder varies because of the waves along a range that contains the mean value. Hence, a statistical analysis was carried out, after which the mean value of the altitudes of the Echo-Sounder of every transect was calculated. This value was used instead of the median since the data presented normal distributions, with kurtosis and skewness values within normal ranges.

Fifth, the altitude of the bottom of the lagoon at each point was calculated as the difference between the altitude of the Echo-Sounder, the mean altitude for each transect (wave correction factor) and the water depths registered.

Finally, the resulting bathymetry was merged with those conducted by INA and MAH. Since it comprised measurements below and above the limit of 98 m set at the beginning, it was found that above 98 m there was a certain degree of overlapping. In those cases, it was decided to adopt the values from INA and MAH.

7.3. Morphometric relationships water level-area-volume

The estimation of the morphometric relationships water level-area-volume of La Picasa lagoon was conducted in three steps. The first step comprised the calculation of a TIN with a GIS software based on the merged bathymetry. A TIN is a "terrain surface modelled by several triangles generated from a set of points distributed over the space according to some selected criteria, each point defined by a triple (x, y, z) with x and y being the coordinates on the horizontal plane, and z being the elevation" (Freitas *et al*., 2016). Afterwards, the generated TIN was used as input to calculate the area and volume of the lagoon at predefined water levels with the tool 'Surface Volume' with the aforementioned software. This tool calculates the area and volume of the region between a surface provided by the TIN and a predefined reference plane. In this case 97.5 m was adopted as the minimum altitude above sea level, increasing the water levels every 1 m until the threshold 102.5 m. This threshold was chosen based on the coverage of the available bathymetry points.

The second step comprised the calculation of the area and volume of the lagoon between the altitudes 102.5 m and the maximum threshold of 105.5 m, which represents the areas without a complete bathymetry. The reason is that INA set a threshold at 102.5 m in 2007 and also because these areas were partially covered by the study of 2005 and by MAH due to the maximum water level of the lagoon at that moment. The threshold of 105.5 m was set according to the maximum water level reached by La Picasa lagoon in 2017. In this sense, a series of contour lines were provided by a technical report conducted by members of LH-CETA (Pagot, 2018). In this study, the contour lines were calculated based on a DEM derived from satellite images from ALOS. These images have a spatial resolution of 12.5 m and a vertical precision of 1 m approximately (Pagot, 2018). Since the DEM was not available, a raster file was first calculated using the contour lines between 102.5 m to 105.5 m as input of the 'Topo to Raster' tool in the GIS software. With this raster, the areas and volumes below each contour line were afterwards calculated with the tool 'Surface Volume'. To estimate the areas and volumes only corresponding to the regions between specified reference altitudes, the differences between them were calculated. The results were then merged to the areas and volumes calculated in the previous step.

In the last step, a linear regression analysis was conducted to develop the morphometric relationships water level-area-volume. To this end, the paired values water level-area and water level-volume were plotted in a scattered plot to graphically analyze their distribution and possible best-fitting functions. With the regression coefficients calculated in both cases the morphometric relationships were built.

7.4. Precipitation

The precipitation over La Picasa lagoon was calculated as an interpolation of the precipitation registered in meteorological stations. Although many stations were found from different sources, not all of them were close enough to the lagoon or contained complete time series for the required period. For example, the automatic stations from INTA, MAGyA and BCCBA had two years of data in the best cases. On the other hand, the manual stations from INTA which had longer time series were located beyond a reasonable distance to obtain accurate results for the interpolation. Based on the criteria to select the closest stations to the lagoon and at the same time with complete monthly time series between the hydrological years 2007 and 2017, the following meteorological stations were considered for the calculations: Rufino (Sociedad Rural de Rufino), Aarón Castellanos (Escuela Agrotécnica), North Pumping Station (Estación de Bombeo Alternativa Norte) and Diego de Alvear (Estancia La Catalina). The data was acquired from SsRH (2017). The location of the stations relative to the lagoon is shown in Figure 10.

The interpolation of monthly precipitation time series was conducted with a GIS software in three steps. First, a spatial interpolation of a weighting factor of the meteorological stations was defined with the IDW method. This method estimates the value of the weighting factor in a specific point or cell (W(x)) calculated by means of a linear combination of weighting factors corresponding to where the stations are located (Wj), weighted by an inverse function of the distance from the point of interest to the stations (Equation 2). The assumption is that the influence of the weighting factor set for each ground station on the specific cell decreases proportionally to the inverse distance between them.

$$W_x = \sum_{j=1}^{n} \frac{{}^{1}/_{L_i^{\alpha}}}{\sum_{i=1}^{n} {}^{1}/_{L_i^{\alpha}}} * W_j \qquad (2)$$

Source: Keblouti *et al*. (2012)

As a result, four raster files encompassing the lagoon with spatial interpolated weighting factors were calculated, each one of them defined by setting a weighting factor of 1 for the respective ground station (for example Aarón Castellanos in Figure 10) and setting the others to 0.

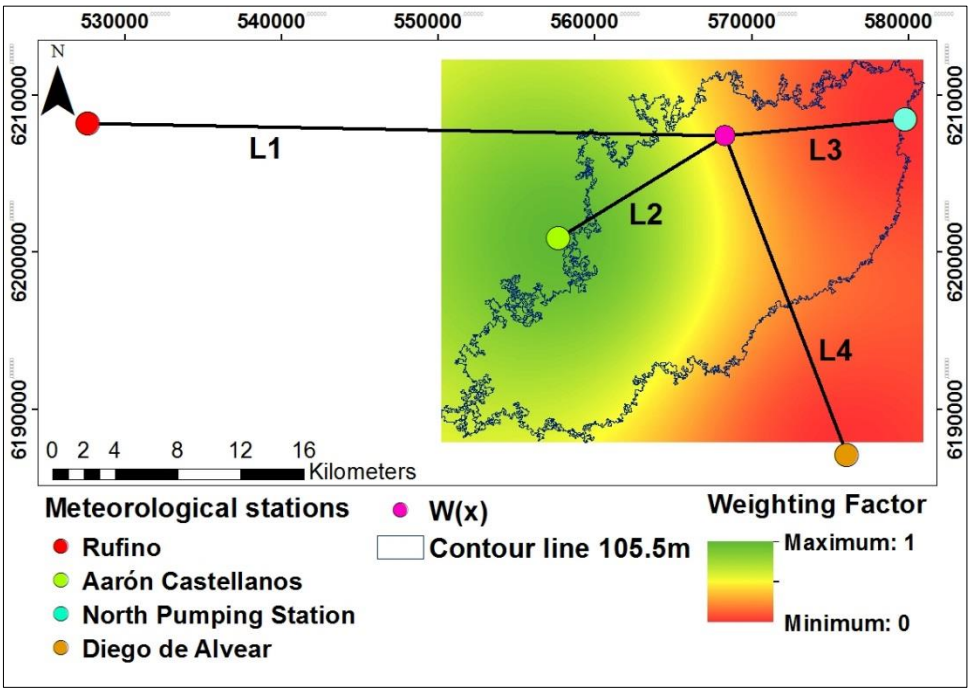

Figure 10 Interpolation of a weighting factor among precipitation ground stations

Source: own elaboration

In the second step, for each of the four raster files corresponding to the ground stations the mean areal weighting factor within the limits of the lagoon corresponding to the contour line 105.5 m was calculated with the tool "Zonal Statistics" in the GIS software (W_1, W_2, W_3 and W_4 in Equation 3). Finally, the monthly precipitation over La Picasa lagoon was calculated as the sum of the monthly precipitation of each ground station multiplied by their respective mean weighting factors (Equation 3):

$$P_{[mm\ month^{-1}]} = P_1 W_1 + P_2 W_2 + P_3 W_3 + P_4 W_4 \qquad (3)$$

Source: own elaboration

Where P_1 is the precipitation in Rufino, P_2 in Aarón Castellanos, P_3 in North Pumping Station and P_4 in Diego de Alvear.

Since the volume of water considered as inflow is also function of the area of the lagoon, the amount of water due to precipitation in volumetric terms was calculated as the monthly precipitation multiplied by the mean area of the lagoon in the respective month using the previously developed morphometric relationship water level - area.

7.5. Evaporation

Several methods have been reported to be useful to estimate water evaporation from lakes, although their performance varies according to the different conditions where they are applied while their use depends on the available data. The empirical methods, such as pan evaporation, are not recommended to estimate evaporation from large lakes. Although they can be adjusted using correction coefficients, they show many uncertainties caused by pan types, lake characteristics and the different meteorological settings (Wang *et al*., 2018; Vallet-Coulomb *et al*., 2006; Morton, 1983a). Bulk transfer methods, like Dalton Method, provide good approximations, although they require a previous parameter optimization (Wang *et al*., 2018). Water budget methods may not be accurate due to errors occurred during measurements of the water budget components, for instance other water losses like seepage from the bottom of the lake or lateral outflows (Wang *et al*., 2018). On the other hand, if water heat storage can be calculated, the Energy Budget Based methods are an adequate option (Vallet-Coulomb *et al*., 2001). For example, the Bowen Ratio Energy Budget, Penman, Priestley-Taylor, Brutsaert-Stricker and DeBruin-Keijman were evaluated using eddy covariance observation-based reference datasets and their results proved to be consistent (Wang *et al*., 2018). In the case that input data is limited, the CRLE Model has also shown to be an accurate method to estimate evaporation from lakes (Troin *et al*., 2010; Dos Reis and Dias, 1998; Morton, 1983a, b).

Since no systematic measurements of water surface temperatures were available, the Bowen Ratio Energy Budget Method, commonly chosen as a standard reference method (Wang *et al*., 2018), could not be applied. Instead, two other energy budget methods were applied to estimate the monthly water loss from La Picasa lagoon due to evaporation between the hydrological years 2007/2017, namely the Penman Method (Penman, 1948) and the CRLE Model (Morton, 1983a, b).

The Penman Method has been already widely applied to estimate daily evaporation from open waters under different conditions with standard meteorological data without considering surface temperatures (Shuttleword, as cited in Valiantzas, 2006; Penman, 1948). However, one of its disadvantages is the requirement of many weather variables that are sometimes missing in meteorological stations (Valiantzas, 2006).

On the other hand, the CRLE model bares the advantage that requires fewer input data at the monthly time step (Troin *et al*., 2010). In fact, it has been already applied in another closed lake in Argentina and in Brazil to estimate monthly evaporation, obtaining relatively accurate results in comparison to Penman and Priestley-Taylor methods (Troin *et al*., 2010; Dos Reis and Dias, 1998). After obtaining and analyzing their results, one of the methods was chosen as input of the water balance.

The input parameters for both methods were obtained from a meteorological station from INTA Pergamino, approximately 150 km away from the lagoon (Figure 11). This station contained the most complete time series with all the parameters required for calculations. In few cases, where daily gaps were found, they were completed using data collected from another meteorological station from INTA San Pedro.

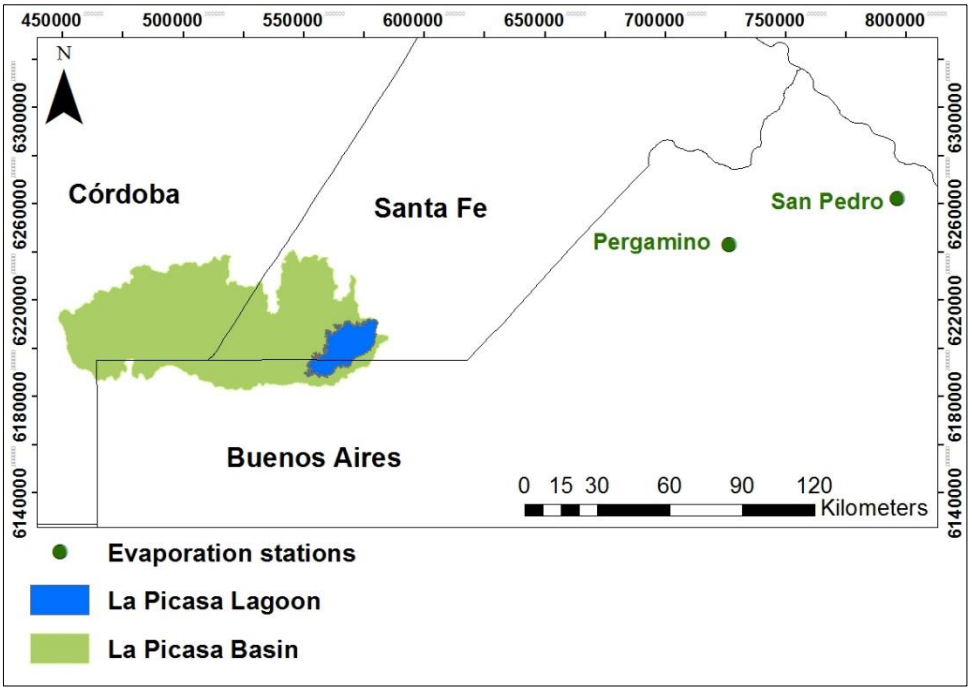

Figure 11 Evaporation ground stations

Source: own elaboration

The first method considered was the Penman Method, which estimates daily evaporation as a result of a combination of an equilibrium evaporation, a lower limit evaporation from moist surfaces, and considering the departure from this equilibrium in the atmosphere (Wang *et al.*, 2018; Penman, 1948). More specifically, evaporation from a saturated surface (lagoon) is calculated based on a combination of an aerodynamic approach which considers the effect of the turbulent vapor transport on evaporation rates by a process of eddy diffusion and at the same time an energy-based approach in which evaporation is considered as an energy transformation of the incoming radiation (Penman, 1948). Therefore, this combination is used to calculate daily evaporation rates expressed in Equation 3 as follows:

$$E_{[mm\ day^{-1}]} = \frac{\Delta}{\Delta + \gamma} * \frac{R_n}{\lambda} + \frac{\gamma}{\Delta + \gamma} * \frac{6.43\ f_u\ D_{(av)}}{\lambda} \qquad (3)$$

Source: Valiantzas (2006)

Where E is potential – open water – evaporation [mm day^{-1}], R_n is net radiation at the surface [MJ m^{-2} day^{-1}], Δ is the slope of the saturation vapor pressure curve [kPa °C^{-1}], γ is the psychrometric coefficient [kPa °C^{-1}], λ is the latent heat of vaporization [MJ kg^{-1}] and f_u is a wind function. Since this method requires a considerable number of meteorological parameters and other physical factors, the calculation was conducted based on a description of the steps suggested by Valiantzas (2006). The parameters highlighted in blue represent those that are already known or are obtained directly from ground stations (Table 1). Finally, the total monthly evaporation was calculated by summing the daily evaporation rates of each corresponding month.

Table 1 Steps and equations to calculate evaporation with Penman Method

Steps	Description	Equations/Parameters	Components
1	Slope of the saturation vapor pressure curve	$\Delta = \frac{4098 e_s}{(T + 237.3)^2}$	Δ: slope of the saturation vapor pressure curve [kPa °C^{-1}] T: mean air temperature for the examined time interval [°C] e_s: saturation vapor pressure [kPa]
2	Daily mean air temperature	$T = 0.5(T_{max} + T_{min})$	T_{max}: maximum air temperature [°C] T_{min}: minimum air temperature [°C]
3	Saturation vapor pressure	$e_{s(T)} = 0.611 e^{(\frac{17.27T}{T+237.3})}$	
4	Latent heat of vaporization	$\lambda = 2.501 - (2.361 * 10^{-3}) + T$	λ: latent heat of vaporization [MJ kg^{-1}]
5	Psychrometric coefficient	$\gamma = 0.0016286 * \frac{P}{\lambda}$	γ: psychrometric coefficient [kPa °C^{-1}] P: atmospheric pressure [kPa]
6	Atmospheric pressure	$P = 101.3 * (\frac{293 - 0.0065 * Z}{293})^{5.26}$	Z: altitude of the ground station above sea level [m]
7	Net radiation at the surface	$R_n = R_{nS} - R_{nL}$	R_{nS}: incoming net short wave radiation [MJ m^{-2}day^{-1}] R_{nL}: outgoing net long wave radiation [MJ m^{-2}day^{-1}]
8	Outgoing net long wave radiation	$R_{nL} = f\varepsilon' \sigma * (T + 273.2)^4$	f: adjustment factor for cloud cover ε': net emissivity between the atmosphere and the ground σ: Stephan – Boltzman constant [MJ m^{-2} K^{-4} day^{-1}]
9	Adjustment factor for cloud cover	$f = (1.35 \frac{R_S}{R_{SO}} - 0.35)$	R_S: measured incoming solar radiation [MJ m^{-2}day^{-1}] R_{SO}: clear sky radiation [MJ m^{-2}day^{-1}]
10	Measured incoming solar radiation	$R_S = R_A * (0.5 + 0.25 \frac{n}{N})$	R_A: extraterrestrial radiation [MJ m^{-2}day^{-1}] n: measured bright sunshine hours per day [h] N: maximum possible duration of daylight [h]
11	Extraterrestrial radiation	$R_A = 37.59 d_r[\omega_s \sin(\phi)\sin(\delta) + \sin(\omega_s)\cos(\phi)\cos(\delta)]$	d_r: relative distance between the Earth and the Sun ω_s: sunset hour angle [radians] ϕ: latitude of the ground station [radians] δ: solar declination [radians]
12	Relative distance between the Earth and Sun	$d_r = 1 + 0.033 \cos(\frac{2\pi}{365} * J)$	J: Julian day number π: Pi number
13	Sunset hour angle	$\omega_S = \arccos(-\tan(\phi)\tan(\delta))$	
14	Solar declination	$\delta = 0.409 \sin(\frac{2\pi}{365} J - 1.39)$	
15	Maximum possible duration of daylight	$N = \frac{24}{\pi} * \omega_s$	
16	Clear sky radiation	$R_{SO} = (0.75 + 2 * 10^{-5} * Z) * R_A$	
17	Net emissivity between the atmosphere and the ground	$\varepsilon' = (0.34 - 0.14\sqrt{e_a})$	e_a: actual vapor pressure [kPa]
18	Actual vapor pressure	$e_a = \frac{RH}{100} e_s(T)$	RH: relative humidity (%)
19	Incoming net short wave radiation	$R_{nS} = (1 - \alpha) * R_s$	α: reflection coefficient or albedo for open water surfaces
20	Wind function	$f_u = a_u + b_u U$	$a_u = 0$ (for large areas of open water); $b_u = 0.536$ U: wind speed at 2 m height [m s^{-1}]
21	Mean vapor pressure deficit	$D_{(av)} = e_{s(av)} * (1 - \frac{RH}{100})$	$D_{(av)}$: mean vapor pressure deficit [kPa] $e_{s(av)}$: mean daily saturation vapor pressure [kPa]
22	Mean daily saturation vapor pressure	$e_{s(av)} = 0.5\,[e_s(T_{max}) + (e_s(T_{min})]$	$e_{s(T_{max})}$: saturation vapor pressure T_{max} [kPa] $e_{s(T_{min})}$: saturation vapor pressure T_{min} [kPa]
23	Potential - open water - evaporation	$E = \frac{\Delta}{\Delta + \gamma} * \frac{R_n}{\lambda} + \frac{\gamma}{\Delta + \gamma} * \frac{6.43 f_u D_{(av)}}{\lambda}$	**E: potential – open water – evaporation [mm day^{-1}]**

Source: adapted from Valiantzas (2006)

The second method applied to estimate evaporation was the CRLE model. This method estimates the evaporation rate of a shallow-lake considering the equilibrium air temperature and the rate of change of stored enthalpy as substitutes of the water surface temperature. The principle of this model is based on Bouchet's theory (Bouchet, 1963), which states that there is a complementary relationship between potential evapotranspiration (E_{TP}) and actual evapotranspiration (E_T), in which for a specific amount of available energy the decrease in actual evapotranspiration due to water restrictions results in a symmetrical increase in potential evapotranspiration and the sum of both equals twice the evapotranspiration of a wet-environment (E_{TW}), which can be considered as a shallow-lake evaporation as expressed by the Equation 4:

$$E_T + E_{TP} = 2E_{TW} \qquad (4)$$

Source: Vallet-Coulomb *et al*. (2001); Morton (1983b)

According to Morton (1983a), shallow-lakes are those which do not undergo significant variations in seasonal subsurface heat storage. On the contrary, the estimation of evaporation from a deep-lake requires a storage routing technique, which is basically affecting the shallow-lake evaporation by a time delay, depending on the lake depth and total dissolved solids, and the results are afterwards routed through a linear "heat" reservoir based on a storage constant (Dos Reis and Dias, 1998).

The shallow-lake evaporation was obtained in two consecutive main steps. First, an equilibrium temperature, the temperature at which the energy balance equation equals the vapor transfer equation for a saturated surface, was estimated after solving those equations simultaneously (Morton, 1983b). Afterwards, the equilibrium temperature was used as input in an equation similar to Priestley-Taylor's to calculate the shallow-lake evaporation (Equation 5):

$$E_{W\ [mm\ month^{-1}]} = b_1 + b_2\left(1 + \frac{\gamma p}{\Delta_p}\right)^{-1} R_{TP} \qquad (5)$$

Source: Dos Reis and Dias (1998); Morton (1983b)

Where E_W is the shallow-lake evaporation [mm month^{-1}], b_1 [13 W m^{-2}] and b_2 [1.12 W m^{-2}] are constants, Δ_p is the slope of the saturation vapor pressure curve at the equilibrium temperature [mbar °C^{-1}], γp [0.66 mbar °C^{-1}], and R_{TP} is the net radiation at the equilibrium temperature [W m^{-2}].

The model requires the ground station parameters, such as latitude, altitude and an estimate of the mean annual precipitation (Morton, 1983a). On the other hand, it is necessary to provide few meteorological parameters, for instance mean monthly air temperatures, mean monthly dew-point temperatures and the ratio of observed to maximum possible sunshine duration (Morton, 1983a).

The required meteorological parameters, the steps followed to estimate the monthly evaporation and the equations used in each step are summarized in Table 2. The parameters highlighted in blue were either directly obtained from ground stations, such as maximum and minimum temperature, or constants and coefficients previously known and used as inputs of the corresponding equations.

Table 2 Steps and equations to calculate shallow-lake evaporation with CRLE Model

Steps	Description	Equations/Parameters	Components
1	**Groundstation inputs**	ϕ, H,PA, T, TD, S, i, n	ϕ: latitude [degrees] H: altitude above sea level [m] P_A: mean annual precipitation [mm] T: mean air temperature [°C] T_D: mean dew – point temperature [°C] S: ratio of observed to maximum possible sunshine duration i: month number from 1 (January) to 12 (December) n: number of days in the month
2	**Pressure correction for the standard atmosphere**	$\frac{p}{p_s} = [\frac{288 - 0.0065 * H}{288}]^{5.256}$	p: atmospheric pressure at the station p_s: atmospheric pressure at the sea level
3	**Saturation vapor pressure and slope of the saturation vapor pressure curve**	$v_D = 6.11e^{[\frac{17.27T_D}{T_D+237.3}]}$ $v = 6.11e^{[\frac{\alpha T}{T+\beta}]}$ $\Delta = \frac{dv}{dT} = \frac{\alpha\beta v}{(T+\beta)^2}$	v_D: saturation vapor pressure at T_D [mbar] v: saturaton vapor pressure at T [mbar] α = 17.27; β = 237.3°C Δ: slope of the saturation vapour pressure curve at T [mbar °C^{-1}]
4	**Extra-atmospheric global radiation**	$\theta = 23.2\sin(29.5i - 94)$ $\cos Z = \cos(\phi - \theta)$ $\cos\omega = 1 - \cos\frac{\cos Z}{(cos\phi * cos\theta)}$ $\cos z = \cos Z + \left[\left(\frac{180}{\pi}\right)sin\frac{\omega}{\omega} - 1\right]cos\phi * cos\theta$ $n = 1 + \left(\frac{1}{60}\right)\sin(29.5i - 106)$ $G_E = \frac{1{,}354}{n^2}\frac{\omega}{180}\cos z$	θ: declination of the Sun [degrees] Z: noon angular zenith distance to the Sun ω: Earth rotation degrees between sunrise and noon z: average angular zenith distance to the Sun n: radius vector of the Sun G_E: extra – atmospheric global radiation [W m^{-2}]
5	**Zenith value of clear-sky albedo and clear-sky albedo**	$a_z = a_{zz} + (1 + c_0^2)(0.34 - a_{zz})$ $a_0 = \frac{a_z[e^{1.08} - (\frac{2.16\cos Z}{\pi} + \sin Z)e^{0.012*Z}]}{1.473(1 - \sin Z)}$	a_{zz}: zenith value of snow – free clear – sky albedo = 0.05 $c_0 = v - v_D$
6	**Precipitable water vapour and turbidity coefficient**	$W = \frac{V_D}{0.49 + \frac{T}{129}}$ $c_1 = 21 - T$ $j = (0.5 + 2.5\,cos^2 z)e^{[c_1(\frac{p}{p_s} - 1)]}$	W: precipitable water vapour[mm] c_1: factor j: turbidity coefficient
7	**Transmittancy of clear skies to direct beam solar radiation**	$\tau = e^{\left[-0.089(\frac{p}{p_s})^{0.75} - 0.083\left(\frac{j}{\cos z}\right)^{0.90} - 0.029\left(\frac{W}{\cos z}\right)^{0.60}\right]}$	τ: transmittancy of clear skies to direct beam solar radiation
8	**Part of τ that is result of absorption**	$\tau_a = e^{[-0.0415(\frac{j}{\cos z})^{0.90} - 0.0029^{0.5}\left(\frac{W}{\cos z}\right)^{0.30}]}$	τ_a: part of τ resulting from absorption
9	**Clear-sky and incident global radiation**	$G_0 = G_E\tau[1 + (1 - \frac{\tau}{\tau_a})(1 + a_0\tau)]$ $G = SG_0 + (0.08 + 0.30S)(1 - S)G_E$	G_0: clear sky global radiation [W m^{-2}] G: incident global radiation [W m^{-2}]
10	**Average albedo**	$a = a_0[S + (1 - S)(1 - \frac{Z}{330})]$	
11	**Proportional increase in atmospheric radiation due to clouds**	$c_2 = 10(\frac{v_D}{v} - S - 0.42)$ $\rho = 0.18[(1 - c_2)(1 - S)^2 + c_2(1 - S)^{0.5}]\frac{p_s}{p}$	c_2: weighting factor ρ: proportional increase in atmospheric radiation due to clouds
12	**Net long-wave radiation loss at air temperature**	$B = \varepsilon\sigma(T + 273)^4[1 - (0.71 + 0.007v_D\frac{p}{p_s})(1 + \rho)]$	B: net long – wave radiation loss at air temperature [W m^{-2}] ε: emissivity σ: Stefan – Boltzmann constant
13	**Net radiation at air temperature, stability factor, vapour pressure coefficient, heat transfer coefficient**	$R_W = (1 - a)G - B$ $\frac{1}{\xi} = 0.28\left(1 + \frac{v_D}{v}\right) + \frac{\Delta R_{TC}}{\gamma p\left(\frac{p_z}{p}\right)^{0.5} b_0 f_z(v - v_D)}$ $f_T = \frac{p_s}{p}^{0.5}\frac{f_z}{\xi}$ $\lambda = \gamma p + 4\varepsilon\sigma\frac{(T + 273)^3}{f_T}$	R_W: net radiation for water surface at air temperature [W m^{-2}] $R_{TC} = R_w$; ξ: stability factor; $b_0 = 1$ γp = 0.66 (T ≥ 0); 0.57 (T < 0)[mbar °C^{-1}] f_z = 25 (T ≥ 0); 28.75 (T < 0)[W m^{-2}mbar^{-1}] f_T = vapour transfer coefficient λ = heat transfer coefficient
14	**Calculate equilibrium temperature by means of a converging iterative solution to solve vapour transfer and energy-balance equations until |[δTp]|<0,01**	$T_p = T'_p + [\delta T_p]$ $v_p = 6.11e^{[\frac{\alpha T_P}{T_P + \beta}]}$ $\Delta_p = \frac{\alpha\beta v_P}{(T_P + \beta)^2}$ $[\delta T_p] = \frac{[\frac{R_W}{f_T} + v_D - v'_p + \lambda(T - T'_P)]}{(\Delta'_P + \lambda)}$	T_P = equilibrium temperature T'_P: trial value = T (iteration 1); $[\delta T_P]$ = correction T'_P: trial value = T (iteration 1) v_P = saturation vapor pressure at T_P v'_P = trial value = v (iteration 1) Δ_P = slope of the aturation vapor pressure curve at T_P Δ'_P = trial value = Δ (iteration 1)
15	**Estimate potential evapotranspiration, net radiation for soil-plant surfaces at Tp and shallow-lake evaporation**	$E_P = R_W - \lambda f_T(T_p - T)$ $R_{TP} = E_P + \lambda p f_T(T_p - T)$ $E_W = b_1 + b_2(1 + \frac{\gamma p}{\Delta_p})^{-1}R_{TP}$	E_P = potential evaporation R_{TP} = net radiation for soil – plant surfaces at Tp[W m^{-2}] **E_W = shallow – lake evaporation [mm month^{-1}]**

Source: adapted from Morton (1983b)

After having estimated the shallow-lake evaporation, the effective depth "d" (meters) (Equation 6), routing constant "k" (months) (Equation 7) and time delay "t" (months) (Equation 8) were calculated to decide whether La Picasa lagoon should be considered as a shallow or deep lake based on the need to consider the effects of seasonal changes in subsurface heat storage:

$$d = \frac{d_A}{1 + 0.00003s} \quad (6)$$

$$k = d[0.04 + \frac{0.11}{1 + \frac{1}{16}d^2}] \quad (7)$$

$$t = 0.50k \quad (8)$$

Source: Morton (1983a)

Where "d_A" is the mean depth (m) and "s" is total dissolved solids (ppm). The total dissolved solids were obtained from literature and accounted for approximately 4,622 ppm (Iriondo and Kröhling, 2007), the mean depth was calculated as the mean ratio between the volume (m^3) and the respective surface area (m^2) for every month. As a result, the mean effective depth of La Picasa lagoon was 1.78 m for the simulation period and the required time delay to account for subsurface heat storage resulted in 0.12 months (between 3 and 4 days). Consequently, since the time delay was less than the time step of the evaporation analysis, the shallow-lake evaporation values were considered for the water balance. To calculate the amount of water evaporation in volumetric terms, the results of evaporation of the CRLE model were multiplied by the mean monthly area of the lagoon.

7.6. Water discharge

Water discharge was considered as the monthly water inflow to the lagoon from the channels A45 and P5 (see Figure 5). Daily time series of water discharge measurements in different discharge gauges located along the main channel (Module I) and the reservoirs (Module II) were acquired during a field trip to the study area (A. Raparo, personal communication, April 19th, 2018). When data for the corresponding channels was not available, the total water discharge was calculated as the sum of water discharge at the outlet of the reservoir OR7 and the contribution of surface runoff calculated for the sub-basins whose outlets are the channels A45 and P5.

The data provided consisted either in water discharges [$m^3\ s^{-1}$], which were used directly in the calculations, or height readings [m] in the scales at each gauge. However, in these cases the geometry of the gauge was not available, for which the flow rating curves H-Q had to be calculated. To fulfil this step, dates with both heights and water discharges were chosen to construct a scatter plot with the paired H-Q data. In general, the most common equation suggested to explain H-Q relationships is Equation 9, where Q_0, n and h_0 are calibration parameters (Manfreda, 2018). Before conducting a simple linear regression analysis, the variables of the function were linearized by calculating the natural logarithms as shown in Equation 10. Using this equation as the linear function to conduct the simple regression analysis, the calibration parameters Q_0 and n were obtained from the regression coefficients and h_0 was obtained from trial and error.

$$Q = Q_o(h + h_0)^n \quad (9)$$

$$lnQ = \ln Q_o + n \ln(h + h_0) \quad (10)$$

Source: Manfreda (2018)

In a second step, the calculated water discharges were used to build the daily time series. However, the measurements were scarce and obtained on an irregular basis, thus presenting a considerable number of gaps. Therefore, a linear interpolation between daily measurements was conducted to fill these gaps and then the daily values were summed up to calculate the monthly time series (Helsel and Hirsch, 2002).

7.7. Pumping

The estimation of the monthly volume of water accounted as outflow due to pumping was the result of the aggregation of measurements on both pumping stations. The time series were built with data mainly obtained from SsRH (2017, 2015) and subsequently conducting a cross-checking with two other sources. One of them was the time series used as input in the HEC HMS model of La Picasa basin (A. Villanueva, personal communication, April 27th, 2018). The other one was a series of technical reports about the operational status and maintenance of the pumping stations, the number of hours that the pumps worked and further required maintenance activities (Raparo, 2015, 2012, 2009).

The North Pumping Station is composed by three pumps (Raparo, 2015), with a maximum pumping capacity of 5 $m^3 s^{-1}$ (SsRH, 2015). Although this station was already projected and executed in 2000 as an emergency response to the first flooding event (Bertoni, 2017), it started operating in 2006. The following year, that is during the first year in the simulation period, the pumping station evacuated 1.5 $m^3 s^{-1}$. From 2008 to 2012, the pumping station was out of service (SsRH, 2015). From the beginning of September 2012 until July 2013, it worked with two pumps and a capacity of 2.5 $m^3 s^{-1}$ and afterwards with one pump and a capacity of 1 $m^3 s^{-1}$ until December 2013 (SsRH, 2015). During 2014, this only pump continued to work but intermittently also draining 1 $m^3 s^{-1}$. The following three years, the pumping station was out of service in 2015 (SsRH, 2015), afterwards it started operating again in 2016 but this time sporadically with a mean discharge of 0.25 $m^3 s^{-1}$. For example, 0.5 $m^3 s^{-1}$ were registered the 20th of July 2016 in the water gauge located 20 km downstream the North Pumping Station (Photograph 6). Finally, in 2017 the station stopped operating again.

Photograph 6 Water gauge downstream North Pumping Station

Source: A. Raparo (2016)

The South Pumping Station was designed to pump the water from the lagoon at 98.5 m above sea level with the objective to regulate its water level (SsRH, 2015). It has four pumps with a pumping capacity of 1.8 m^3 s^{-1} each, yet its total pumping capacity is 5.4 m^3 s^{-1} because one of them was considered to operate only in contingency cases (SsRH, 2015). It was not part of the water infrastructure of the basin during the first half of the simulation period. Although its execution already started in 2009, it took two years to be completed in 2011 (SsRH, 2015). Among the reasons of the delay to finish the station was the need to conduct an expropriation of the land where the pumping station was supposed to be built (Sogno, 2009). From 2012 onwards, the pumping station could not work properly because a channel connecting the lagoon to the pumping station needed to be constructed. Since this channel has considerable dimensions, 9 meters depth and 50 m width where it connects to the pumping station, the construction had to be conducted in stages, draining the groundwater table from the area (SsRH, 2015). As shown in Photograph 7, this channel was still under construction the 5th of September 2013.

Photograph 7 Connection of South Pumping Station with La Picasa lagoon, Sep. 5th, 2013

Source: SsRH (2015)

Since in 2015 precipitations above average were expected together with the emergency situation of an increasing water level of the lagoon, a smaller channel started to be constructed in order to rapidly connect the lagoon to this station. Finally, the South Pumping Station could be connected to the lagoon in December 2016 and started its operations (SsRH, 2017).

7.8. Surface runoff

Aiming to estimate the total amount of water flowing into the lagoon originated from surface runoff, a previous analysis of the characteristics of the basin was conducted. In this respect, La Picasa basin was divided in a series of sub-basins in the framework of the preliminary results of the aforementioned HEC HMS model (A. Villanueva, personal communication, April 27th, 2018).

Based on this subdivision, the surface runoff occurring upstream Reservoir 7 was already accounted as water discharge measured in the gauge station OR7 of the corresponding reservoir (Figure 12). Downstream OR7, there are two channels flowing into the lagoon with their respective gauge stations (A45 and P5). The precipitation occurring downstream OR7 over the sub-basins whose outlets are the channels A45 and P5 were already accounted as part of the inflow to channels (Sub-basin A45 and P5 in Figure 12). In fact, since there were months when the only water discharge measurement available was in OR7, the results of the surface runoff of these two sub-basins were

summed up to their water discharge. Consequently, the total surface runoff accounted as inflow in the water balance was the sum of the direct contribution of all the sub-basins surrounding the lagoon. As shown in Figure 12, there is a sub-basin (Ext) which was not considered by SsRH (2017) as being part of La Picasa basin, yet it was considered in the HEC HMS model.

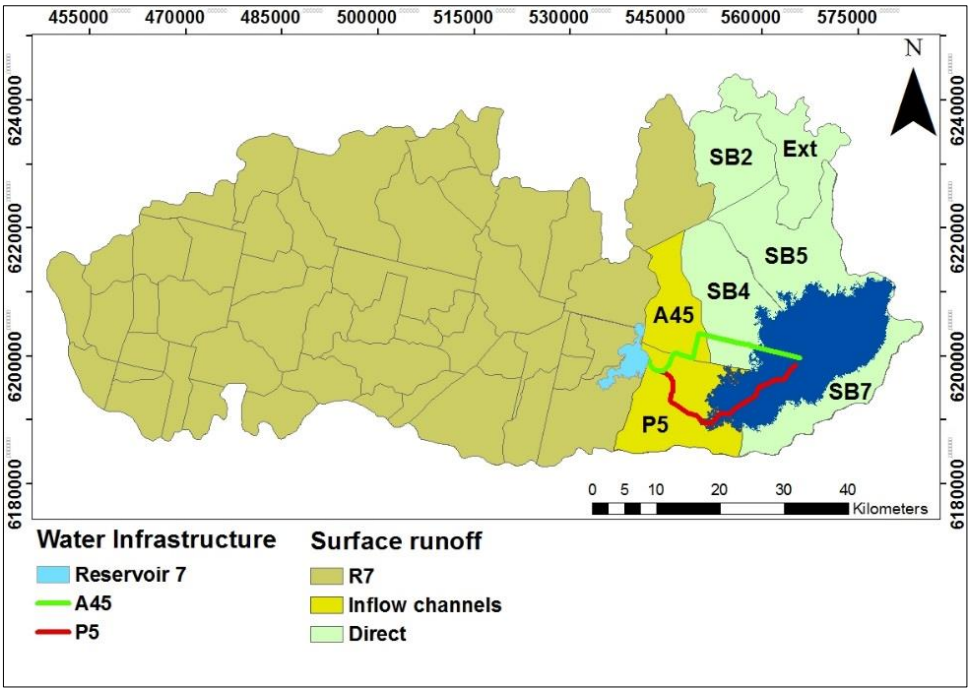

Figure 12 Surface runoff

Source: own elaboration based on A. Villanueva (personal communication, April 27th, 2018)

The estimation of direct surface runoff was conducted in a series of sequential steps based on a conceptual model of the water balance of the sub-basins surrounding the lagoon (Ponce and Shetty, 1995). These authors stated that precipitation (P) is either transformed into surface runoff (S) or into the so-called catchment wetting (W). Afterwards, this component of the water balance is transformed into baseflow (U) or lost by vaporization (V), with is the combined contribution of direct evaporation (E) and transpiration (T) (Figure 13).

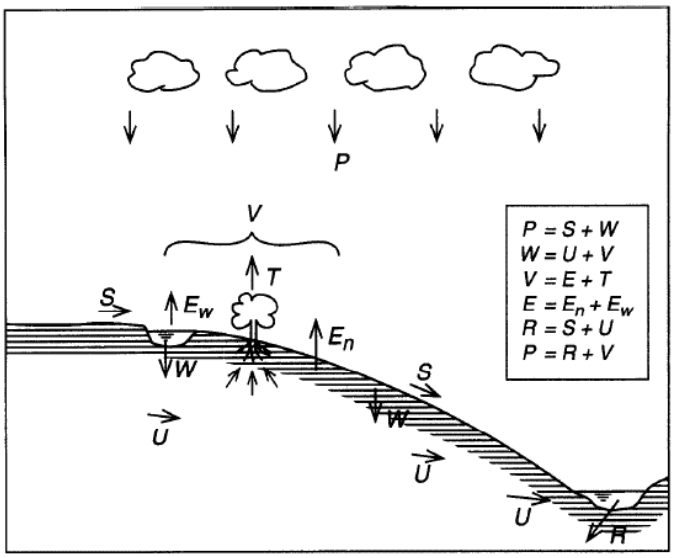

Figure 13 Components of the water balance in the sub-basins

Source: Ponce and Shetty (1995)

Although deep percolation was neglected by these authors, arguing that it only accounts for less than 1.5% on a global scale (Ponce and Shetty, 1995), in the current water balance it was considered as an important component recharging the groundwater table. On the other hand, although the authors further divide evaporation in sub-components, the total amount of water lost due to vaporization (E+T) was completely accounted in the calculations of evapotranspiration. Re-arranging the equations shown in Figure 13, the water balance can be expressed with the following equation:

$$P = S + U + V \qquad (11)$$

Source: Ponce and Shetty (1995)

Since Equation 11 represents an annual water balance of a basin, the soil moisture storage from year to year was neglected. However, since the time step selected in this water balance is monthly, this component was also considered within the calculations. In this sense, there are two different storages in the sub-basins and the areas of reservoirs that are currently not under water, a sub-surface storage (root zone) and groundwater storage (Pedraza *et al*., 2010).

Following the processes of the water balance presented by Ponce and Shetty (1995), first monthly precipitation time series between the hydrological years 2007/2017 were calculated for each sub-basin. This was conducted by means of precipitation interpolations using the same meteorological stations showed in the section “7.4 Precipitation”. Although the same methodology was applied, the limits taken to calculate the mean weighting factors were each sub-basin respectively.

Second, surface runoff for each sub-basin was estimated based on the SCS-CN method (SCS-USDA, 1986). This method computes surface runoff (Q) based on precipitation (P), initial abstraction (Ia), which are losses before surface runoff begins, and potential maximum retention (S), which are losses after surface runoff begins. Particularly, the initial abstraction set as conditional threshold was established to account for water retained in surface depressions, water intercepted by vegetation, evaporation or infiltration (SCS-USDA, 1986). If the precipitation does not surpass the threshold Ia, then the runoff does not occur (Equation 12). It was found by empirical approximations that Ia = 0.2S (Shadeed and Almasri, 2010).

$$Q = \begin{cases} \dfrac{(P - I_a)^2}{P - I_a + S} & P > I_a \\ 0 & P \leq I_a \end{cases} \qquad (12)$$

Source: SCS-USDA (1986)

The potential maximum retention (S) is function of the CN basin parameter, which ranges from 0 to 100, where a high CN means high runoff and low infiltration and vice versa (Equation 13).

$$S = \frac{25400}{CN} - 254 \qquad (13)$$

Source: Shadeed and Almasri (2010)

The CN was calculated based on two factors. One of them is the HSG, a classification of soils into four categories (A, B, C, D) based on their minimum infiltration rate obtained for bare soils after prolonged wetting, where Soils A have high infiltration rates and low surface runoff potential and vice versa (SCS-USDA, 1986). Nevertheless, since soils are found under different conditions depending on the study area, the HSG categories are determined indirectly based on the proportion of different soil textures, ranging from sandy (A) to clay (D) (SCS-USDA, 1986). The other factor is land cover, specifically type and hydrologic condition, which indicates its effects on the surface runoff potential (SCS-USDA, 1986). For each land cover type, standard tables have been developed with four associated CN curves depending over which HSG they are found. Thus, the aggregated CN of each sub-basin was calculated with Equation 14 as the combination of sub-areas with different CN values, which represent different combinations of soil types and land covers:

$$CN = \frac{CN_1 A_1 + CN_2 A_2 + \cdots + CN_i A_i + CN_n A_n}{\sum_{i=1}^{n} A_i} \qquad (14)$$

Source: Shadeed and Almasri (2010)

To calculate Equation 14, a GIS-based method suggested by Shadeed and Almasri (2010) was followed. First, global soil types were acquired from the HWSD (FAO/IIASA/ISRIC/ISS-CAS/JRC, 2012). After extracting the soil types from the global scale to the basin scale, the HSG were calculated based on the proportion of each texture. Afterwards, land covers were obtained from (EU, 2003). Also, from the global dataset an area encompassing La Picasa basin was extracted. Based on these land covers, the respective CN values were added from a standard table (SCS-USDA, 1986). Afterwards, having obtained the CN values for each sub-basin with Equation 14 and calculating their potential maximum retention with Equation 13, monthly time series of surface runoff were calculated applying Equation 12. The restrictive conditions were employed, that is when precipitation was less or equal to the estimated initial abstraction the surface runoff was equaled to zero, if not it was considered for the monthly time series. To calculate the volume of water as inflow from each sub-basin, the estimated precipitation being transformed to surface runoff was multiplied by each corresponding area. The total volume was obtained as the sum of the volume of surface runoff of each sub-basin surrounding La Picasa lagoon.

Since during humid periods an enhanced lateral movement of water in the basin takes place (Pedraza, 2000), the further steps in the calculations of the water balance of the sub-basins were conducted aiming to verify possible water inflows due to interflow. Therefore, following the model suggested by Ponce and Shetty (1995) the third step after having accounted for the amount of water transformed into surface runoff, was the calculation of the catchment wetting as the difference between the precipitation and surface runoff.

Fourth, from the amount of water considered as catchment wetting a modification to the model suggested by Ponce and Shetty (1995) was included to account for the second storage identified by Pedraza *et al*. (2010), that is the deep percolation recharging the groundwater table. An assessment of the soil water content using SWAT in the headwaters of the Arrecifes basin, whose westernmost part is located at approximately 67 km from La Picasa basin, showed that the deep aquifer percolation fraction, which is the fraction of percolation from the root zone which recharges the deep aquifer, was around 0.47 (Havrylenko *et al*., 2016).

Afterwards, from the remaining unsaturated soil water the Reference Potential Evapotranspiration (ET_O) was calculated with the FAO Penman-Monteith Method (Allen *et al*., 1998), as expressed in Equation 15:

$$ET_0 = \frac{0.408\Delta(R_n - G) + \gamma\frac{900}{T+273}u_2(e_s - e_a)}{\Delta + \gamma(1 + 0.34u_2)} \qquad (15)$$

Source: Allen *et al*. (1998)

Where ET_O is the reference potential evapotranspiration [mm day^{-1}], R_n is the net radiation at the crop surface [MJ m^{-2} day^{-1}], G is the soil heat flux density [MJ m^{-2} day^{-1}], γ is the psychrometric constant [kPa $°C^{-1}$], T is the mean daily air temperature at 2 m height [°C], u_2 is the wind speed at 2 m height [m s^{-1}], e_s is the saturation vapor pressure [kPa], e_a is the actual vapor pressure [kPa], (e_s - e_a) is the saturation vapor pressure deficit [kPa] and Δ is the slope of the saturation vapor pressure curve [kPa $°C^{-1}$]. To achieve this step, the same meteorological data from INTA Pergamino as used for the calculation of evaporation was employed.

After that, the crop potential evapotranspiration ET_C [mm day^{-1}] was calculated by multiplying the values of ET_0 with the crop coefficient Kc, which accounts for the characteristics that distinguish the crop from reference grass, namely crop height, albedo, canopy resistance and evaporation from soil (Allen *et al*., 1998). In this case, a Kc = 0.80 was selected to represent the mean value between the typical crops produced in the region, similar to the Kc employed as input of the HEC HMS model (A. Villanueva, personal communication, April 27th, 2018). The following step was the aggregation of the ET_C to the monthly time step.

Afterwards, the monthly crop potential evapotranspiration values were subtracted from the catchment wetting. A conditional procedure was established because when the difference in precipitation and crop potential evapotranspiration resulted in negative values during a specific month, the amount of water remaining in the soil was neglected.

Finally, the remaining soil water content was accounted as interflow with the assumption that the water available in a specific month reached the outlet of the respective sub-basin the following month. The assumption was based on lateral flow travel times of 51 days (Havrylenko *et al.*, 2016), which is the time that a water particle in the soil layer spends travelling in the subsurface through the basin until it reaches the outlet (Rinaldo *et al*., 2011). As shown in Figure 12, the outlets of the sub-basins EXT and 2 reach the sub-basin 5. Therefore, their contributions were accounted as part of the interflow from sub-basin 5 to the lagoon with the respective lateral flow travel time.

7.9. Sensitivity analysis

After quantifying the monthly contributions of the hydrological components to inflow and outflow of the water balance of La Picasa lagoon, a sensitivity analysis was conducted aiming to determine the model structure and comprehend the relationships between the model and the most dominant physical processes occurring in the lagoon and associated components of the water balance (Atkinson *et al*., 2002).

This type of analysis basically assists in defining the rate of change of the simulated values as a response to variations in the input parameters (Moriasi *et al*., 2007). In other words, it is commonly used to recognize which parameters are more important to determine the model and their precision during the calibration process (Ma *et al*., as cited in Moriasi *et al*., 2007).

Sensitivity analyses have been already applied to the case of identifying main factors defining lake variations. For example, Troin *et al*. (2010) performed this analysis as a way to compare the potential contribution of each hydrological component to the water level variations of Mar Chiquita lagoon in Córdoba, Argentina. Similarly, Vallet-Coulomb *et al*. (2006) conducted a sensitivity analysis to study the responses of lake Ihotry (Madagascar) to potential climate and hydrological changes.

There are different possibilities to test the sensitivity of the input parameters. In this regard, Troin *et al*. (2010) examined the impact of each input parameter by increasing or decreasing their values in 10% and computing the resulting change in proportion of lake level variations. In the current study, the sensitivity analysis was conducted following the methodology suggested by Schulze (as cited in Aduah *et al*., 2017). In this regard, after the parameters were modified iteratively by increasing and decreasing their values by 10%, their effects on the model output were accounted with Equation 16:

$$\Delta O\% = \frac{(O - O_{base})}{(O_{base})} * 100\% \qquad (16)$$

Source: Aduah *et al*. (2017)

Where $\Delta O\%$ is the percentage of change in volume of the lagoon, O_{base} is the volume of the lagoon corresponding to the initial parameter and "O" is the output volume of the lagoon after changing the value of the parameter.

The sensitivity of each parameter was assessed based on the ranking shown in Table 3, where ΔI is the change in input parameter:

Table 3 Sensitivity criteria

Sensitivity Class	Description
Extremely sensitive	$\Delta O\% > 200\%\Delta I$
Highly sensitive	$200\%\Delta I > \Delta O\% > 100\%\Delta I$
Moderately sensitive	$100\%\Delta I > \Delta O\% > 50\%\Delta I$
Slightly sensitive	$50\%\Delta I > \Delta O\% > 10\%\Delta I$
Insensitive	$\Delta O\% < 10\%\Delta I$

Source: Aduah *et al*. (2017)

7.10. Calibration

Calibration is a process aiming to include slightly changes to the model to adjust as much as possible its predictions of the measured values (Rodríguez *et al*.,2006). It can also be defined as the process by which the model parameters are modified, within logical limits, until the simulated values yield reasonable results compared with the observed ones (Aduah *et al*., 2017).

The calibration process assisted in the confirmation if the conceptual model previously developed accurately represented the hydrological system of La Picasa lagoon and if the chosen parameters were able to explain its water balance (Troin *et al*., 2010). It was mainly conducted on the model parameters whose results were obtained from estimations, such as precipitation, evaporation and surface runoff. The reason is that these parameters could be adjusted to account for possible prediction errors, thus improving the overall model performance. Although the parameters that resulted from measurements, such as water discharge and pumping, might also present measurements errors, their prediction errors might be smaller compared to the estimated ones (Vallet-Coulomb *et al*., 2001). For example, it was suggested that part of the uncertainties or prediction errors occurring during the use of Penman Method or CRLE Model to estimate evaporation are due to assumptions, empirical equations or coefficients, whose errors are difficult to estimate (Vallet-Coulomb *et al*., 2001).

From the simulation period considered for the water balance model, nine hydrological years between September 2007 to August 2016 were selected for the calibration process. To assess the accuracy of simulated values compared to measured values during the calibration process, three quantitative statistics were selected based on recommendations from Moriasi *et al*. (2007). The first one was the Nash-Sutcliffe Modelling Efficiency Index (NSE):

$$NSE = 1 - \left[\frac{\sum_{i=1}^{n}(Y_I^{obs} - Y_i^{sim})^2}{\sum_{i=1}^{n}(Y_I^{obs} - Y_i^{mean})^2}\right] \quad (17)$$

Source: Nash and Sutcliffe (1970)

where Y_i^{obs} is the i_{th} observation of the volume of the lagoon, Y_i^{sim} is the i_{th} simulated volume of the lagoon, Y_i^{mean} is the mean observed volume of the lagoon and n is the total number of observations. This index ranges from -∞ to 1 inclusive, where 1 is the optimal value. Values between 0 and 1 represent acceptable levels of performance and values less than 0 are considered with unacceptable performance (Moriasi *et al*., 2007). This is a common performance test used in hydrological modelling and has already been used to test the performance from a water balance of lakes (Troin *et al*., 2010) or basins (Aduah *et al*., 2017).

The second one was the Percent Bias (PBIAS):

$$PBIAS = \frac{\sum_{i=1}^{n}\left(Y_i^{obs} - Y_i^{sim}\right) * 100}{\sum_{i=1}^{n} Y_i^{obs}} \quad (18)$$

Source: Gupta *et al*. (1999)

Where PBIAS expresses the deviation of the simulated values in percentage; Y_i^{obs} is the i_{th} observation of the volume of the lagoon and Y_i^{sim} is the i_{th} simulated volume of the lagoon. This error index calculates the mean tendency of the simulated values to be larger or smaller than the observed ones (Gupta *et al*., 1999). The optimal value is 0, while positive values indicate underestimation bias and negative values vice versa (Gupta *et al*., 1999).

The third one was the RMSE-Observations Standard Deviation Ratio (RSR):

$$RSR = \frac{RMSE}{STDEV_{obs}} = \frac{\sqrt{\sum_{i=1}^{n}(Y_i^{obs} - Y_i^{sim})^2}}{\sqrt{\sum_{i=1}^{n}(Y_i^{obs} - Y_i^{mean})^2}} \quad (19)$$

Source: Singh *et al*. (2005)

Where RSR standardizes the root mean square error with the standard deviation of the measured values. Y_i^{obs} is the i_{th} observation of the volume of the lagoon and Y_i^{sim} is the i_{th} simulated volume of the lagoon and Y_i^{mean} is the mean observed volume of the lagoon (Singh *et al*., 2005). The optimal value is 0, which indicates zero residual variation, thus perfect model simulation. However, a general rule suggests that a lower the RSR represents a better performance (Moriasi *et al*., 2007).

7.11. Validation

Validation is understood as the comparison between measured values and simulated values of the model, calculated with input data that are different from those used to build the model (Rodríguez *et al*., 2006). In particular, to validate a model is making use of the input parameters defined in the calibration process and analyzing if the model is capable of providing "sufficiently accurate" simulations (Moriasi *et al*., 2007). If the simulated values yield an acceptable coincidence with the measured values, the model is considered validated (Rodríguez *et al*., 2006).

As previously mentioned, the suggested water balance model was validated with data from the last hydrological year of the simulation period between September 2016 and August 2017, for which a complete data set with all relevant variables was available. The performance was evaluated with the same criteria as used in the calibration method.

8. Results

8.1. Precipitation

The interpolations conducted during the simulation period resulted in a mean monthly precipitation of 77.5 mm over La Picasa lagoon. In addition, the distribution of monthly precipitations resembled the typical intra-annual variability of the Central Pampa, showing a dry season and a humid season (Iriondo *et al.*, 2009).

The dry season, with a mean precipitation of 42 mm, started in May and prolonged until September. In this month, the start of a new hydrological year, as proposed by Pedraza (2000), was characterized by a considerable higher amount of precipitation in comparison with the preceding months. For example, the mean precipitation in September was 48 mm higher than August, clearly marking a change in the intra-annual patter of precipitations.

Complementary, the humid season presented a mean precipitation of 111 mm. It started in October and lasted until April. The months with the highest precipitation rates were January and February, with 130 mm and 127 mm respectively. Between September 2007 and August 2017, the estimated absolute maximum monthly precipitation was 282.4 mm in February 2012. Conversely, four months did not account for precipitation, three of them during the years 2008 and 2009 (Figure 14).

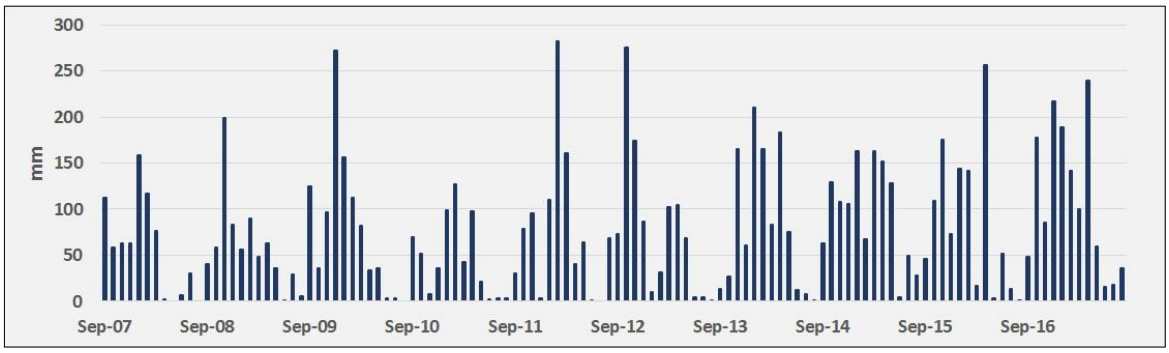

Figure 14 Monthly precipitation over La Picasa lagoon (mm)

Source: own elaboration

Although the monthly precipitations clearly illustrate an intra-annual pattern, they do not depict a trend throughout the simulation period. In this regard, after aggregating them to an annual time step, two aspects became more evident. First, the mean annual precipitation resulted in 931 mm, barely higher than the historical mean annual of the basin (Pedraza, 2000) (Figure 15). That means at first sight that the simulation period was not characterized by water excesses. However, the second aspect is that the annual precipitation displayed increasing values on the second half of the period (Figure 15). For instance, even though that the three months with the largest precipitations values occurred before 2013/2014, after aggregating them to an annual time step, the data showed that from the beginning of the simulation period to 2011/2012 the mean annual precipitations were about 133 mm below the historical mean annual. Contrarily, the last four hydrological years presented more humid conditions, surpassing the historical mean annual in approximately 200 mm (21%). It was especially marked in 2017, when the total precipitation was 1,328 mm, 43% higher than the historical mean annual.

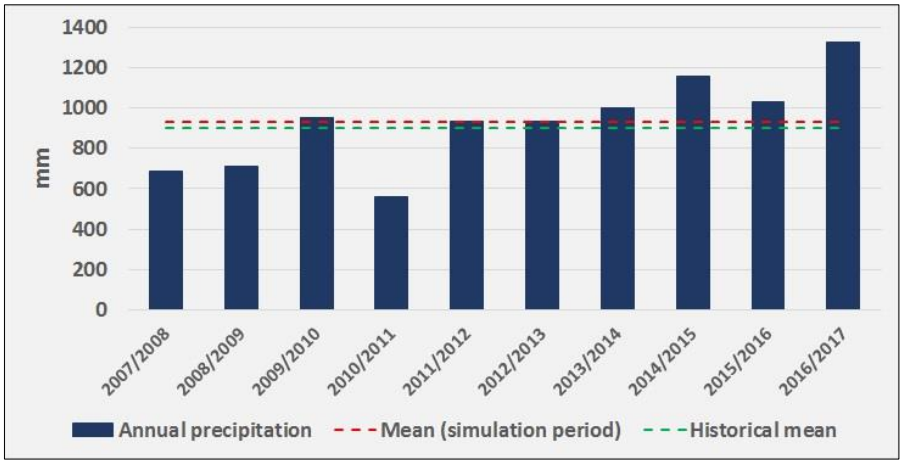

Figure 15 Annual precipitation over La Picasa lagoon (mm)

Source: own elaboration

The mean monthly volume of water inflow due to precipitation resulted in 13.1 hm^3. As expected, the intra-annual variability did not present the same pattern as shown in Figure 14, since the variable area of the lagoon played an important role in enhancing or diminishing the total monthly water inflow. Despite it was possible to differentiate dry and humid seasons, the mean maximum water inflow was calculated in September (18.4 hm^3) and the mean minimum in March (5.5 hm^3). In absolute terms, 7 out of the 10 maximum monthly water inflows during the simulation period occurred in the last two hydrological years 2015/2016 and 2016/2017, with an absolute peak reaching 89.1 hm^3 in April 2017 (Figure 16).

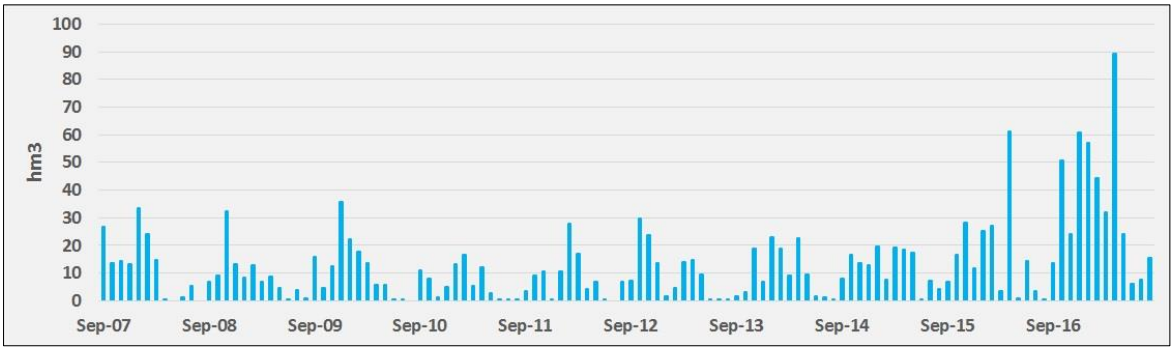

Figure 16 Monthly water inflow to La Picasa lagoon from precipitation (hm^3)

Source: own elaboration

After these values were aggregated to the annual time step, the mean annual water inflow from precipitation resulted in 157 hm^3 (Figure 17). In addition, the inter-annual variability was characterized by a slightly decreasing trend from the beginning of the simulation period until 2011/2012, after which it almost steadily increased until the end of the simulation period. This behavior was not only explained by changes in the annual precipitation (Figure 15) but also by changes in the area of the lagoon.

An enhancing effect of the area of La Picasa lagoon on this hydrological component was more visible in the last part of the simulation period. In this regard, from September 2007 to August 2015, the inflow was approximately 33% less than the mean annual. On the other hand, from September 2015 onwards, the inflow surpassed this threshold in 50% (312 hm^3), being the year 2017 the one with the highest contribution to water inflow, exceeding the mean annual in 171% (425 hm^3).

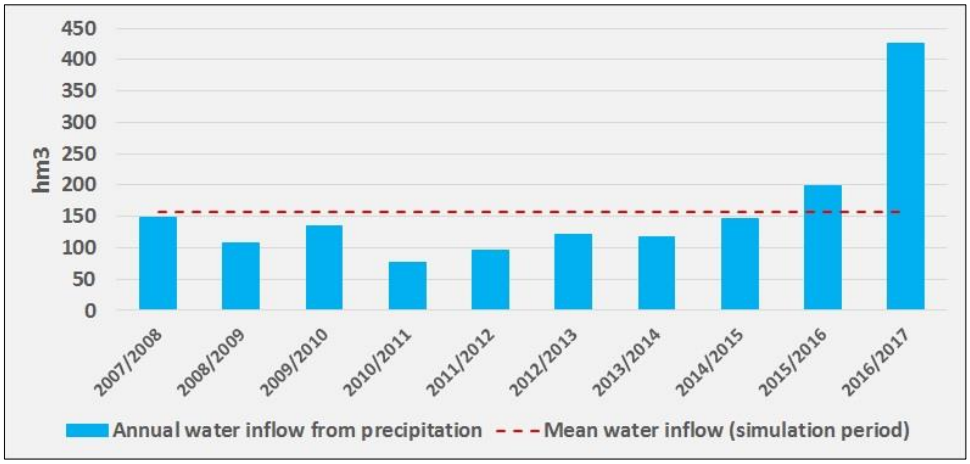

Figure 17 Annual water inflow to La Picasa lagoon from precipitation (hm^3)

Source: own elaboration

8.2. Evaporation

After applying the Penman Method and the CRLE model to estimate the open water evaporation from La Picasa lagoon, the mean monthly evaporation resulted in 191 mm and 131 mm respectively. However, the intra-annual variability of these methods presented considerable differences. On one hand, the seasonality of the CRLE model was more evident, expressed by range of 162 mm. More specifically, larger evaporation rates were estimated from October to March, with the maximum mean monthly in January (221 mm), while smaller evaporation rates from April to September, with the minimum mean monthly in June (59 mm) (Figure 18). Contrarily, the Penman Method showed a less marked intra-annual variability, with a range of 57 mm. Surprisingly, larger evaporation rates occurred from March to September, with the maximum mean monthly in April (216 mm), a similar value to CRLE model but three months afterwards, while smaller evaporation rates were estimated from October to February, with the minimum mean monthly in February (159 mm), considerably higher than the CRLE model (Figure 18).

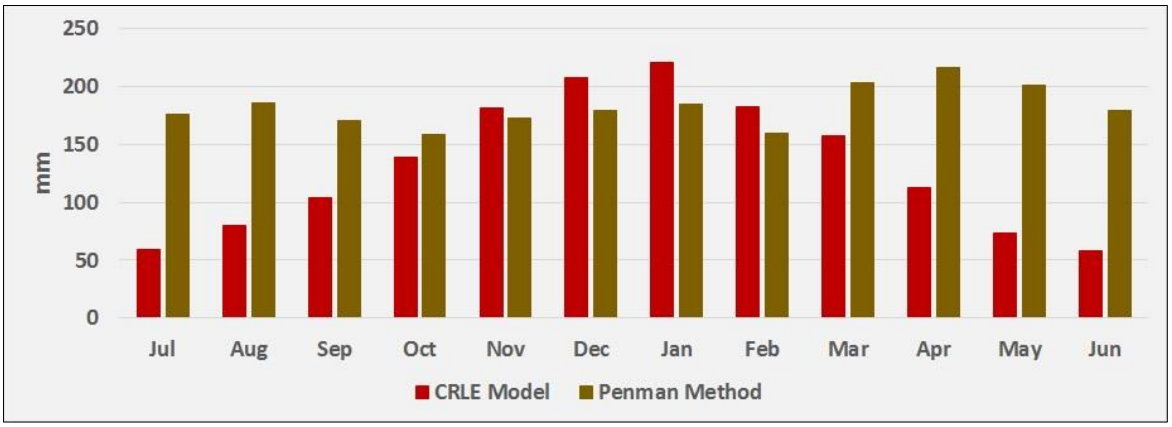

Figure 18 Mean monthly evaporation estimated with Penman Method and CRLE model

Source: own elaboration

Considering the estimations obtained with the CRLE model and aggregating them to the annual time step, the mean annual evaporation resulted in 1,574 mm. It is also important to highlight that this value did not remain constant throughout the simulation period because it showed a marked inter-annual variability with an overall descending trend. In this regard, the range between the

maximum and minimum annual evaporation totalized 330 mm. In addition, the first half of this period showed values above average in approximately 80 mm, with a maximum in the hydrological year 2008/2009 (1,758 mm), while the second half showed evaporations below average in 79 mm, with a minimum in the hydrological year 2013/2014 (1,428 mm).

Similar to the estimation of water inflow from to precipitation, the area of La Picasa lagoon was also a key factor enhancing or diminishing the volume of water lost from evaporation. On a monthly time step, the mean water outflow from the lagoon was 22 hm^3. However, unlike precipitation, it showed a smaller variability throughout the simulation period with a total range of 60 hm^3, determined by a maximum monthly water outflow of 66.6 hm^3 and a minimum monthly of 6.5 hm^3.

In turn, when the values were aggregated to the annual time step, the effect of the area of the lagoon became more explicit, copying the behavior of the variations in the water level (SsRH, 2017). In this sense, Figure 19 stresses a descending trend in annual evaporation rates from 346 hm^3 in the beginning of the simulation period until the absolute minimum annual evaporation of 174 hm^3 in 2013/2014. Afterwards, the water lost due to evaporation increased substantially, reaching the absolute maximum of 491 hm^3 in 2016/2017, which represented 85% more than the mean annual evaporation of the simulation period.

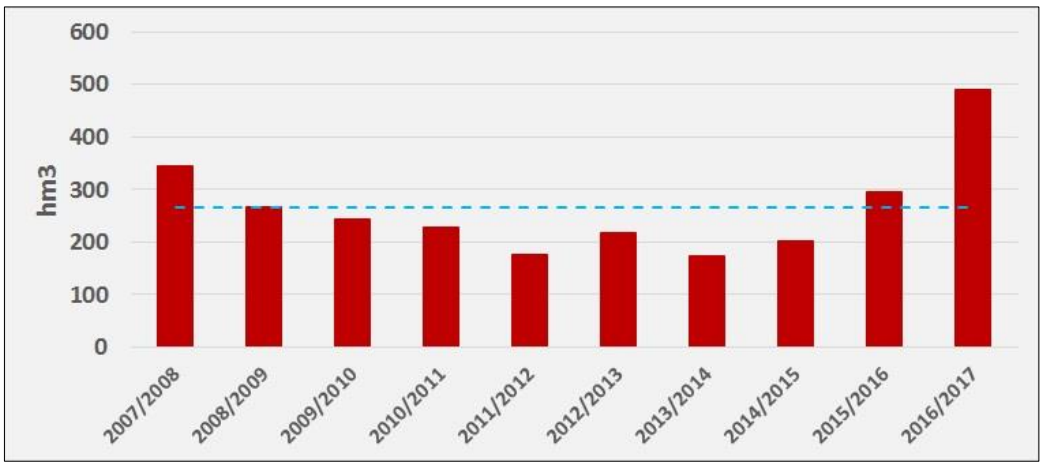

Figure 19 Annual water outflow from La Picasa lagoon from evaporation (hm^3)

Source: own elaboration

When the difference between both vertical hydrological processes, namely precipitation and evaporation, was calculated to estimate the annual net evaporation rates during the simulation period, the mean value resulted in 644 mm (Figure 20). More importantly, the inter-annual variability of net evaporation showed a substantial reduction during the simulation period (Figure 20), caused by a coupled effect in descending trend of evaporation and ascending trend in precipitation.

Furthermore, the difference between the maximum of 1,057 mm in the hydrological year 2010/2011 and minimum of 157 mm in the last hydrological year (2016/2017) increased in relation to those from evaporation and precipitation, totalizing 901 mm, which represented 39.9% more than the mean net evaporation for the simulation period. It is also worthwhile mentioning that the net evaporation presented values below average from the hydrological year 2012/2013 onwards, suggested as the starting point of a more humid period in the region (Giordano *et al.*, 2017).

Additionally, when the net evaporation was analyzed in volumetric terms, it was noticeably that the increase in the area of the lagoon, which enhanced the total water lost due to evaporation, could not outweigh the descending trend in net evaporation. For instance, when these values were summed to the annual time step, the mean volume of net evaporation totalized 108 hm^3, as shown in Figure 20. But the variability of the volume of water lost due to net evaporation during the period under analysis showed a descending trend with two marked periods. Figure 20 stresses that the net evaporation was above the mean value from the beginning of the simulation period until 2010/2011. After that, it continued to fall below the mean, with the 3 lowest values in 2013/2014, 2014/2015 and 2016/2017, which represented barely 53%, 54% and 62% of the mean net evaporation in the simulation period respectively.

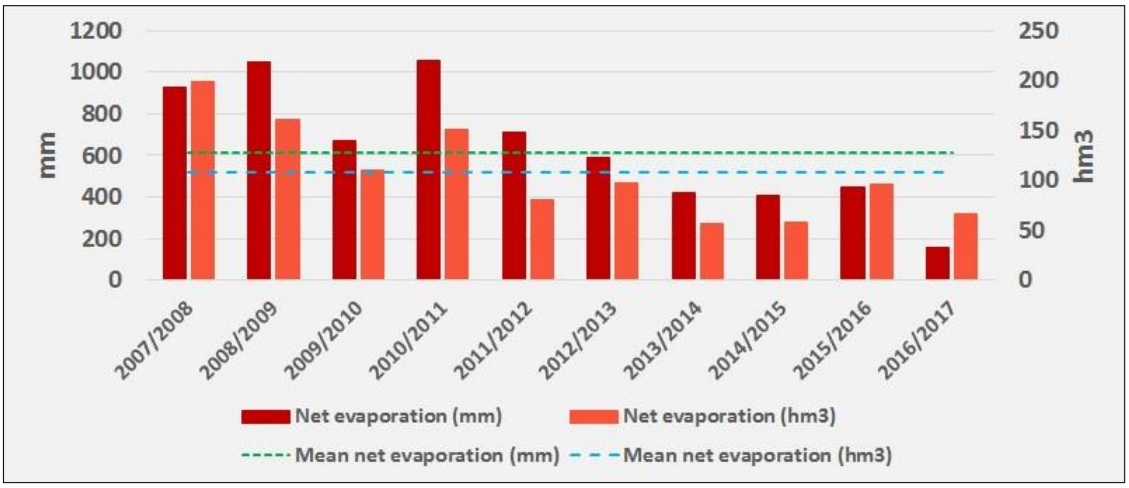

Figure 20 Annual net evaporation

Source: own elaboration

8.3. Surface runoff

The estimated CN of the sub-basins surrounding the lagoon did not show great differences between them, meaning that the characteristics affecting their hydrological behavior, such as HSG and land cover, did not have a high spatial variability. For example, the CN of all sub-basins contributing with direct runoff resulted in 74, thus the potential maximum retention of these areas was calculated in 89 mm. From the sub-basins indirectly contributing with surface runoff to the channels A45 and P5, only the latter one presented a different CN of 73, which means a slightly higher potential maximum retention of 94 mm (Figure 21).

Half of the area of the sub-basins surrounding the lagoon was characterized by the fraction A of the HSG. In turn, the fractions B and D represented 30% and 20% respectively. Consequently, most of the soils presented sandy, sandy loam or loamy sand textures, followed by patches with sandy clay loam and a smaller proportion of finer textures, such as clay loam or sandy clay. Regarding land cover, approximately 90% was represented by intensive agriculture or parts of agriculture with degraded vegetation.

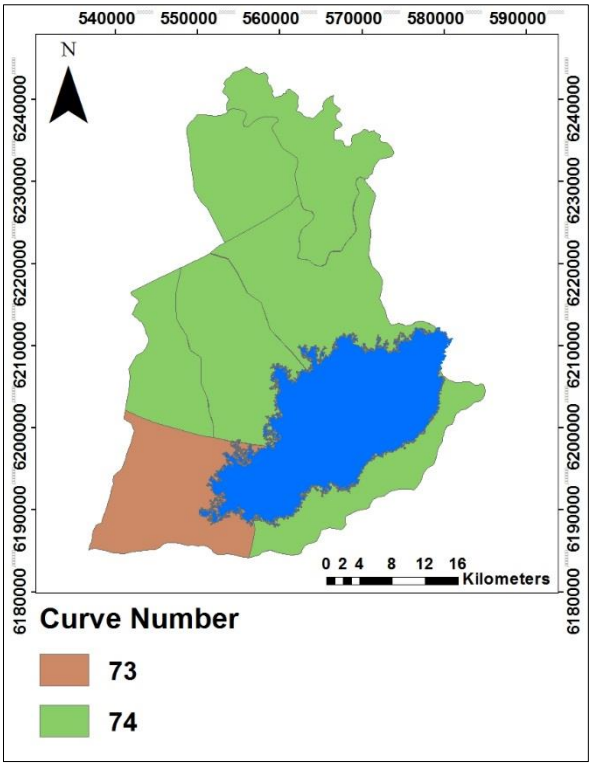

Figure 21 Spatial distribution of Curve Numbers (CN)

Source: own elaboration

After having interpolated the precipitation to all the sub-basins surrounding the lagoon, the mean monthly surface runoff resulted in 4.8 hm^3 during the simulation period. Additionally, a high intra-annual variability was apparent, naturally following the pattern of precipitations (Figure 22). In this sense, higher values during summer months between October to February were estimated, with a maximum mean surface runoff of 9.5 hm^3 in January, while lower values occurred during winter months from March to September, with a minimum mean surface runoff of 0.1 hm^3 estimated in July. Nevertheless, it is important to stress that April also resulted with a mean surface runoff of 8.4 hm^3 mainly due to relatively higher values registered in 2016 (23.1 hm^3) and 2017 (21.9 hm^3). In absolute terms, there were certain months with no contribution of surface runoff to the water balance of the lagoon, while in some others this contribution ascended to an absolute maximum above 25 hm^3.

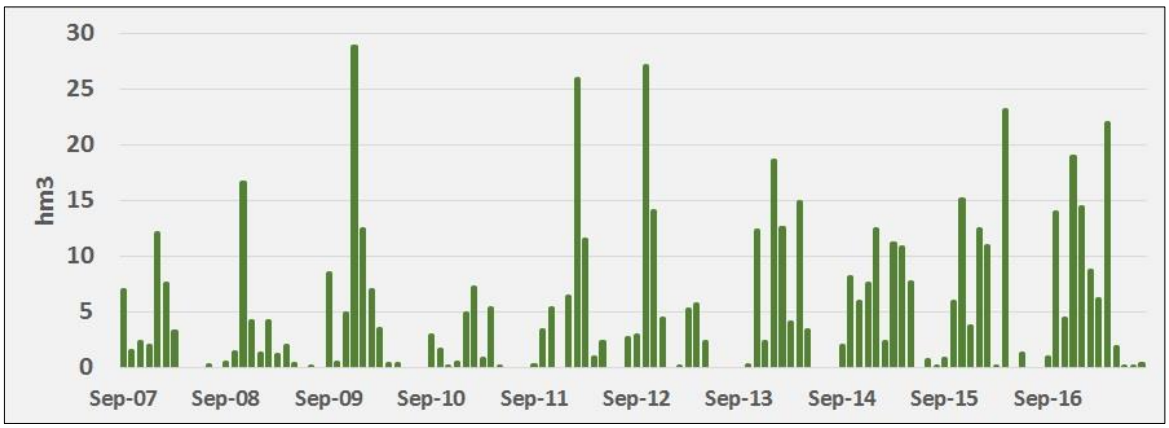

Figure 22 Monthly surface runoff (hm^3)

Source: own elaboration

Afterwards, when the monthly contribution of surface runoff was aggregated to the annual time step, the amount of water flowing into the lagoon was variable. Under relatively dry conditions, it accounted for 23 hm^3, while in the last hydrological year with more humid conditions it ascended to a maximum of 92 hm^3, representing approximately 9.4% of the mean volume of the lagoon in the same year.

Like precipitation estimations, the contribution of surface runoff to the water balance also showed a positive trend throughout the simulation period, determined not only by an increase in the total amount of precipitation over the sub-basins but also by a variable proportion of precipitation being transformed into surface runoff. As shown in Figure 23, from the total water fluxes in the sub-basins, the mean surface runoff for the simulation period resulted in 22%, ranging from 12% in the hydrological year 2008/2009 to a maximum of 30% in 2016/2017. On the other hand, the mean percolation during the period under analysis resulted in 13% of the total water fluxes. However, it presented a slightly different behavior than surface runoff because its standard deviation was 1.16% in comparison to 6.97% of the latter one, with a minimum of 11% and a maximum of 15%. Lastly, the third component of evapotranspiration showed a decreasing trend in relative proportions to the increase in surface runoff, showing a mean proportion of the total water fluxes of 65% but ranging from a maximum of 77% in the hydrological year 2008/2009 to a minimum of 56% in the last one. The outcomes of the analysis of the water balance in the surrounding sub-basins showed that the proportion of interflow in the total water fluxes was negligible.

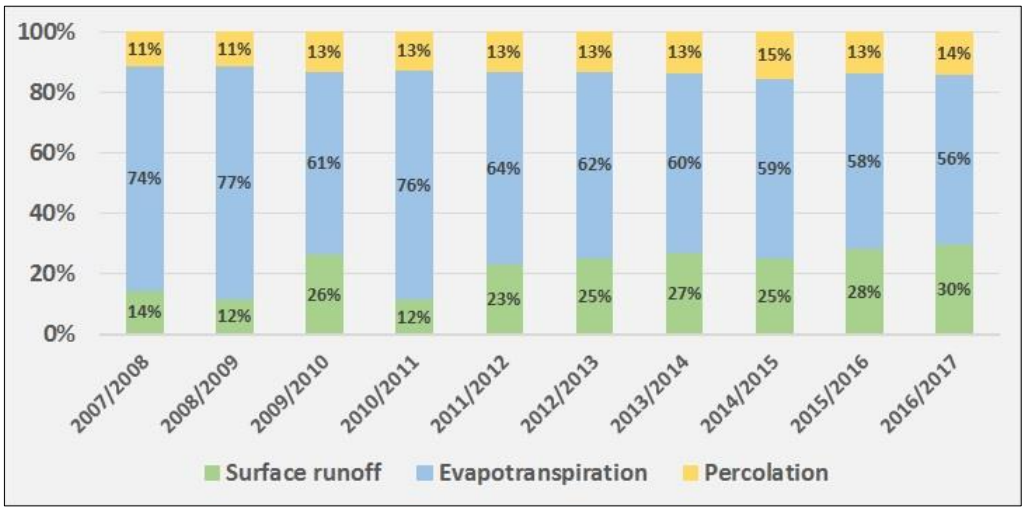

Figure 23 Relative contribution of surface runoff, evapotranspiration and percolation

Source: own elaboration

8.4. Water discharge

The water discharge gauges considered to calculate the inflow from channels to the lagoon were OR7, A45 and P5. However, only the channel A45 consisted in water discharge data. The other two gauges consisted either in water discharges or scale measurements at each gauge. In these cases, two flow rating curves were developed by least-squares fitting. In the first case, the gauge OR7 consisted in 20 available measurements with both water discharge and height (m) of the scale. After having plotted the paired H-Q data, the flow rating curve obtained was a power function (Figure 24). The coefficient of determination (R^2) obtained showed a very good performance. Therefore, it was used to estimate the water discharge of the measurements where only heights were available.

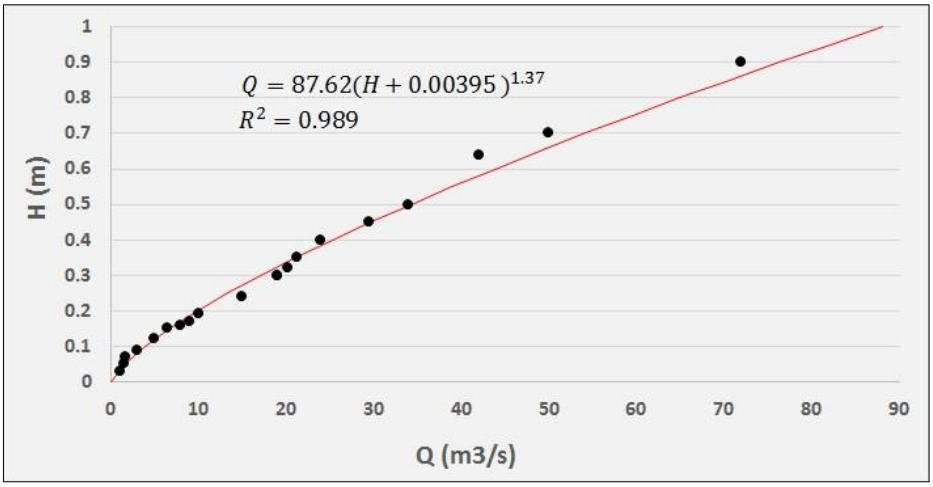

Figure 24 Rating curve OR7

Source: own elaboration

In the second case, following the same procedure as in OR7, most of the water discharges in P5 were estimated by developing a flow rating curve. In contrast to the first gauge, P5 only presented 7 available measurements with both water discharge and heights of the scale. Despite the limited availability of data, especially those with higher flow readings, the performance of the least-squares fitting expressed by R^2 was very good, showing a good fit between the rating curve and the discharge samples extracted from the data provided (Figure 25).

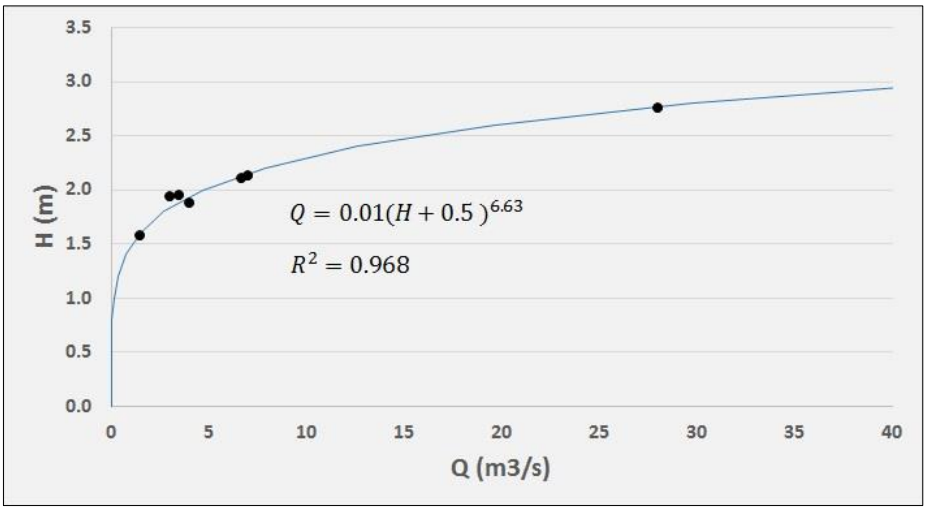

Figure 25 Rating curve P5

Source: own elaboration

Applying the flow rating curves previously developed, calculating daily water discharge by means of a linear interpolation and aggregating them to the monthly time step between September 2007 and August 2017 resulted in a mean monthly water discharge of 12.74 hm^3. This value was rather not representative of the time series, since the aggregation to monthly time step also helped to visualize the irregular contribution of water discharge to the total inflow to the lagoon. In this regard, the intra-annual variability showed that between June and December water discharges were below the monthly mean, with a minimum mean of 6.8 hm^3 in August, while from January to May these were above, with a maximum mean of 27.4 hm^3 in April. In absolute terms, during the period under consideration, there were months with no water discharge, while others showed peak discharges, such as 125 hm^3 in April 2017 (Figure 26).

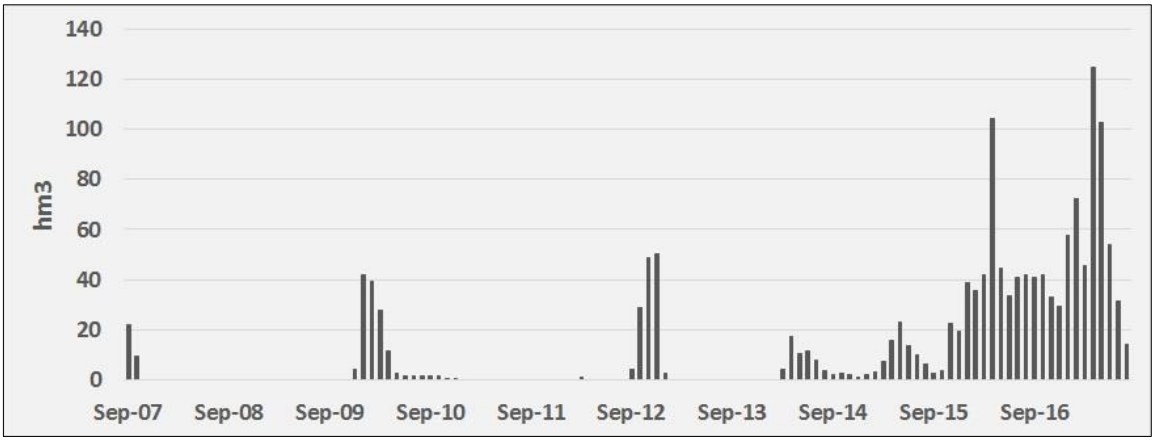

Figure 26 Monthly water discharge (hm³)

Source: own elaboration

Relative to the other inflow components, the water discharge represented approximately 26% of the total water inflow to the lagoon. However, the influence of this component increased in the last two hydrological years (September 2015 to August 2017) when it accounted for almost 60%. This represented a mean ratio between water discharge to volume of the lagoon of 0.06, an increase of roughly 140% with respect to the previous hydrological years.

Afterwards, the monthly water discharges were aggregated into the annual time step, showing a mean value of 152.9 hm^3. During the simulation period, it ranged from a minimum of 0 hm^3 in the hydrological year 2008/2009, when no water flowed through the channels, to a maximum of 648.3 hm^3 in 2016/2017 (Figure 27).

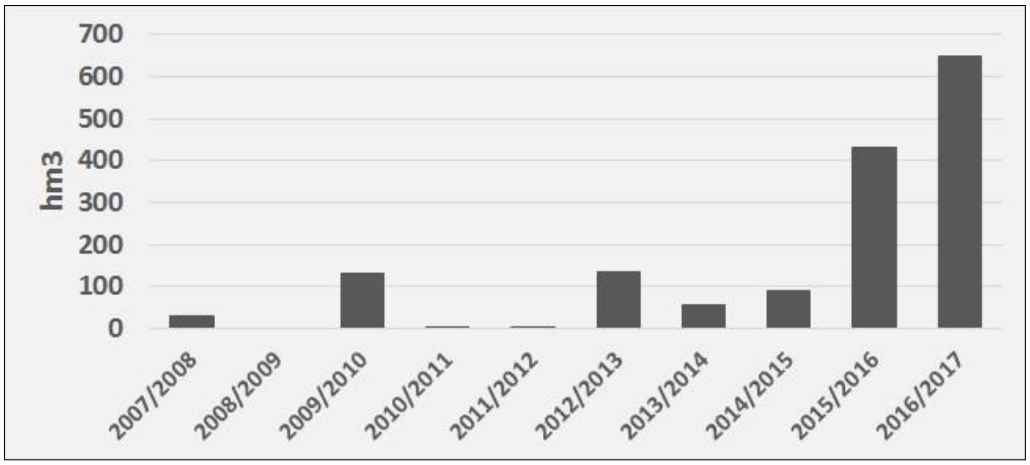

Figure 27 Annual water discharge (hm³)

Source: own elaboration

Interesting is to focus that throughout the simulation period, only water discharges in the last two hydrological years exceeded the mean annual value in 182% and 324% respectively. Since these extreme values might have distorted the mean water discharge, the median was calculated resulting in 72.7 hm^3. In this case, although there were also some hydrological years above the median, particularly the water discharges in 2015/2016 and 2016/2017 clearly showed that they were extraordinary values, exceeding the median in 493% and 792% respectively.

Organizing the water discharges to the calendar year as calculated by SsRH (2017), the results showed a similar behavior most of the simulation period. Nevertheless, the water discharges

calculated in the current study resulted in general 25% larger than those suggested by SsRH (2017), except for the year 2010 when it resulted 3.9% less. This difference was variable throughout the period. Although the maximum difference occurred in 2014 (90.6%), the last two hydrological years presented the biggest differences in absolute terms, with 192 hm^3 in 2016 and 76 hm^3 in 2017 (Figure 28)

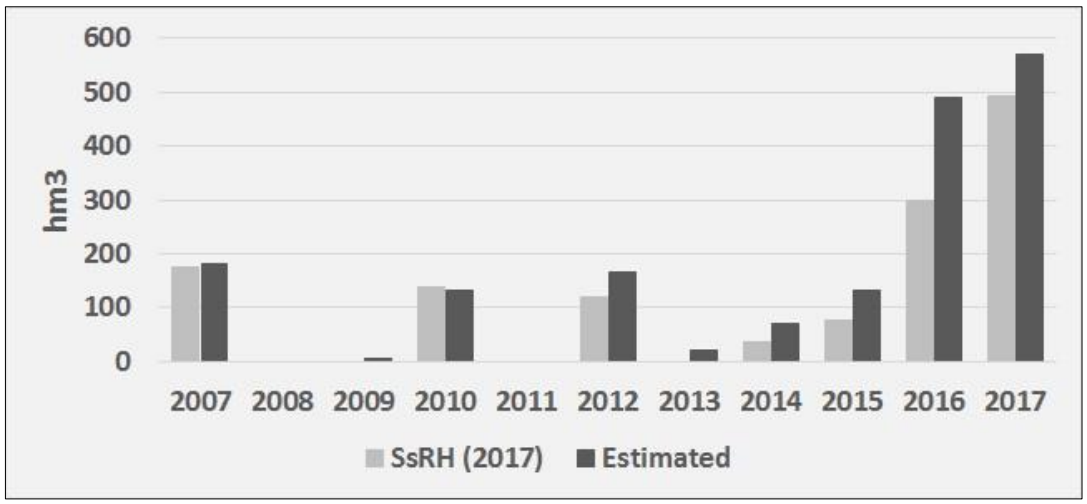

Figure 28 Comparison annual water discharge (hm^3)

Source: own elaboration

The contribution from surface runoff of the sub-basins A45 and P5 to water discharge of the respective channels showed a variable behavior. After having estimated the rating curves, an increase in water discharge was observed between the gauge OR7 and the effective discharge to the lagoon from A45 and P5. In cases when no water discharge was measured in OR7 but there was inflow to the lagoon, it was totally explained by this hydrological process. In absolute terms, the difference ranged from barely 0.0012 m^3/s the 4th of February 2012 to 5.97 m^3/s the 12th of January 2013. In cases when water discharge was measured in OR7, these differences ranged from 0.36 m^3/s the 9th of April 2014 to 23.65 m^3/s the 20th of February 2017. However, in relative terms, in the first case the water discharge almost doubled that one registered in OR7 (107%) while in the second case it totalized more than quadruple of the discharge in OR7 (438%).

8.5. Pumping

The estimation of total monthly outflow from both pumping stations showed that there were at least 60 months of the simulation period with no pumping, specifically between October 2008 and August 2012 and between December 2014 to December 2015 (Figure 29). That is the same to say that the only outflow component of La Picasa lagoon in half of the period considered was evaporation.

Considering the months with active pumping, the mean monthly water outflow was 4.12 hm^3, ranging from 0.63 hm^3 in February 2016 to 12.26 hm^3 in May 2017. Relative to the volume of La Picasa lagoon during these months, the pumping represented a minor proportion (1.13%).

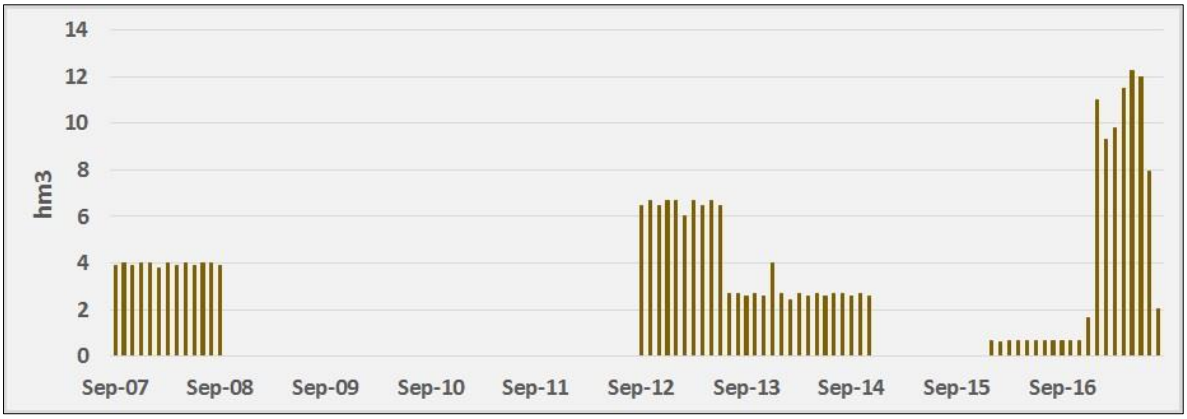

Figure 29 Monthly pumping (hm³)

Source: own elaboration

When the monthly pumping was aggregated to the annual time step, the mean annual outflow resulted in 25 hm³. However, the annual pumping ranged in absolute values from no pumping between the hydrological years 2009/2010 and 2011/2012 to a maximum pumping of 79 hm³ during the last one (2016/2017), followed by 2012/2013 with 71 hm³ (Figure 30).

It is important to stress that simultaneously with an increase in water inflow from precipitation, water discharge and surface runoff in the last two hydrological years, the contribution from pumping to outflows was important only in the last one, when it exceeded the mean annual in approximately 220%. This also represented an increase in the ratio between the water outflow from pumping and the mean volume of La Picasa lagoon of 7.1% in the period.

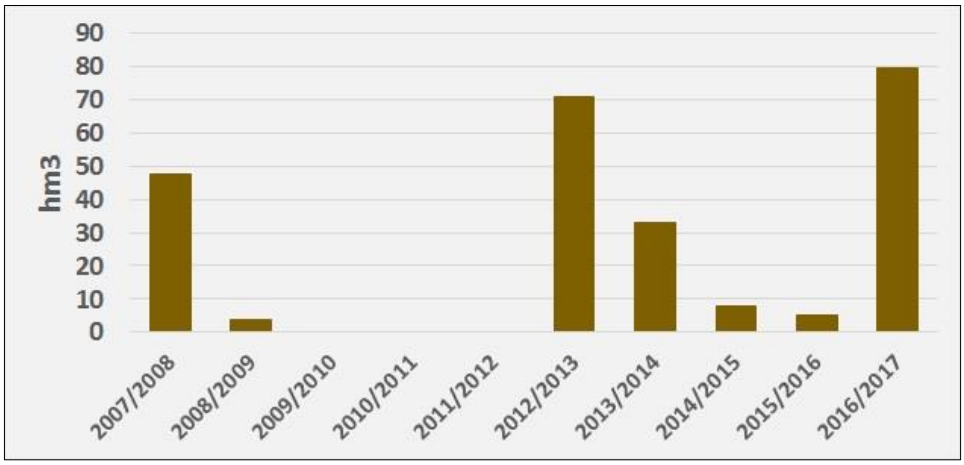

Figure 30 Annual pumping (hm³)

Source: own elaboration

8.6. Morphometric relationships water level-area-volume

The measured water level of La Picasa lagoon between September 2007 and August 2017 presented three well-defined periods (Figure 31). The first one, between September 2007 and September 2012, was characterized by a general negative trend. In particular, the water level dropped from 103.3 m to 100.83 m, a total decrease of 2.47 m in 61 months, representing a mean reduction rate of 4 cm per month. In contrast with this general trend, there was a short interval between November 2009 and April 2010 (6 months) when the water level increased 73 cm (12 cm per month).

The second period, between September 2012 to February 2015, showed an intermittent behavior. It was characterized by two positive intervals, the first of which showed a relatively high increase rate of 24.2 cm per month, followed by two negative ones. Despite this erratic behavior, the water level varied within a restricted range between a minimum of 100.83 m and a maximum of 101.20 m. This determined an overall slightly ascending trend, characterized by a total increase of only 37 cm in 30 months, that is a mean increase rate of 1.2 cm per month.

The third period, between February 2015 and August 2017, was marked by a clearly positive trend, yet with variable increase rates. The total water level ascended 4.49 m in 31 months, from 101.2 m to 105.69 m, representing a mean increase rate of 14.48 cm per month. Nevertheless, in this interval the maximum increase rate reached 64 cm in April 2017 followed by 38 cm in May.

Figure 31 Variation of the water level of La Picasa lagoon (September 2007 – August 2017)

Source: own elaboration based on SsRH (2017)

The DEM resulting from the bathymetry conducted in the frame of the current study and complemented with the processing of satellite images by Pagot (2018) and the bathymetric studies from SsRH (2008) and INA-CRL (2007) is shown in Figure 32. To better visualize the results, the red colors indicate the deepest areas of the lagoon while the blue the shallowest ones. The legend indicates the altitude of the bottom of the lagoon above sea level in meters.

The outcomes showed that the mean slope of the bottom of the lagoon is approximately 0.19%, with a minimum altitude of 97.36 m above sea level. Since during the bathymetry the water level was 104.78 m, the maximum altitude of 105.5 m above sea level shown in Figure 32 corresponds to the contour line calculated with satellite images (Pagot, 2018).

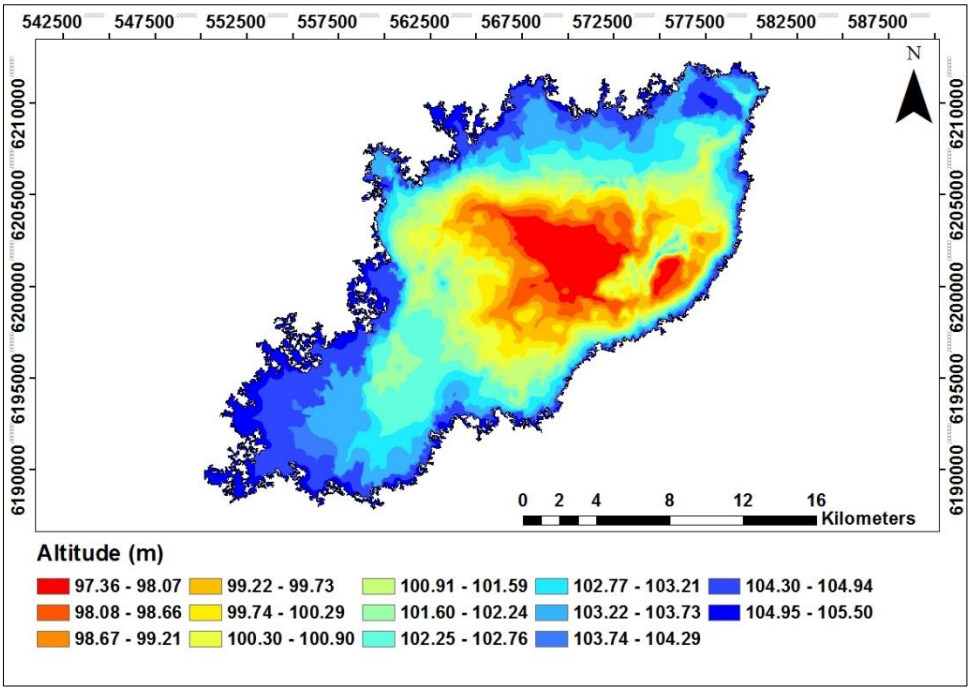

Figure 32 DEM of La Picasa lagoon

Source: own elaboration based on own bathymetry and Pagot (2018), SsRH (2008) and INA-CRL (2007)

After applying the two sequential steps mentioned in the methodology, the area and volume of La Picasa lagoon at different bathymetric water levels were calculated, starting from 97.5 until 105.5 m (Table 4). Due to the shape of the bottom of the lagoon and the mean slope, these results showed that the incremental volume of the lagoon when the water level increased 1 m varied from a minimum of approximately 14.39 hm^3 between 97.5 to 98.5 to a maximum of 352.4 hm^3 between 104.5 to 105.5. Similarly, incremental values of the area ranged from a minimum of 2,532.3 ha to a maximum of 11,989.3 ha for the same water level intervals.

Table 4 Estimated area and volume of La Picasa lagoon

Water Level (m)	Area (ha)	Volume (hm3)
97.5	145.6	0.1
98.5	2,677.9	14.5
99.5	5,785.1	55.0
100.5	9,398.5	130.4
101.5	13,234.9	243.4
102.5	17,449.0	394.6
103.5	24,953.7	611.3
104.5	30,586.7	886.9
105.5	42,576.0	1,239.3

Source: own elaboration

The morphometric relationships water level-area-volume developed based on the results of Table 4 are shown in Figure 33. After a first graphical analysis, it was decided to adjust two different polynomial functions. First, a quadratic function best fitted the distribution of the area of La Picasa lagoon as a function of the water level (Z). In the second case, a cubic function was found to be more appropriate to the distribution of the paired values volume and water level (Z).

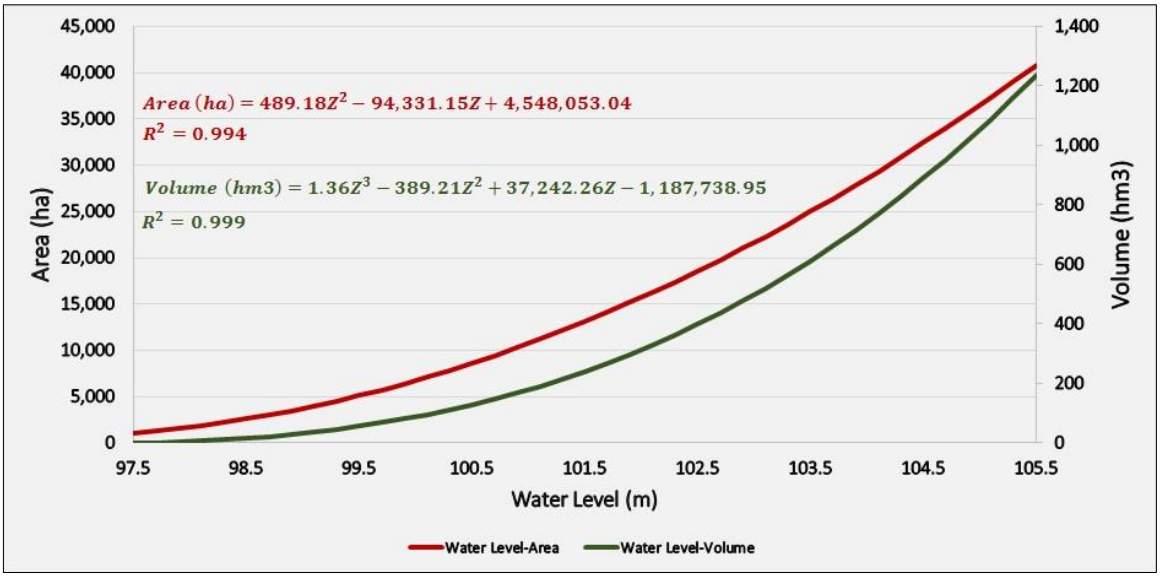

Figure 33 Morphometric relationships water level-area-volume

Source: own elaboration

8.7. Sensitivity analysis

The ranking of sensitivities of the components considered to build the water balance model stressed the noticeable differences among them (Table 5).

Table 5 Ranking of sensitivities

Parameter	Sensitivity	Ranking
Evaporation	339%	Extremely sensitive
Precipitation	164%	Highly sensitive
Water discharge	84%	Moderately sensitive
Surface runoff	66%	Moderately sensitive
Pumping	25%	Slightly sensitive

Source: own elaboration

Based on these results, the remarkable aspect among the natural components of the water balance is that the most sensitive parameter was evaporation. A variation of 10% in its contribution to the overall outflow modified the volume of La Picasa lagoon in 339% on average. The second most sensitive parameter was precipitation, assessed as highly sensitive. Although a rather small change in their values had a great impact in the volume of the lagoon, it represented almost half of the effect of evaporation. These outcomes certainly highlight the importance of both vertical physical processes in determining the volume variations of the lagoon over the lateral ones, such as surface runoff, which resulted in moderately sensitive.

On the other hand, the anthropogenic components considered in the water balance were generally less sensitive. For example, the current functioning of the pumping stations resulted in slightly sensitive, reflecting its rather low influence relative to the total volume of the lagoon at the monthly time step. Additionally, water discharge resulted in moderately sensitive, same as surface runoff. Despite the sensitivity of water discharge represented approximately half of the precipitation component, the outcomes clearly show that this inflow component, as well as surface runoff, can have a considerable impact on the variations of the volume of the lagoon during humid periods.

8.8. Performance tests

During the calibration process, four simulations were conducted by introducing different modifications to the water balance model. The results of the performance tests applied to the simulations are shown Table 6.

Table 6 Performance tests for calibration and validation

Performance test	NSE	PBIAS	RSR
Simulation 1	-2.91	75.06	1.98
Simulation 2	-1.07	50.99	1.44
Simulation 3	0.86	-11.72	0.38
Simulation 4	0.97	-0.28	0.19
Validation	0.85	-7.64	0.39

Source: own elaboration

The first simulation considered four parameters to estimate the water balance, namely precipitation, evaporation, water discharge and pumping. The component of direct surface runoff was initially neglected, considering only the contributions of surface runoff to the channels A45 and P5, which were accounted as part of their water discharge. Furthermore, the evaporation was estimated with the Penman Method. The first results showed that the behavior of the model relatively reproduced that one of the measured values, yet it consistently underestimated them (Figure 34). The NSE confirmed that the performance was unacceptable because its value was below zero. In addition, the considerable underestimation of the volume of the lagoon was corroborated by the results of the PBIAS, which indicated a mean tendency of underestimation bias of approximately 75%. Likewise, the RSR displayed that the residual variation almost doubled the standard deviation of the measured volume. Therefore, in light of the outcomes of the performance tests, the first simulation was considered not adequate to estimate the water balance of La Picasa lagoon.

A second simulation was performed applying the evaporation estimations from the CRLE model instead of the Penman Method. Although the simulated values remarkably improved in comparison to the first simulation, the water balance model still underestimated the measured values (Figure 34). After applying the performance tests, the NSE showed that also the second simulation was not acceptable because the index resulted in a negative value (Table 6). Although improving approximately 24%, the PBIAS still yielded a high positive bias, proving that the model underestimated the measured volume of the lagoon. In turn, the RSR showed that the residual variation was above acceptable levels of the standard deviation of the measured volume.

Consequently, the results of the performance tests suggested the existence of an additional hydrological process leading to an increased water inflow, thus reducing the underestimation of the simulated values rather than an outflow component, since these were already identified. In this regard, the evaporation was considered and calibrated. In turn, the pumping component not only showed a reduced sensitivity but was also considered as a measured component. That means that its estimation error is small compared to the estimated parameters and would not require further calibrations. Therefore, one of the hydrological processes considered to be responsible of additional water inflows to the lagoon was direct surface runoff and interflow from surrounding

sub-basins. In this regard, after having pursued the calculations of the water balance on these sub-basins and considering the proportions of surface runoff, evapotranspiration and percolation in their total water fluxes, the component of interflow was already discarded from the water balance.

Having included the component of surface runoff as part of the water balance, a third simulation was conducted. In this opportunity, the results considerably improved, almost reproducing the variation of the volume of the lagoon in the calibration period (Figure 34). This was reflected in the results of the NSE, which showed that the performance was not only acceptable but also close to its optimal (Table 6). The conclusion from this test reinforces the inclusion of the surface runoff from surrounding sub-basins as an inflow component of the water balance of La Picasa lagoon. Another point to consider are the result of the PBIAS and the RSR tests. Although the second one showed a reduced residual variation relative to the standard deviation of the measured volume, being in line with the results from NSE, the first one expressed a slightly overestimation of the simulated values over the measured ones.

In view of the outcomes of the third simulation, a fourth simulation was performed including an adjustment factor to optimize the model. Following the results of Vallet-Coulomb *et al*. (2001), this factor was included to the evaporation estimation with the CRLE model to account for errors in the predictions and optimize its results. The adjustment factor that yielded the best performance was 3%. As a consequence, the results of the NSE showed an almost optimal performance of the water balance model (Table 6). In turn, the PBIAS test also displayed an almost perfect fit between the measured and simulated volume of the lagoon, with a slightly overestimation (Figure 34). Similarly, the RSR presented a residual variation of the model of approximately 20% of the standard deviation of the observed variations. As a result, the water balance model of La Picasa lagoon was considered calibrated.

After having assessed and defined the structure of the model, seeking to include the most important components explaining the water balance of La Picasa lagoon, the validation process was applied using the model already calibrated but to the hydrological year 2016/2017. In this context, both the NSE and PBIAS tests showed an acceptable performance (Table 6), but with a slightly underestimation. In turn, the RSR showed a very good performance, since the residual variation of the model was approximately 39% of the standard deviation of the measured volume. Based on the results of the performance tests, the modelled values yielded an acceptable coincidence with the measured ones. Therefore, the model was considered validated.

8.9. Water balance of La Picasa lagoon

After having conducted the performance tests for the calibration and validation, the most important components and processes of the water balance of La Picasa lagoon were defined, either representing inflows or outflows, thus allowing to reproduce the monthly volume variation of the lagoon with a high degree of accuracy. In Figure 34, the measured volume (red solid line) was obtained with the use of the morphometric relationship water level-volume, utilizing as input the water level measurements provided by SsRH (2017). As can be seen, the calibrated and validated hydrological model corresponding to the Simulation 4 fitted the measured volume with a high performance and a minor overall overestimation.

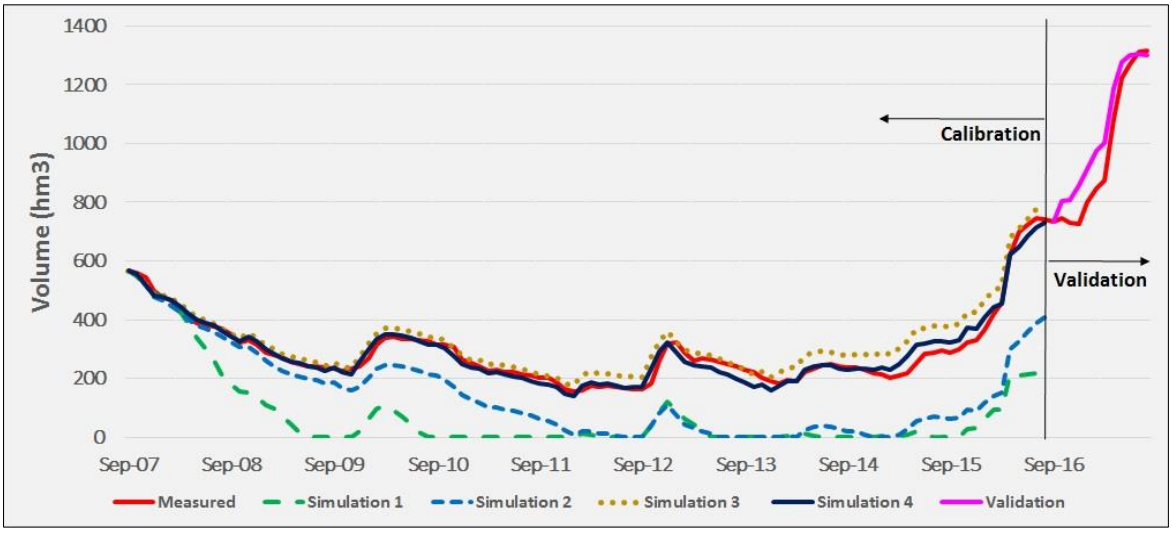

Figure 34 Monthly volume variation of La Picasa lagoon (September 2007 – August 2017)

Source: own elaboration

The mean monthly relative contribution to inflow and outflow of each component of the water balance stressed the importance of the natural hydrological processes, such as precipitation and evaporation, above the considered anthropogenic ones, such as water discharge from channels and pumping (Figure 35). More specifically, despite that three months of the simulation period did not account for any water inflow, particularly May 2008, August 2008 and July 2012, for the rest of the months precipitation was the most important component with a mean monthly contribution of 59%. Analyzing the variability of its contribution along the hydrological year and recognizing that it showed increases and decreases between certain months, a general descending trend from the beginning to the end of the hydrological year could be observed. For instance, it ranged between a maximum of 68% in September to a minimum of 52% in August of the following year. This abrupt change in two consecutive months might be explained by an increase of the mean monthly precipitation from 14 mm in August to 62 mm in September at the beginning of the hydrological year, since water discharge not only did not show a reduction in the same period, but also an increase of 0.5 hm^3. The variability of the contribution of precipitation was more evident when the results were analyzed in absolute terms, since there were months with no precipitation and others when it was the only inflow.

The mean monthly contribution of the second and third inflow components in importance, namely water discharge and surface runoff, accounted for approximately 27% and 14% respectively. The behavior of water discharge was different than precipitation in the sense that its contribution presented an ascending trend throughout the hydrological year with a range double than its mean value between the minimum contribution of roughly 15% in October to a to a maximum of 45% in August. Again, in absolute terms there were months with no water discharge and others when the inflow to the lagoon was exclusively explained by this component. Similarly, the mean monthly contribution from surface runoff also presented a considerably variability, with very limited contributions in winter (almost no contribution in June with 0.3%) to larger contributions in summer (23% in January). Although this component was on average less determinant than the other ones, there were some months when it explained almost half of the inflow to the lagoon.

Regarding outflows, it is undoubtedly that evaporation was the most determinant component of the water balance, since its mean monthly relative contribution ascended to 92% during the simulation period. In contrast to the inflow components, it displayed a more limited variability between a minimum of 87% in December to a maximum of 96% in June. Although evaporation was the only outflow component in half of the simulation period in absolute terms, its contribution decreased to almost half of it in specific months with active pumping. In this regard, the reduction of the contribution during summer months was not explained by a decrease in evaporation rates, since it was already shown that the CRLE model yielded larger evaporation rates in this period of the year (see Figure 18), but rather by an increase in the contribution of the pumping.

The pumping component represented a minor contribution during the simulation period, accounting for 8% of the total water outflows. Contrarily to evaporation, it presented higher relative values in summer with a maximum of 13% in December and lower relative values in winter with a minimum of 4% in June. Rather than a recognized seasonality, its intra annual variation can only be explained by the erratic functioning of both pumping stations. In addition, complementing the contributions from evaporation, this component ranged from months with no pumping to months when it almost accounted for half of the outflow in absolute terms.

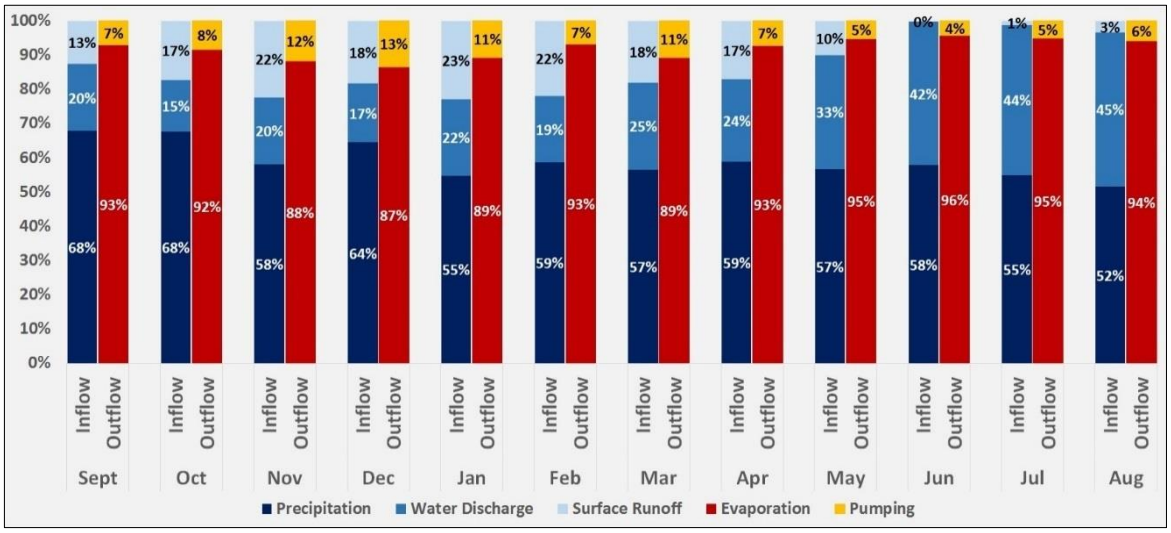

Figure 35 Mean monthly relative contribution of the water balance components

Source: own elaboration

The inter-annual variability in the contribution to inflow and outflow of each component of the water balance in absolute terms facilitated the observation of their combined effects determining the evolution of the volume of La Picasa lagoon and their relative changes (Figure 36). In this regard, the results showed that there were hydrological years in the simulation period when the annual water loss from the lagoon reached 178 hm^3 (2007/2008) and others when the water surplus ascended to 594 hm^3 (2016/2017). Nevertheless, the most remarkable aspect was that the overall water balance showed a clear positive trend, mainly driven by an increment in water inflows rather than a decrease in water outflows. In fact, taking 2013/2014 as a base year, both total inflow and total outflow increased, yet the first one did it at a considerable higher rate than the second one, specifically 74% and 45% respectively.

Figure 36 also stresses that the main reason of the relatively large positive water balance of La Picasa lagoon in the last two hydrological years was the water discharge rather than precipitation

or surface runoff. For instance, considering only these two components in the hydrological year 2016/2017, the total inflows would have surpassed the outflows only by 25.5 hm^3. However, the contribution from water discharge of 648.3 hm^3 led the total water inflow to outweigh the outflow, thus resulting in a positive balance of 594.36 hm^3.

On the other hand, it is also worthwhile indicating the low impact of the pumping factor to reduce the water level of the lagoon in the current scenario, stressing that evaporation was the main outflow component to counterbalance the inflow. For example, during years when the water balance was negative, the evaporation itself showed to be higher than all the combined inflows together, while pumping contributed with a small fraction of water losses, as shown in the hydrological years 2007/2008 or 2008/2009 (Figure 36).

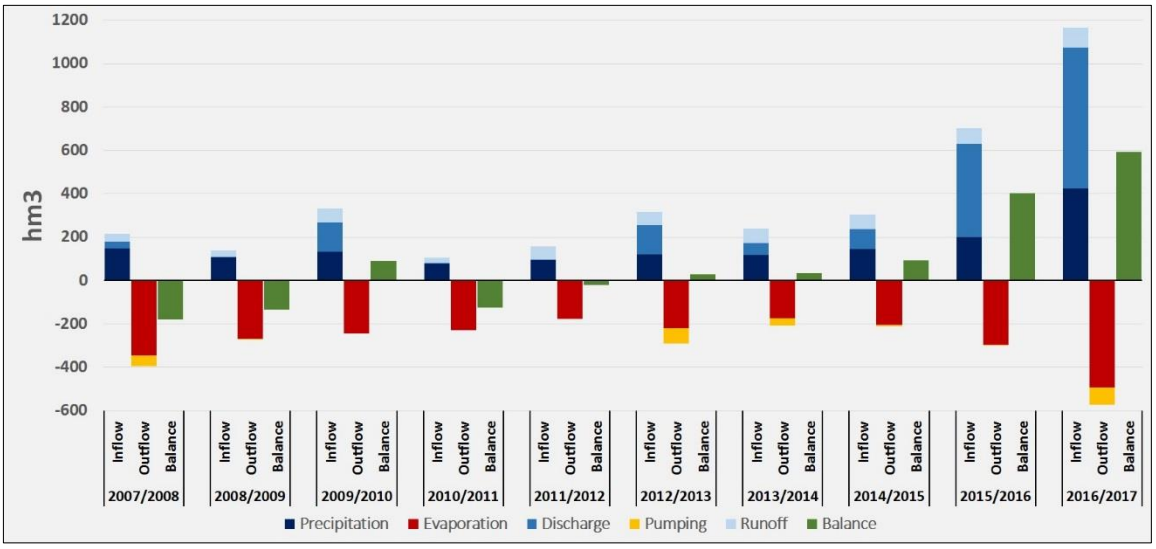

Figure 36 Absolute annual contribution of the water balance components

Source: own elaboration

8.10. Simulation Scenarios

Once having identified the most determinant inflow and outflow components with the sensitivity analysis together with the water balance model that explains the variations of the volume of La Picasa lagoon with an acceptable performance, two hypothetical simulation scenarios were proposed to reflect the trajectories of the volume based on different pumping operation schemes.

A first hypothetical simulation scenario 'Potential pumping' was developed, characterized by a continuous operation of the North Pumping Station at full capacity from the beginning of the simulation period and the South Pumping Station from 2011 onwards (when it should have been finished according to SsRH (2015)) (Figure 37).

For this scenario, the mean monthly pumping discharge would have risen to 15.51 hm^3 between the hydrological years 2007/2008 and 2010/2011 and to 27.36 hm^3 for the rest of the period. At the annual step, this would have represented a mean annual water outflow of 158 hm^3 until August 2010, after which this would have ascended to 217 hm^3 in the hydrological year 2010/2011 and finally to 328 hm^3 in the remaining period. In this case, the pumping would have been the most important outflow component for the simulation period, draining approximately 15% more water than evaporation.

A second hypothetical simulation scenario was proposed called 'Adjusted pumping', in which the operation of the pumping stations would have been adjusted according to the climatic conditions and the operation of the water infrastructure. The aim of this scenario would have been to increase the pumping efficiency aiming to fulfil the objective of regulating the water level of La Picasa lagoon between 98.5 m and 102.5 m above sea level (corresponding to the Minimum projected volume of 14.5 hm^3 and Maximum projected volume of 394.6 hm^3 in Figure 37). This is the range that would theoretically allow the lagoon to have a sufficient storage capacity to buffer the increased water discharges, surface runoff and precipitation during humid periods. Therefore, three operation periods were defined (Figure 37).

The 'Adjusted no pumping' was defined for a period characterized by net evaporations above average and without considerable water discharges or surface runoff. It consisted in not operating the pumping stations because they would have not been required to regulate the water level. In turn, the 'Adjusted minimum pumping' was matched with the time interval when the start of more humid conditions were suggested. It was estimated that both stations operating continuously with one pump each would have been capable of maintaining the water level within a safe range. Lastly, the 'Adjusted full capacity pumping' would have tried to cope with the noticeably increase in water discharge and surface runoff coupled with the reduction in net evaporation in the last two hydrological years by utilizing both pumping stations at its maximum capacity.

For this scenario, the mean monthly pumping discharge would have obviously been 0 hm^3 from September 2007 to August 2012, ascending then to 9.12 hm^3 between September 2012 until August 2015, finishing with 27.36 hm^3 until the end of the simulation period. At the annual step, this would have represented a mean annual water outflow of 109 hm^3 for the minimum pumping and 328 hm^3 for the full capacity pumping as already expressed for the potential pumping scenario.

It is also important to highlight the possible trajectories of the volume of the lagoon according to the hypothetical simulation scenarios developed. In the case of 'Potential pumping', the Figure 37 stresses that most of the simulation period would have presented negative monthly balances, causing La Picasa lagoon to be almost dried up except during exceptionally humid periods, such as between December 2009 and July 2010 or between October 2012 and January 2013 coincident with the start of the humid period. Furthermore, it is vital to remark that despite a potential functioning of both pumping stations, the water excesses estimated in the last two hydrological years would have outweighed the pumping capacity of both stations operating together. Consequently, the volume of the lagoon would have increased to 534 hm^3, representing a water level of 103.16 m.

With respect to the second scenario, the water level would have also been kept between the minimum and the maximum projected volume during most of the simulation period (Figure 37). Nevertheless, it would have anyways surpassed the latter one, reaching 626 hm^3, which represents a water level of 103.55 m. More specifically, the first period of this scenario stresses that the pumping component would not have been required, since the water level would have also followed a descending trend, copying the actual measured ones. In the second period 'Adjusted minimum pumping', the use of one pump per station would have been enough to break the ascending trend in the water level and even draining more water than the increased inflow. Lastly, although both pumping stations working at full capacity would have not avoided the water level of the lagoon to exceed the maximum projected volume, it would have rather limited them at 103.55 m.

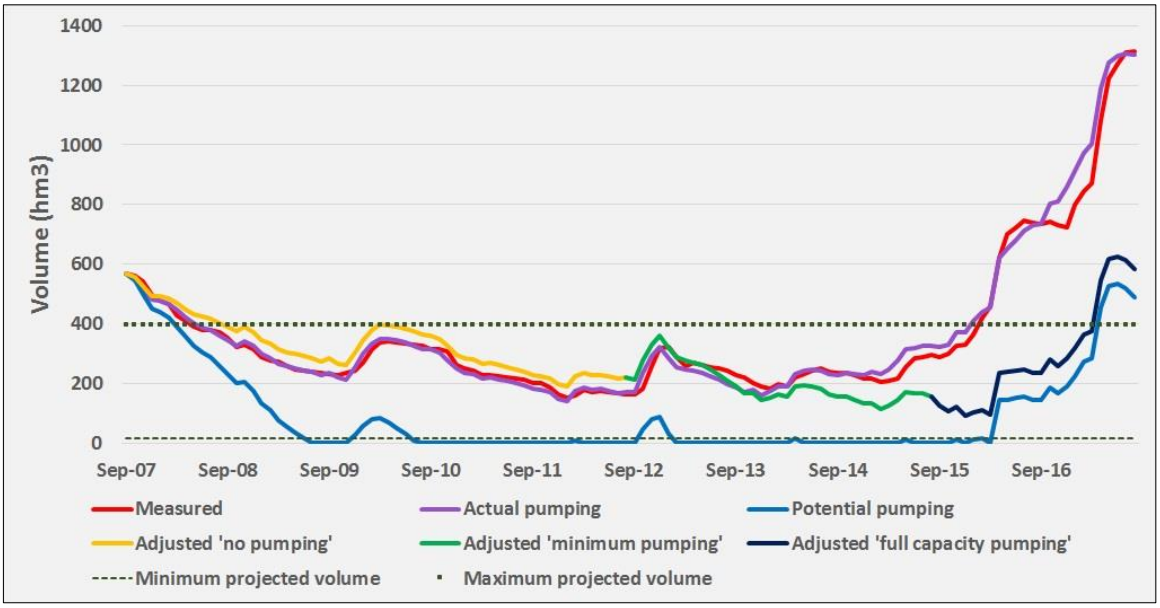

Figure 37 Monthly volume variation of La Picasa lagoon for the simulation scenarios

Source: own elaboration

Finally, the inter-annual variability in the contribution of each component considering the 'Potential pumping' scenario is shown in Figure 38. The difference is that the increased water outflow due to the pumping component would have caused to have more noticeably water losses during most of the simulation period, reaching 395 hm^3 in the hydrological year 2010/2011. Simultaneously, the maximum water surplus would have been reduced to 346 hm^3 in 2016/2017, representing a reduction of 42%. Moreover, the longer positive trend shown in Figure 36 starting in 2011/2012 would have been shortened, showing that the pumping component balanced most of the additional water inflows during the humid period. However, even a pumping at full capacity could not have coped with the incremental growth of water inflows in the last two hydrological years, which basically determined the positive water balances in this period. A last important remark is the fact that the pumping component would have been the main outflow of the lagoon.

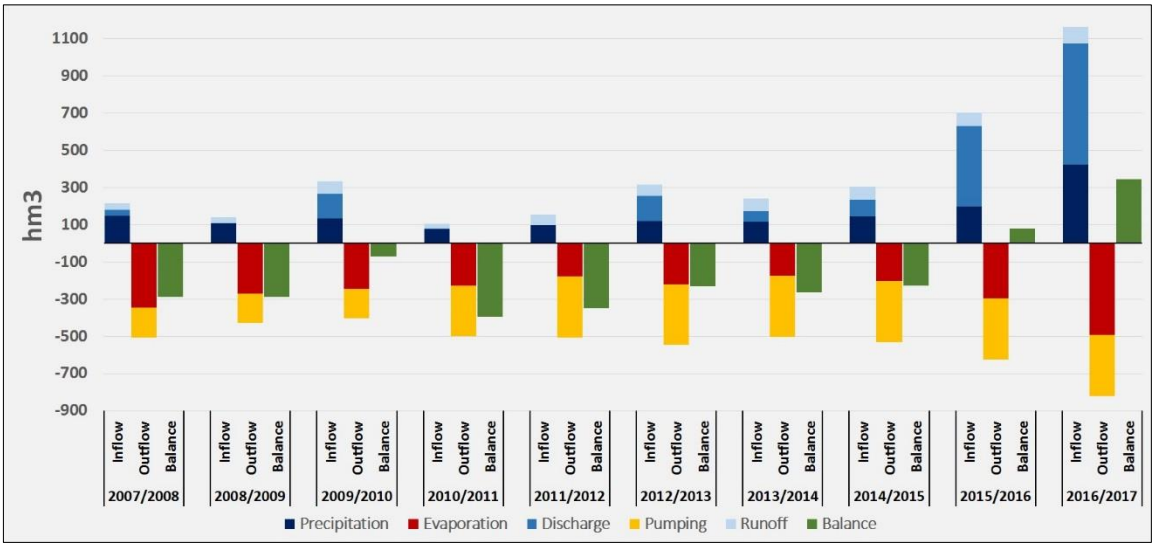

Figure 38 Effect of a potential pumping on the absolute annual water balance

Source: own elaboration

9. Discussion

Although previous studies have already estimated the mean areal precipitation with interpolation methods from ground stations in La Picasa basin (A. Villanueva, personal communication, April 27th, 2018; Pedraza *et al*., 2010), this thesis provides the first estimation of the monthly volumetric inflow from this component to the overall water balance of La Picasa lagoon. Therefore, it contributes to previous modelling approaches, which sought to quantify the components and processes of the water cycle at the basin scale and analyze this water body without having estimated the volumetric inflow from precipitation. In addition, as mentioned in the section "4. State of the Art", the previous attempts to measure the volume of water flowing into the lagoon considered either inflow from reservoirs and channels (SsRH, 2017; Pedraza *et al*. 2010; Pedraza, 2000), accounted in this study as part of the water discharge component, or from surface runoff coming from the surrounding sub-basins (A. Villanueva, personal communication, April 27th, 2018; Pedraza *et al*. 2010; Pedraza, 2000). However, the analysis of the relative contribution of the hydrological factors to the water balance revealed that precipitation over the lagoon should also be considered as one of the most determinant components, since it explained 59% of the monthly water inflow during the simulation period.

The mean annual precipitation of 931 mm for the overall simulation period corresponds to the findings of INA (2016), who suggested that La Picasa basin has not experienced a period with water excesses during the time interval under analysis. Indeed, this value resulted only 3.5% above the historical mean of the basin (Pedraza, 2000). Nevertheless, the evolution of precipitations showed a positive trend leading to exceed the historical mean in the last four hydrological years in approximately 26%. This trend is in line with the conclusions of Giordano *et al*. (2017), who stated that from 2012 onwards a humid period is taking place in the region. In this regard, the relatively high monthly precipitation values estimated between December 2016 and April 2017 might have been a result of a series of precipitation events over Córdoba, northern Buenos Aires and center and south Santa Fe, which fostered the existence of water excesses over the Central Pampa in this specific period of time (Giordano *et al*., 2017).

The outcomes of precipitation also implied the existence of a feedback loop between the volume of precipitation and the area of the lagoon. More specifically, not only does the total volume accounted as inflow depend on the amount of precipitation, but it has also a strong dependency on the area of the lagoon as an enhancing or lessening effect. In other words, high precipitation values increase the area of the lagoon, which in turn enhances the total volume of water as inflow from precipitation. For example, the consecutive hydrological years 2011/2012 and 2012/2013 accounted for a very similar total annual precipitation of 934.4 mm and 933.7 mm respectively. However, between these years the surface of La Picasa lagoon increased by approximately 3,116 ha due to other factors. As a result, the total volume from precipitation showed an incremental growth of 24 hm^3. In relative terms, this represented 7.57% of the total water inflow of the hydrological year 2012/2013. Although the last four hydrological years were above the historical mean, the enhancing effect of the area of the lagoon played a key role in the last two, when precipitations were above mean 11% and 43% respectively, but their inflow volume were 27% and 171%.

All the previous estimations of evaporation conducted in the basin were obtained from evaporation pans (SsRH, 2017; Pedraza *et al*., 2010; Pedraza, 2000). In this context, this thesis provides the first quantification of evaporation from the open waters of La Picasa lagoon using Energy Budget Based methods, such as the Penman Method and the CRLE model.

It is important to highlight that both methods showed different degrees of prediction error. For example, after including the component of surface runoff in the water balance model and without considering any adjustment factor, the mean prediction error of the simulated values of the volume of the lagoon compared to the measured ones during the calibration period were 73% for the Penman Method and 14% for the CRLE model. These results are in line with the higher cumulative prediction error of the Penman Method compared to the CRLE model suggested by Vallet-Coulomb *et al*. (2001). After equalizing all errors in the input variables to 10%, these authors found that the Penman Method provided a consistent inter-annual evaporation rate with a cumulative error of 20.1%, while in the case of the CRLE model the cumulative error was 9.3%. Other studies aiming to assess lake water balances also compared both methods. In this regard, Troin *et al*. (2010) applied the CRLE model to estimate the evaporation from Mar Chiquita lagoon and obtained an estimation 3% higher than the one by Shipper (as cited by Troin *et al*., 2010), who applied the Penman Method.

It is possible that the larger prediction errors of both Energy Budget Based methods in this study might have been due to the lack of meteorological input data near the lagoon. The use of a ground station located in Pergamino could have certainly increased the amount of uncertainties and errors of the input variables beyond 10% as suggested by Vallet-Coulomb *et al*. (2001). However, even considering these uncertainties, the prediction error of CRLE model only surpassed the suggested cumulative error in 4.7% while in the case of Penman Method it ascended to 52.9%.

The lower performance of the latter one may have arisen from its disadvantages, namely the great number of required weather variables and parameters. Since most of them are not directly available from ground stations, they are commonly estimated from other variables (Valiantzas, 2006), thus increasing the magnitude of its uncertainties (Troin *et al*., 2010).

Therefore, the CRLE model has some advantages over the Penman Method. One of them is the reduced input requirement (Dos Reis and Dias, 1998). Additionally, it has been mentioned that the influence of wind speed, required in the Penman Method, is eliminated by an empirical coefficient, which may result in less errors because it does not require any site-specific calibration (Troin *et al*., 2010). Moreover, when a layer of air over a moist area is saturated with vapor and there are small changes in temperature and vapor pressure at different altitudes and times (the case for a lake or lagoon), it is recommended to use a method that takes the equilibrium evaporation in a state of low advection, such as the case of the CRLE model (Wang et al., 2018). In light of these advantages, the results implied that the CRLE model was more appropriate for the study area with the available data.

The aggregation of evaporation and pumping components provided enough evidence to state that the first one was the main outflow of La Picasa lagoon during the simulation period, being in line to what has been previously expressed by INA (2016). Although the estimated mean monthly evaporation rate during the simulation period (131 mm) resulted only 11 mm higher, the intra-annual variability resembled the findings from these authors, showing that the summer evaporation is the highest with a mean of 204 mm per month, that is 138 mm more than during

winter. At the annual time step, it was assumed that the estimated evaporation also yielded acceptable results, based on comparisons with annual evaporation rates from SsRH (2017) and Fili *et al*. (2000). Despite the mean evaporation for the simulation period resulted 334 mm higher than the one reported by Fili *et al*. (2000), it was only 74 mm above the results from SsRH (2017), who estimated a mean annual evaporation in the basin of 1500 mm between 2005 and 2013.

Conversely, the mean annual net evaporation calculated for the simulation period showed differences to the 500 mm specified by SsRH (2017). Although it was 144 mm higher, the analysis of the time series showed a negative trend throughout this period, driven by a decreasing evaporation coupled with an increasing precipitation. From September 2014 onwards, the mean annual net evaporation was less than the estimated by SsRH (2017), reaching a minimum of 157 mm in 2016/2017. This effect fostered an important reduction in the water losses from the lagoon to the atmosphere equivalent to a volume of 117 hm^3 in the mentioned year.

The inclusion of surface runoff from the surrounding sub-basins to the lagoon as a component of the water balance is supported by the results of Pedraza *et al*. (2010). They proposed surface runoff as one of the mechanisms of water transport in La Picasa basin, the so-called “superficial saturation flux”. This mostly occurs during years with water excesses in which the reduction of water table depths saturates the soil profile, reducing its infiltration capacity. Similarly, Fili *et al*. (2000) also suggested that during long humid periods, instead of the predominant vertical processes, namely precipitation, evaporation and infiltration, the soil storage capacity is saturated and surface runoff takes place. In this regard, it is interesting to note that the ascendant trend in this component occurred especially after the hydrological years 2011/2012, simultaneously with the start of a humid period in the region indicated by Giordano *et al*. (2017).

One of the key inputs to estimate surface runoff was the calculation of the Curve Numbers (SCS-USDA, 1986). Although Pedraza *et al*. (2010) included a modification of the original SCS-CN method, proposing variable CN at a daily time step to account for the mean soil humidity based on the water table depths, the estimated CN values calculated with the traditional SCS-CN method were accordingly to the suggested for the Central Pampa. For example, Bert *et al*. (2007) reported a variation range of CN in Pergamino between 76 to 82 (see Figure 11), while Savin *et al*. (1995) also reported CN values of 83 in Pergamino and 75 in Marcos Juarez, located in Córdoba, further North of the study area.

The reasons of the agreement between the calculated CN in this thesis to those found in the literature might be based on similar soil textures used to calculate the HSG to those described for the region by Viglizzo and Frank (2006) and Pedraza (2000), specifically coarser textures in higher areas and some patches characterized by finer textures. In the same line, the land cover utilized was similar to the one published by FAO-LCCS (2007), which proposed 87% of intensive agriculture, without considering the water bodies.

Based on the results shown in Figure 23, the estimated mean contribution of surface runoff to the total water fluxes in the sub-basins surrounding the lagoon was almost the same to the ones found by Nosetto *et al*. (2012) for a soybean-dominated vegetation cover (24%) and a rotation wheat-soybean cover (19%). Likewise, the mean contribution of evapotranspiration was only 3.6% higher than that reported for a soybean cover and barely 2.4% less than that for a rotation soybean-wheat

(Nosetto *et al*., 2012). In turn, the mean contribution of percolation resulted slightly less than the deep drain suggested for soybean (12%) and for soybean-wheat (10%) (Nosetto *et al*., 2012).

The fact that interflow was not considered as an important component of the water balance of La Picasa lagoon after having calculated the total water fluxes of the sub-basins is comprehensively in line with the conclusions of Fili *et al*. (2000). After estimating the mean inflow from this source in 0.02 $m^3 s^{-1}$, which represents 0.05 hm^3 per month or 0.63 hm^3 per year, they decided to discard the influence of subsurface and groundwater inflow to the lagoon (Fili *et al*., 2000).

Water discharge from channels, representing a quarter of the total water inflow, was found to be the second inflow component of La Picasa lagoon at a monthly time step after precipitation. However, during months with precipitation below average, its contribution ascended to almost three quarters and in extreme cases with no precipitation it represented the total water inflow.

Regarding its intra-annual variability, the fact that water discharge presented higher relative contributions during winter months (June, July, August) compared to the other inflow components could not be explained by an increase of its absolute monthly contribution in this period of the year, since they were registered during summer months (December, January, February). It was rather explained by the behavior of surface runoff, which also presented higher relative contributions during late spring and summer, with a peak in January (22.9%), while in winter its influence was drastically reduced to be almost neglected with 0% and 0.01% in June and July respectively.

The analysis of the behavior of water discharge throughout the simulation period highlighted that during the humid period its absolute contribution to the total inflow at the annual time step considerably increased over precipitation. One of the reasons was its close relationship to surface runoff at the basin scale. In line with Pedraza (2000), despite vertical processes are dominant during normal or dry periods, these results stressed that in the humid period the storage capacity of soils was surpassed, increasing the amount of surface runoff flowing to drainage channels, regulation reservoirs and finally La Picasa lagoon. This situation can be illustrated analyzing the hydrological years 2012/2013 onwards, characterized by more humid conditions in the region (Giordano *et al*., 2017). In this regard, although the mean contribution from water discharge was 62 hm^3 less than precipitation until 2015/2016, from this hydrological year until the end of the simulation period, its high increase rate led the water discharge to exceed precipitation in 227 hm^3.

As can be perceived, the increase in water discharge presented a delay compared to the start of the humid period. These results are similar to those found by SsRH (2017) and INA (2016), who stated that during the first six months of 2016 the OR7 drained double the discharge than 2012 with a similar amount of precipitation. One of the reasons of this delay could have been due to the storage capacity of lagoons and lowlands in dells, a hydrological process described not only for the Central Pampa in general but also for this basin in particular (Paoli, 2015; Latrubesse and Brea, 2009; Iriondo and Kröhling, 2007; Pedraza, 2000). These lagoons, located on the sides of the main channel, might have had the capacity to naturally regulate water excesses during the start of the humid period. However, after the groundwater table started to rise, as showed the time series of groundwater table depths provided by members of SRH (A. Robul, personal communication, July 3rd, 2018), their storage capacity might have been exceeded and the time of residence of the water reduced, altogether leading to increase the water discharge reaching the lagoon. The second reason of the delay might have been additional water inflows in certain sections of the basin in the last two

hydrological years due to the execution of a number of irregular drainage channels after the water infrastructure was built (SsRH, 2017; INA, 2016). These changes in the basin might have accelerated the time of concentration of water excesses in the main channel and regulation reservoirs, leading to enhanced annual discharges. These results provided evidence to the findings of SsRH (2017), who suggested that the increase in water discharge is related to additional inflows of approximately 100% in a short section of 20 km between the union of Reservoirs 6 and 7. Additionally, the lower water discharges obtained by SsRH (2017) in the last two hydrological years compared to those estimated in this study could be explained by additional inflows flowing into the channels A45 and P5 from surface runoff of the sub-basins located between OR7 and the lagoon.

This situation was probably one of the main causes leading to the second flooding event of the lagoon. For example, after the construction of the main water infrastructure of the basin and the presumed connection of irregular channels, a punctual measurement of water discharge reaching La Picasa lagoon totalized 51 $m^3 s^{-1}$, similar to those reported by Fili *et al*. (2000) of 50 $m^3 s^{-1}$ flowing to the lagoon from Rufino in 1999 during the first flooding event.

The outcomes of this thesis also provide a numerical evidence to the conclusion drew by INA (2016), who expressed that it is of utmost importance to implement a more efficient pumping to control the water level of La Picasa lagoon. In this regard, the role that pumping stations played as an outflow component in the water balance clearly showed that its contribution was rather low because it represented on average less than 2% of the volume of the lagoon, being evaporation the main outflow component.

Moreover, INA (2016) also mentioned that in case of precipitations above average and without additional inflows, the water level of the lagoon would increase and the required volume to be discharged in order to reduce it would outweigh the maximum pumping capacity in a reasonable short period of time (3 months) by 193.5%. In this respect, there were time intervals during the simulation period, such as the hydrological years 2011/2012 and 2012/2013, when the incremental growth in volume of inflow from precipitation, only considering the variations of the area of the lagoon, outweighed the pumping component of the respective year in 641% (20.76 hm^3).

The variation of the water level of La Picasa lagoon in the first half of the Period 1 as shown in Figure 31 corresponded to the one suggested by Pereira *et al*. (2014), who also presented a descendent trend from 2007 to 2009. These authors related the decrease in water level to a reduction in precipitation as part of a dry period during those years. However, the current study highlighted that it was a net evaporation above average the main factor determining the decreasing water level of the lagoon in the first period rather than only a reduction in precipitation. Additionally, from the second half of the Period 1 onwards, the water level matched those proposed by INA (2016), who expressed that the lagoon was below 102.5 m between 2008 and 2015.

Another point to consider was that INA (2016) did not stress the increase in water level already starting from 2012, coupled with the beginning of the humid period as suggested by Giordano *et al*. (2017). On the contrary, Pereira *et al*. (2014) did indirectly provide evidence in that sense because they displayed the growth in the fraction of maximum annual flooded area of La Picasa basin using MODIS from less than 0.01 in 2011 to over 0.03 in 2016.

The second period in the variations of the water level, characterized by an overall slightly ascending trend, but above all the third period, displaying a noticeable ascending trend, demonstrated that

the storage capacity of La Picasa lagoon had already decreased before the start of the higher precipitation values registered in 2016 and 2017. In this sense, it exposed a similar behavior to most of the lagoons in the Central Pampa, which according to Giordano *et al*. (2017) presented a high water level since November 2016. Nevertheless, La Picasa lagoon presented a more accelerated increase rate already in 2015, alike the Sub-Basin A1 of the Salado Basin, adjacent of La Picasa basin in the East (Giordano *et al*., 2017). These authors mentioned that the storage capacity of the different hydrological components of A1, such as lagoons, had already been saturated especially after two important recharge events in August 2015.

After analyzing regional changes in water storage from spatio-temporal variations of the Equivalent Water Height (EWH) from GRACE at the basin scale, Pereira *et al*. (2014) stated that the water level of La Picasa lagoon could continue to increase until it reaches the maximum level before it overflows, which in this case is at 105.8 m above sea level (Pedraza, 2000). Despite the fast water level increase during the third period, the maximum level of La Picasa Lagoon reached 105.69 during the simulation period, that is 11 cm below the overflowing point.

Although there were already morphometric relationships water level-area-volume developed for La Picasa lagoon, they were rather conducted based on a different objective than this study. Specifically, the former bathymetric measurements sought to replace previous measurements of the perimeter of the lagoon for those parallel to the bathymetry conducted in 2005 aiming to define the contour line 102.5 (INA-CRL, 2007). In this regard, they intended to densify the bathymetry to determine the relief of flooded areas of the lagoon based on a higher density of points (INA-CRL, 2007). Another difference with these studies was the maximum water level of the lagoon at the moment of the field campaigns. For instance, when INA-CRL (2007) conducted the bathymetric measurements, the water level was at approximately 103.5 m above sea level (Pereira *et al*., 2014), more than one meter below the water level when the bathymetric measurements in the framework of this study were conducted and almost two meters below the maximum level reached during the simulation period. That was the reason of the inclusion of the contour lines until the bathymetric level 105.5 with the use of satellite images from ALOS (Pagot, 2018).

Compared to the previous morphometric relationships developed for La Picasa lagoon to obtain the area and volume at different water levels, the application of a quadratic function and a cubic function in the current study yielded satisfactory results with minor differences, suggesting that they can be employed with an acceptable degree of error. For instance, based on the water level-area function used as input on the HEC HMS model of the basin, the lagoon had 17,600 ha at a water level of 102.5 m, while in this thesis it was estimated in 17,449 ha. The difference of 151 ha represented only a 0.84% error (A. Villanueva, personal communication, April 27th, 2018). In relation to the water level-volume function, SsRH (2017) stated that an area of La Picasa lagoon equal to 17,300 ha corresponds to a volume of 380 hm^3. At the same water level for which the lagoon equals this area (102.28 m), the developed morphometric water level-volume function predicted a volume of 359 hm^3. The difference represented an error of roughly 5%.

Many sensitivity analyses have been conducted in the frame of hydrological modelling of lagoons and lakes aiming to identify their main components and relative roles determining the variations in their overall water balances (Troin *et al*., 2010; Vallet-Coulomb *et al*., 2006). In this regard, the components of the water balance of La Picasa lagoon found to be the most sensitive, such as

evaporation or precipitation, were also highlighted as showing a high sensitivity in other lakes. For example, Troin *et al*. (2010) found that evaporation was the most sensitive parameter in determining the water level of Mar Chiquita Lagoon. Nevertheless, there was a difference related to the accumulated sensitivity of the other components, for which the influence of evaporation resulted lower than the combined sensitivity of river discharge and precipitation (Troin *et al*., 2010). Contrarily, in the case of La Picasa lagoon it was found that evaporation yielded a higher sensitivity than the combined water discharge and precipitation, presumably because the importance of the surface runoff and lateral movements in this case is not as important as in the case of Mar Chiquita, whose surface inflow is explained by the combined inflows of three rivers.

The monthly water balance of La Picasa lagoon integrated the combined effects of the different components of the hydrological system. In this regard, Bohn *et al*. (2016) had already stated that it is not enough to study the climatic drivers of the variation of shallow lakes in the Central Pampa but also other hydrological components that enhance or diminish the climatic effects, such as anthropogenic actions. Consequently, the results made clear which were the natural and anthropogenic drivers of the variations in volume, area and water level during the simulation period.

The general negative water balance estimated between the hydrological years 2007/2008 and 2011/2012 that determined the descendant trend registered in the water level of the lagoon were consistent with the findings from Pereira *et al*. (2014). In particular, these authors detected a general negative tendency in precipitation, soil humidity and water level using GRACE products in the same time interval. Hence, this tendency was reflected in a mean net evaporation of 884 mm between the aforementioned hydrological years, which were 77% higher compared to the net evaporation of 500 mm suggested by SsRH (2017). A second reason of this negative tendency was the relatively lower antecedent soil moisture suggested by Pereira *et al*. (2014), which might have had an impact in the annual surface runoff estimated in this period, being on average 30 hm^3 less than between 2012 and 2015.

A contrasting short-term fast increase in the volume of the lagoon within this period, specifically in the beginning of 2010 as shown in Figure 34, was based on a mean positive water balance of approximately 89 hm^3. Although an increase in annual precipitation was registered, expressed by Pereira *et al*. (2014), the net evaporation was also above the mean for the simulation period and the net evaporation suggested by SsRH (2017) in approximately 9.5% and 34% respectively. Therefore, the reasons were presumed to be not only a higher water discharge but also a higher surface runoff. These assumptions were based on an increase in soil humidity for the same period exposed by Pereira *et al*. (2014), who calculated an increase in soil humidity with GLDAS from around 70 kg m^{-2} to 165 kg m^{-2}.

The variations in the volume of La Picasa lagoon between the hydrological years 2012/2013 and 2016/2017, with generally positive water balances, were consistent with the findings from SsRH (2017). Nevertheless, they contrasted with INA (2016), who mentioned that the flooding emergency was not explained by a hydrological scenario of water excesses. To this end, the results of the water balance evidenced that this emergency was fostered partly by anthropogenic drivers and partly by natural drivers.

One of the natural drivers of floods was already mentioned and was related to the negative tendency in net evaporation, which caused that this important outflow component of the water balance dropped to 66% below mean in this period. One explanation of this hydrological dynamic was found in an unequal enhancing effect of the increase in area of the lagoon, which determined that the increase in the volume of water lost from evaporation did not outweigh the increase in volume of water inflow from precipitation. The other natural driver of floods was the additional water inflow due to an enhanced surface runoff, which represented up to a maximum of 30% of the total water fluxes of the surrounding basins.

On the other hand, one of the anthropogenic drivers of floods identified was the net water inflow from the main channel and the regulation reservoirs, in accordance with INA (2016). In other words, the calculated additional water inflow due to water discharge from the channels A45 and P5 was not balanced with the outflow from the North and South Pumping Stations. This could be illustrated by analyzing the dynamics of the water discharged and pumped in this period. First, a major increase in water discharge occurred, especially since 2015, possibly due to the construction of irregular drainage channels along the basin, leading to modify the regulation conditions of the system of reservoirs. Simultaneously, the amount of water lost from pumping could only outweigh water discharge in the first two hydrological years, while from 2012 onwards it represented almost half of the total water discharge in the best cases.

The fact that the performance of the model obtained to quantify the water balance of La Picasa lagoon was acceptable showed that the most important hydrological processes were considered. This was in accordance to the results from Fili *et al*. (2000), who mentioned that the groundwater recharge and seepage are not important factors contributing to inflows or outflows and could be neglected. Moreover, accounting for surface runoff and estimating the water losses due to evapotranspiration and percolation in the surrounding sub-basins of the lagoon reinforced the assumption to neglect the possibility of interflow as an important inflow component (Fili *et al*., 2000).

Finally, the results of the water balance in both hypothetical simulation scenarios provided evidence to the impact that the intermittent functioning of the pumping component could have had in the variations of the volume of the lagoon and its effectiveness as a long-term and continued strategy to keep the water level between 98.5 m and 102.5 m as it was projected (Bertoni, 2017; Silvosa, 2017; INA 2016).

In this context, it is important to remark that the contribution of this component could considerably increase as an additional outflow to evaporation, the only natural outflow below 105.8 m as mentioned by Pedraza (2000). In other words, since this component could be temporary outweighed by the inflows, this study found that the only possibility to effectively regulate the water level of the lagoon without building new infrastructure is the continuous operation of the pumping stations. In fact, SsRH (2017) highlighted that the temporal connection of natural reservoirs in lowlands next to the main drainage channels could contribute up to 8 $m^3 s^{-1}$, which would approximate the pumping capacity of both stations. Additionally, the outcomes are in line with Bertoni (2017) and INA (2016), who based the success of the pumping component only as being part of a long-term strategy to achieve the objective of maintaining the water level of the lagoon between the 98.5 m and 102.5 m.

Contrasting with these conclusions, the hypothetical simulation scenario of potential pumping coupled with the already existing water infrastructure in the basin provided evidence against the possibility of regulating the water level of La Picasa lagoon within a safe operation range only with the use pumps. In cases of maintained humid periods, with a combined effect of low net evaporation and increased water discharges together with high inflow due to surface runoff from surrounding sub-basins, this component would not be sufficient to keep the water level of La Picasa lagoon below 102.5 m. Nevertheless, it is worthwhile highlighting that an optimal pumping would have increased its storage capacity anyways, making possible to buffer the additional water inflows, thus stressing this component as an effective measure to reduce the risk of flooding of surrounding towns and public infrastructure (Bertoni, 2017). For instance, both pumping stations working at full capacity during the simulation period would have been vital to avoid the increase in water level beyond 103.15 m, thus preserving the railways and the National Route 7, whose altitude is 104.5 m above sea level (INA, 2016), from being flooded.

Regarding the second hypothetical simulation scenario, up to now there is no record of technical reports promoting a variable operation scheme of the pumping stations according to the climatic and basin conditions. In this regard, the results showed that it would not have been required to operate both pumping stations at full capacity to maintain the water level of the lagoon within the safe range from the beginning of the simulation period. This was expressed by the 'Adjusted no pumping' scenario, which indicated that during normal to dry periods, the negative water balances driven by higher net evaporation values outweigh the sporadic inflows from discharge and surface runoff.

Contributing to Bertoni (2017), this scenario particularly confirmed that the pumping would be effective as a long-term strategy to regulate the water level but suggested the fact that a variable operation scheme would increase its efficiency. In this context, this operation scheme would have delayed the occurrence of an exceeding water level above the maximum projected from January 2016 to April 2017 (fifteen months), while limiting it almost two meters below the maximum water level reached in the simulation period. Finally, this outcome provided an answer to the question on how long the pumping stations should have worked to avoid the flooding of the public infrastructure and the increase in the flooding risks.

10. Conclusions

In summary, a first water balance model of La Picasa lagoon was developed, identifying the components of the hydrological system and their interrelationships. After quantifying the monthly water fluxes, either coming into the lagoon (inflow) or water losses (outflow), it was possible to account for their relative contribution and variability. These components showed to play a major role in determining the changes in volume of the lagoon during the simulation period between the hydrological years 2007/2008 and 2016/2017.

In order to calculate the area and volume of the lagoon based on the available water level measurements, the master's thesis contributed to update the morphometric relationships water level-area-volume previously developed by including a new bathymetry aiming to densify the measurements in the deepest areas of the lagoon bellow 98.5 meters above sea level. In addition, after La Picasa lagoon reached its historical maximum water level, this study also integrated the topographic estimations of the shallowest areas of the lagoon based on satellite products conducted by researchers of LH-CETA.

The adoption of the CRLE model and the Penman Method can be considered as the first systematic approach to quantify the open water evaporation from the lagoon with Energy Budget Based methods. In this regard, the relatively low prediction error of the CRLE model suggested that it was a more appropriate method, since it reduced the cumulative errors of measurements of the meteorological variables and calculations.

The implementation of a sensitivity analysis permitted to determine the importance of the relative contributions of each component to the overall water balance of La Picasa lagoon. Among the outflows, evaporation was identified as the most important component, while pumping represented a minor proportion. In fact, in the current scenario with precipitations above mean and water excesses, the pumping component was found to be not sufficient to reduce and control the water level in the short-term.

On the other hand, precipitations over La Picasa lagoon represented the most determinant component among the inflows. Although it did not present the characteristics of a period with water excesses considering the complete simulation period, after the hydrological year 2011/2012 a positive trend in precipitations indicated the start of a more humid period with values above mean. In addition, water discharge was estimated as the second water inflow in importance, representing the total water flowing through the main channel and the series of regulation reservoirs. Moreover, the sensitivity analysis helped to identify the component of surface runoff from surrounding sub-basins of the lagoon as an additional source of water inflow contributing to its volume variations, representing the third inflow component in importance. Furthermore, the calculations of the water balance in the surrounding sub-basins suggested the no inclusion of interflow as an inflow component. Although the contribution of surface runoff increased in the second half of the simulation period in response to higher precipitation values, the water discharge presented the highest increase rate to the extreme that it exceeded the inflow volume of precipitation in this period. Therefore, these components played an important role explaining the last flooding event that occurred between the hydrological years 2015/2016 and 2016/2017

The flooding event might have been fostered by a coupled effect of anthropogenic and natural drivers. In fact, during the last hydrological years when the highest water level was registered, the extraordinary increase in water discharge might suggest that the storage capacity of reservoirs and wetlands located in dells along the main channels was surpassed, reducing the water retention capacity of the basin and causing that a higher proportion of the additional precipitations occurring in this period was transformed into water discharge. Ultimately, this process might be reflecting other profound changes of the hydrological equilibrium of the basin, from land use changes towards more intensive agriculture schemes to the introduction of water infrastructure and irregular drainage channels to regulate the water fluxes. Simultaneously, it was estimated a noticeably reduction in the capacity of the hydrological system to evaporate the water excesses from this additional water discharge. In particular, the combined contributions of precipitation and evaporation resulted in a decreasing trend of the net evaporation throughout the simulation period, with values below mean specifically after 2012/2013. This effect was even enhanced in volumetric terms due to the increase in the area of the lagoon.

The hypothetical simulation scenarios stressed that both a potential and an adjusted pumping operation as an additional outflow component could have been an important strategy to increase the water losses in the medium-term during the normal and dry period, thus increasing the storage capacity of the lagoon to buffer water excesses and regulate the water level between the safe range of operation. But most importantly, it also showed that during long humid periods with water excesses, the pumping component alone might not be enough to outweigh the additional inflows and control the water level of the lagoon, suggesting the need of establishing additional integrated measures.

It is evident that La Picasa basin has undergone changes in the hydrological equilibrium, which was reflected in the noticeable increase of the water level of La Picasa lagoon. In a potential scenario with longer and maintained humid periods, the current water infrastructure would not be capable of coping with additional water excesses. This situation stresses the need to consider other non-structural measures, such as changes in the agricultural production paradigm or re-establishing the hydrological functionality of wetlands and small lagoons in lowlands and dells within the basin as natural reservoirs to increase the evaporation capacity and ultimately the self-regulatory capacity of the system.

In conclusion, the water balance of La Picasa lagoon showed with concrete evidence which hydrological components and processes had an influence in determining the extraordinary water level rise, which caused one of the most important disasters in the basin, disrupting livelihoods, flooding agricultural land and affecting infrastructure. In this scenario, it represents a decision support tool that aims to consider all factors having a significant role in the evolution of a flooding event in the basin, thus contributing to develop better and more effective flood control and mitigation measures in the future.

11. References

Aduah, M. S., Jewitt, G. P., & Toucher, M. L. (2017). Assessing suitability of the ACRU hydrological model in a rainforest catchment in Ghana, West Africa. *Water Science, 31*, 198-214.

Alconada-Magliano, M. M., Fagundo-Castillo, J. R., Carrillo-Rivera, J. J., & Hernández, P. G. (2011). Origin of flooding water through hydrogeochemical identification, the Buenos Aires plain, Argentina. *Environmental Earth Sciences, 64*, 57-71.

Allen, R. G., Pereira, L. S., Raes, D., & Smith, M. (1998). *FAO Irrigation and Drainage Paper No. 56.* Rome, Italy: Food and Agriculture Organization of the United Nations. 56. 26-40.

Aradas, R. D., & Thorne, C. R. (2001). Modelling groundwater and surface water interaction for water resources management in Buenos Aires Province, Argentina. *World Water and Environmental Resources Congress* (pp. 120-129). Orlando, FL: Integrated Surface and Ground Water Management.

Atkinson, S. E., Woods, R. A., & Sivapalan, M. (2002). Climate and landscape controls on water balance model complexity over changing timescales. *Water Resources Research, 38*(12), 1314.

Badano, N. D. (2010). *Modelación Integrada de Grandes Cuencas de Llanura con Énfasis en la Evaluación de Inundaciones.* Buenos Aires: Tesis de grado en Ingeniería Civil - Facultad de Ingeniería Universidad de Buenos Aires.

Badano, N., Lecertua, E., Re , F., & Re, M. (2012). *Evaluación de las inundaciones y las obras de drenaje en la cuenca del Salado (Prov. de Buenos Aires) mediante simulación numérica.* Ezeiza: Laboratorio de Hidráulica - INA (Instituto Nacional del Agua).

Bert, F. E., Laciana, C. E., Podestá, G. P., Satorre, E. H., & Menéndez, A. N. (2007). Sensitivity of CERES-Maize simulated yields to uncertainty in soil properties and daily solar radiation. *Agricultural Sciences, 94*, 141-150.

Bertoni, J. C. (2017, November 8). *Se realizó una audiencia pública ante la Corte Suprema en una causa vinculada con la situación de emergencia de las aguas de la laguna La Picasa*. Retrieved from Centro de Información Judicial. Agencia de noticias del Poder Judicial: https://www.cij.gov.ar/nota-28237 Se realizó una audiencia pública ante la Corte Suprema en una causa vinculada con la situación de emergencia de las aguas de la laguna La Picasa.html

Bohn, V. Y., Delgado, A. L., Piccolo, M. C., & Perillo, G. M. (2016). Assessment of climate variability and land use effect on shallow lakes in temperate plains of Argentina. *Environmental Earth Sciences, 75*(818), https://doi.org/10.1007/s12665-016-5569-6.

Bouchet, R. J. (1963). Evapotranspiration réelle et potentielle, signification climatique. *General Assembly, Berkeley. International Association of Hydrological Sciences, 62*, 134-142.

Brandolin, P. G., Ávalos, M. A., & De Angelo, C. (2012). The impact of flood control on the loss of wetlands in Argentina. *Aquatic Conservation: Marine And Freshwater Ecosystems*.

Cobby, D., Morris, S., Parkes, A., & Robinson, V. (2009). Groundwater flood risk management: advances towards meeting the requirements of the EU floods directive. *Journal of Flood Risk Management, 2*, 111-119.

Collins, J. (2005). Calibración de un modelo hidrodinámico con el apoyo de imágenes satelitales. In J. D. H. D. Farias (Ed.), *RIOS 2005: Principios y Aplicaciones en Hidráulica de Ríos. Segundo Simposio Regional sobre Hidráulica de Ríos.* Neuquén, Argentina.

Dalponte, D., Rinaldi, P., Cazenave, G., Usunoff, E., Vives, L., Varni, M., . . . Clausse, A. (2007). A validated fast algorithm for simulation of flooding events in plains. *Hydrological Processes, 21*, 1115-1124.

Devi, G. K., Ganastri, B. P., & Dwarakish, G. S. (2015). A Review on Hydrological Models. *Aquatic Procedia, 4*, 1001-1007.

Dos Reis, R. J., & Dias, N. L. (1998). Multi-season lake evaporation: energy-budget estimates and CRLE model assessment with limited meteorological observations. *Journal of Hydrology, 208*, 135-147.

European Commission, Joint Research Centre. (2003). *Global Land Cover 2000 Dataset.* Retrieved from http://forobs.jrc.ec.europa.eu/products/glc2000/data_access.php

FAO/IIASA/ISRIC/ISS-CAS/JRC. (2012). *Harmonized World Soil Database (version 1.2).* Rome, Italy and Laxenburg, Austria: FAO and IIASA.

FAO-LCCS. (2007). *Geoportal IDESA*. Retrieved from http://geoportal.idesa.gob.ar

Fili, M., Tujchneider, O., D'Elia, M., Paris, M., & Pérez, M. (2000). La influencia de las aguas subterráneas en el anegamiento de un sector de la llanura pampeana en la República Argentina. *Revista Aguas Subterráneas*, 1-14.

Freitas, H. d., Freitas, C. d., Rosim, S., & Oliveira, J. d. (2016). Drainage networks and watersheds delineation derived from TIN-based digital elevation models. *Computers & Geosciences, 92*, 21-37.

García Montaldo, M. (2012). Agua, factores que limitan su gestión integral. Algunas sugerencias para su superación a partir del análisis de la conformación y actuación de la Comisión Interjurisdiccional de la Cuenca de la Laguna La Picasa. *UBP Serie Materiales de Investigación, Año 5*(10), 1-15.

Giacosa, R., Paoli, C., & Collins, J. (2005). Modelación hidrológica continua para verificación de parámetros de diseño en el proyecto La Picasa – Arroyo Pavón. *Anales del XX Congreso Nacional del Agua y III Simposio de Recursos Hídricos del Cono Sur.*, (pp. ISBN 987-22143-0-1). Mendoza, Argentina.

Giordano, L., Bianchi, J., & Calvi, T. (2017). *Inundaciones en la cuenca A1 del Río Salado bonaerense. Elementos para el diagnóstico de situación.* Instituto Nacional del Agua (INA). Dirección de Sistemas de Información y Alerta Meteorológico. Área de Sensores Remotos y SIG.

Guerra, L., Piovano, E. L., Córdoba, F. E., Tachikawa, K., Rostek, F., García, M., . . . Sylvestre, F. (2016). Climate change evidences from the end of the Little Ice Age to the Current Warm Period

registered by Melincué Lake (Northern Pampas, Argentina). *Quaternary International*, http://dx.doi.org/10.1016/j.quaint.2016.06.033.

Gupta, H. V., Sorooshian, S., & Yapo, P. O. (1999). Status of automatic calibration for hydrologic models: comparison with multilevel expert calibration. *Journal of Hydrologic Engineering, 4*(2), 135-143.

Havrylenko, S. B., Bodoque, J. M., Srinivasan, R., Zucarelli, G. V., & Mercuri, P. (2016). Assessment of the soil water content in the Pampas region using SWAT. *Catena, 137*, 298-309.

Helsel, D. R., & Hirsch, R. M. (2002). Statistical methods in water resources. In USGS, *Hydrologic Analysis and Interpretation* (pp. 1-503). U.S. Geological Survey.

IGN (Instituto Geográfico Nacional). (2016, 12 02). *Introducción Geoide-Ar 16 - Modelo de Geoide Argentino*. Retrieved from Instituto Geográfico Nacional: http://www.ign.gob.ar/NuestrasActividades/Geodesia/Geoide-Ar16

Instituto Nacional del Agua (INA). (2016). *Plan Director para la Gestión Integrada y Sustentable de los Recursos Hídricos de la Cuenca "Laguna La Picasa".* Buenos Aires: Subsecretaría de Recursos Hídricos (SsRH).

Instituto Nacional del Agua-Centro Regional Litoral (INA-CRL). (2007). *Relevamiento batimétrico de la Laguna La Picasa. Informe Final 2° Etapa.* Santa Fe: Author.

Iriondo, M. H., & Drago, E. C. (2004). The headwater hydrographic characteristics of large plains: the Pampa case. *International Journal of Ecohydrology & Hydrobiology, 4*(1), 7-16.

Iriondo, M., & Kröhling, D. (2007). Geomorfología y sedimentología de la Cuenca Superior del Río Salado (Sur de Santa Fe y Noroeste de Buenos Aires, Argentina). *Latin American Journal of Sedimentology and Basin Analysis, 14*(1), 1-23.

Iriondo, M., Brunetto, E., & Kröhling, D. (2009). Historical climatic extremes as indicators for typical scenarios of Holocene climatic periods in the Pampean plain. *Palaeogeography, Palaeoclimatology, Palaeoecology, 283*, 107-119.

Keblouti, M., Ouerdachi, L., & Boutaghane, H. (2012). Spatial Interpolation of Annual Precipitation in Annaba-Algeria-Comparison and Evaluation of Methods. *Energy Procedia, 18*, 468-475.

Kuppel, S., Houspanossian, J., Nosetto, M. D., & Jobbágy, E. G. (2015). What does it take to flood the Pampas?: Lessons from a decade of strong hydrological fluctuations. Floods and the water cycle in the Pampas. *Water Resources Research, 51*(4), 2937-2950.

Latrubesse, E. M., & Brea, D. (2009). Floods in Argentina. In J. F. Shroder (Ed.), *Natural Hazards and Human-Exacerbated Disasters in Latin America. Special Volumes of Geomorphology* (Vol. 13, pp. 1-510). Developments in Earth Surface Processes. Elsevier.

Manfreda, S. (2018). On the derivation of flow rating curves in data-scarce environments. *Journal of Hydrology, 562*, 151-154.

Moradkhani, H., & Sorooshian, S. (2009). General review of rainfall-runoff modeling: model calibration, data assimilation, and uncertainty analysis. In S. Sorooshian, K.-l. Hsu, E. Coppola, B. Tomassetti, M. Verdecchia, & G. Visconti, *Hydrological Modelling and the Water*

Cycle: Coupling the Atmospheric and Hydrolical Models (p. 291). Springer. ISBN 978-3-540-77842-4.

Moriasi, D. N., Arnold, J. G., Van Liew, M. W., Bingner, R. L., Harmel, R. D., & Veith, T. L. (2007). Model evaluation guidelines for systematic quantification of accuracy in watershed simulations. *Transactions of the ASABE, 50*(3), 885-900.

Morton, F. I. (1983a). Operational estimates of lake evaporation. *Journal of Hydrology, 66*, 77-100.

Morton, F. I. (1983b). Operational estimates of areal evapotranspiration and their significance to the science and practice of hydrology. *Journal of Hydrology, 66*, 1-76.

Nash, J. E., & Sutcliffe, J. V. (1970). River Flow Forecasting Through Conceptual Models Part I- A Discussion of Principles. *Journal of Hydrology, 10*, 282-290.

Nosetto, M. D., Jobbágy, E. G., Brizuela, A. B., & Jackson, R. B. (2012). The hydrologic consequences of land cover change in central Argentina. *Agriculture, Ecosystems and Environment, 154*, 2-11.

Nosetto, M. D., Paez, R. A., Ballesteros, S. I., & Jobbágy, E. G. (2015). High water-table levels and flooding risk under grain vs. livestock production systems in the subhumid plains of the Pampas. *Agriculture, Ecosystems and Environment*(206), 60-70.

Odumosu, J. O., Ajayi, O. G., Idowu, F. F., & Adesina, E. A. (2018). Evaluation of the various orthometric height systems and the Nigerian scenario – A case study of Lagos State. *Journal of King Saud University – Engineering Sciences, 30*, 46-53.

Pagot, M. (2018). *Modelo digital de elevaciones y seguimiento satelital en Cuenca Interprovincial de la Laguna La Picasa.* Córdoba: Laboratorio de Hidráulica - Facultad de Ciencias Exactas, Físicas y Naturales - Universidad Nacional de Córdoba.

Paoli, U. C. (2015). *Gestión integrada de crecidas. Guía y caso de estudio.* Luxembourg: European Comission. Joint Research Centre. Institute for Environment and Sustainability.

Pedraza, R. A. (2000). Simulación hidrológica del sistema de la Laguna La Picasa (República Argentina). *XIX Congreso Latinoamericano de Hidráulica Córdoba*, (pp. 367-376). Córdoba.

Pedraza, R., Ingaramo, J., & Cammissi, N. (2010). Modelación hidrológica de cuencas de llanura con áreas fuente variables. Caso de estudio: Cuenca de la Laguna La Picasa (República Argentina). *I Congreso Internacional de Hidrología de Llanuras* (pp. 507-514). Azul, Buenos Aires, Argentina: IHLLA (Instituto de Hidrología de Llanuras "Dr. Eduardo Jorge Usunoff".

Penman, H. L. (1948). Natural Evaporation from Open Water, Bare Soil and Grass. *Proceedings of the Royal Society of London. Series A, Mathematical and Physical Sciences., 193*(1032), 120-145.

Pereira, A., Cornero, C., Pacino, M. C., & Oliveira Cancoro De Matos, A. C. (2014). Uso de geotecnologias para el mapeo de la variación del almacenamiento de agua en la region pampeana a partir de datos GRACE. *Geoacta, 39*(1), 1-10.

Phillips, F. M., Person, M. A., & Muller, A. B. (1986). A numerical lumped-parameter model for simulating the isotopic evolution of closed-basin lakes. *Journal of Hydrology, 85*(1-2), 73-86.

Ponce, V. M., & Shetty, A. V. (1995). A conceptual model of catchment water balance: 1. Formulation and calibration. *Journal of Hydrology, 173*, 27-40.

Rabah, M., El-Hattab, A., & Abdallah, M. (2017). Assessment of the most recent satellite based digital elevation models of Egypt. *NRIAG Journal of Astronomy and Geophysics, 6*, 326-335.

Raparo, A. A. (2009). *Funcionamiento de estación de bombeo Alternativa Norte-Informe N° 15.* Buenos Aires: Subsecretaría de Recursos Hídricos.

Raparo, A. A. (2012). *Funcionamiento de estación de bombeo Alternativa Norte-Informe N°37.* Buenos Aires: Subsecretaría de Recursos Hídricos.

Raparo, A. A. (2015). *Funcionamiento de estación de bombeo Alternativa Norte-Informe N°57.* Buenos Aires: Subsecretaría de Recursos Hídricos.

Rinaldo, A., Beven, K. J., Bertuzzo, E., Nicotina, L., Davies, J., Fiori, A., . . . Botter, G. (2011). Catchment travel time distributions and water flows in soils. *Water Resources Research, 47*, doi:10.1029/2011WR010478.

Rodríguez, A., Pagot, M. R., Hillman, G. D., Pozzi, C. E., Plencovich, G. E., Nelli Camaño, G., . . . Bucher, E. H. (2006). *Modelo de Simulación Hidrológica. In: Bañados del Río Dulce y Laguna de Mar Chiquita (Córdoba, Argentina).* Academia Nacional de Ciencias. Córdoba, Argentina: Ed. Bucher E.H.

Romagnoli, M., Portapila, M., Rigalli, A., Maydana, G., Burgués, M., & García, C. M. (2017). Assessment of the SWAT model to simulate a watershed with limited available data in the Pampas region, Argentina. *Science of the Total Environment, 596-597*, 437-450.

Rosenstein, S., Montico, S., Bonel, B., & Rosenstein, C. (2009). El caso de las inundaciones en la Laguna La Picasa: ¿una oportunidad para la construcción de una representación colectiva del "desastre ambiental"? *Revista de Investigaciones de la Facultad de Ciencias Agrarias - UNR, 9*(15), 011-025.

Sammartino, F. (2017, April 8). *Productores sumergidos: el incontenible avance de la laguna La Picasa. La Nación*. Retrieved from https://www.lanacion.com.ar/2006430-productores-sumergidos-el-incontenible-avance-de-la-laguna-la-picasa

Savin, R., Satorre, E. H., Hall, A. J., & Slafer, G. A. (1995). Assessing strategies for wheat cropping in the monsoonal climate of the Pampas using the CERES-Wheat simulation model. *Field Crops Research, 42*, 81-91.

Shadeed, S., & Almasri, M. (2010). Application of a GIS-based SCS-CN method in West Bank catchments, Palestine. *Water Science and Engineering, 3*(1), 1-13.

Silvosa, R. (2017, November 8). *Se realizó una audiencia pública ante la Corte Suprema en una causa vinculada con la situación de emergencia de las aguas de la laguna La Picasa*. Retrieved from Centro de Información Judicial. Agencia de noticias del Poder Judicial:

https://www.cij.gov.ar/nota-28237 Se realizó una audiencia pública ante la Corte Suprema en una causa vinculada con la situación de emergencia de las aguas de la laguna La Picasa.html

Singh, J., Vernon Knapp, H., Arnold, J. G., & Demissie, M. (2005). Hydrologic Modeling of the Iroquois River Watershed Using HSPF and SWAT. *Journal of the American Water Resources Association, 41*, 343-360.

Siniscalchi, A. G., Kopprio, G., Raniolo, L. A., Gomez, E. A., Diaz, M. S., & Lara, R. J. (2018). Mathematical modelling for ecohydrological management of an endangered endorheic salt lake in the semiarid Pampean region, Argentina. *Journal of Hydrology, 563*, 778-789.

Sogno, G. (2009, 08 01). *Tras nueve meses sin bombeo, temen volver a perder tierras en La Picasa*. Retrieved from La Capital: https://www.lacapital.com.ar/tras-nueve-meses-bombeo-temen-volver-perder-tierras-la-picasa-n330314.html

Soil Conservation Service, United States Department of Agriculture (SCS-USDA). (1986). *Urban Hydrology for Small Watersheds.* Washington, D.C.: Goverment Printing Office.

Sontek. (2011). *River Surveyor S5/M9 System Manual Firmware Version 2.00.* San Diego, USA: SonTek, a Division YSI Inc.

SOUTH (South Surveying & Mapping Technology CO, LTD). (2014). *SOUTH*. Retrieved from http://www.southinstrument.com/userdata/UploadFiles/down/201842593919839.pdf

Subsecretaría de Recursos Hídricos de la Nación (SsRH). (2008). *Plan Federal de Control de Inundaciones - Canal Aductor Estación de Bombeo Alternativa Norte - Laguna La Picasa.* Author.

Subsecretaría de Recursos Hídricos de la Nación (SsRH). (2015). *Gestión integrada de los recursos hídricos aplicada a la Cuenca de La Picasa y área de drenaje.* Buenos Aires: Subsecretaría de Recursos Hídricos de La Nación.

Subsecretaría de Recursos Hídricos de la Nación (SsRH). (2017). *Proyecto: Monitoreo de Caudales Obras Internas Cuenca Laguna La Picasa.* SsRH (Subsecretaría de Recursos Hídricos) - Secretaría de Obras Públicas - Ministerio del Interior, Obras Públicas y Vivienda.

Tanco, R., & Kruse, E. (2001). Prediction of seasonal water-table fluctuations in La Pampa and Buenos Aires, Argentina. *Hydrogeology Journal, 9*, 339-347.

Tripaldi, A., & Forman, S. L. (2016). Eolian depositional phases during the past 50 ka and inferred climate variability for the Pampean Sand Sea, western Pampas, Argentina. *Quaternary Science Reviews, 139*, 77-93.

Troin, M., Vallet-Coulomb, C., Sylvestre, F., & Piovano, E. (2010). Hydrological modelling of a closed lake (Laguna Mar Chiquita, Argentina) in the context of 20th century climatic changes. *Journal of Hydrology, 393*, 233-244.

UNISDR. (2009). *Global assessment report on disaster risk reduction.* Geneva, Switzerland: International Strategy for Disaster Reduction Secretariat.

Valiantzas, J. D. (2006). Simplified versions for the Penman evaporation equation using routine weather data. *Journal of Hydrology, 331*, 690-702.

Vallet-Coulomb, C., Gasse, F., Robison, L., Ferry, L., Van Campo, E., & Chalié, F. (2006). Hydrological modeling of tropical closed Lake Ihotry (SW Madagascar): Sensitivity analysis and implications for paleohydrological reconstructions over the past 4000 years. *Journal of Hydrology, 331*, 257-271.

Vallet-Coulomb, C., Legesse, D., Gasse, F., Travi, Y., & Chernet, T. (2001). Lake evaporation estimates in Tropical Africa (Lake Ziway, Ethiopia). *Journal of Hydrology, 245*, 1-18.

Venencio, M. D., & García, N. O. (2011). Interannual variability and predictability of water table levels at Santa Fe Province (Argentina) within the climatic change context. *Journal of Hydrology, 409*, 62-70.

Viglizzo, E. F., & Frank, F. C. (2006). Ecological interactions, feedbacks, thresholds and collapses in the Argentine Pampas in response to climate and farming during the last century. *Quaternary International*(158), 122-126.

Wang, B., Ma, Y., Ma, W., Su, B., & Dong, X. (2018). Evaluation of ten methods for estimating evaporation in a small high-elevation lake on the Tibetan Plateau. *Theoretical and Applied Climatology, https://doi.org/10.1007/s00704-018-2539-9*, 1-13.

Wheater, H. (2007). Modelling hydrological processes in arid and semi-arid areas: an introduction. In H. Wheater, S. Sorooshian, & K. Sharma (Eds.), *Hydrological Modelling in Arid and Semi-Arid Areas* (pp. 1-20). Cambridge: Cambridge University Press. doi:10.1017/CBO9780511535734.002.

Zimmermann, E. D., & Riccardi, G. A. (2003). Modelo hidrológico superficial y subterráneo desarrollado para la simulación de sistemas de llanura. 1. Aplicación en el sistema Ludueña (Santa Fe, Argentina). *Boletín Geológico y Minero, 114*(2), 147-158.

Declaration in lieu of oath

by Juan Sebastian Salva

This is to confirm that my Master's Thesis was independently composed/authored by myself, using solely the referred sources and support.

I additionally assert that this Thesis has not been part of another examination process.

Place and Date Signature